DOT/FAA/TC-26/5

Federal Aviation Administration
William J. Hughes Technical Center
Aviation Research Division
Atlantic City International Airport
New Jersey 08405

AIA Recommendations for Ultrasound Inspection of New-Make Turbine Engine, Life-Limited Rotating Parts

January 2026

Final report

U.S. Department of Transportation
Federal Aviation Administration

NOTICE

This document is disseminated under the sponsorship of the U.S. Department of Transportation in the interest of information exchange. The U.S. Government assumes no liability for the contents or use thereof. The U.S. Government does not endorse products or manufacturers. Trade or manufacturers' names appear herein solely because they are considered essential to the objective of this report. The findings and conclusions in this report are those of the author(s) and do not necessarily represent the views of the funding agency. This document does not constitute FAA policy. Consult the FAA sponsoring organization listed on the Technical Documentation page as to its use.

This report is available at the Federal Aviation Administration William J. Hughes Technical Center's Full-Text Technical Reports page: actlibrary.tc.faa.gov in Adobe Acrobat portable document format (PDF).

TECHNICAL REPORT DOCUMENTATION PAGE

1. Report No. DOT/FAA/TC-26/5	2. Government Accession No.	3. Recipient's Catalog No.
4. Title and Subtitle AIA Recommendations for Ultrasound Inspection of New-Make Turbine Engine, Life-Limited Rotating Parts		5. Report Date January 2026 6. Performing Organization Code:
7. Author(s) AIA Civil Aviation Regulatory & Safety (CARS) Committee Propulsion Subcommittee AIA A-18-003 NDE Working Group		8. Performing Organization Report No.
9. Performing Organization Name and Address Aerospace Industries Association 1000 Wilson Blvd., Suite 1700 Arlington, VA 22209		10. Work Unit No. 11. Contract or Grant No.
12. Sponsoring Agency Name and Address Federal Aviation Administration Policy and Standards Division 12 New England Executive Park Burlington, MA 01803		13. Type of Report and Period Final Report 14. Sponsoring Agency Code AIR-625

15. Supplementary Notes
This research was sponsored by Jeffrey Stillinger, Policy and Standards Division, AIR-625.

16. Abstract

The aero gas turbine industry has collaborated with the Federal Aviation Administration (FAA) to study and provide guidance regarding the inspection process for the subsurface volume of critical nickel-based engine hardware, through the Aerospace Industries Association (AIA) team AIA A-18-003. Data from across a broad spectrum in the industry is needed for this work since the probability of an uncontained rotor event from any cause has proven to be extremely low. Following an uncontained event from a melt anomaly in a nickel high pressure turbine (HPT) disk in 2016, industry teams including this team AIA A-18-003, team AIA A-18-004, the AIA Jet Engine Nickel Quality Committee (JENQC), and the AIA Rotor Integrity Steering Committee (RISC) have collected data and considered ways to improve rotor damage tolerance through improvements in inspection technologies, melting and manufacturing practices, and part design and lifing. This report documents the findings from the evaluation of Ultrasonic (UT) forging inspections. The inspection guidance and recommendations provided here are integral components of a broader damage tolerance strategy for critical parts. A comprehensive damage tolerance strategy includes part manufacturing, service management, and engineering design characteristics to effectively minimize potential threats.

The position of AIA A-18-003 Team is that aircraft safety is enhanced by the inclusion of subsurface UT inspections. The most effective and desirable method to detect subsurface anomalies and remove defective material from the supply chain is through original equipment manufacturer (OEM) UT inspections of billets and forgings prior to finished part machining. Focusing on the UT inspection of forgings, anomaly detection capability could be enhanced beyond the current baseline by adopting a Multi Zone Multi Angle (MZMA) inspection approach. Evaluation and recommendations for the UT inspection of billets will be addressed in a separate report to be published later. Additionally, another opportunity to detect anomalies is visual inspection of the etched surface of forging and/or finish machined parts, as part of a series of inspection processes.

17. Key Words	18. Distribution Statement
Ultrasonic inspection, damage tolerance, turbine engine, life-limited rotating part, uncontained engine failure, nickel alloy, melt anomaly, forging	No restrictions. This document is available to the public through the National Technical Information Service, Springfield, VA 22161. http://www.ntis.gov

19. Security Classif. (of this report)	20. Security Classif. (of this page)	21. No. of Pages	22. Price
Unclassified	Unclassified		

Form DOT F 1700.7 (8-72) Reproduction of completed page authorized

TEAM AIA 18-003 REPORT: RECOMMENDATIONS FOR ULTRASOUND INSPECTION OF NEW-MAKE TURBINE ENGINE, LIFE-LIMITED ROTATING PARTS

Tasking Letter from FAA

U.S. Department
of Transportation
**Federal Aviation
Administration**

800 Independence Ave
Washington, DC 20591

November 9, 2018

Aerospace Industries Association
Attn: David Silver, Vice President, Civil Aviation
1000 Wilson Boulevard, Suite 1700
Arlington, VA 22209-3928

Dear Mr. Silver:

The National Transportation Safety Board (NTSB) recently released a report of the NTSB investigation, NTSB/AAR-18-01, regarding the uncontained engine failure event of American Airlines Flight 383 that occurred on October 28, 2016. This report contains seven safety recommendations issued to the Federal Aviation Administration (FAA). The following two NTSB Safety Recommendations are particularly pertinent to the engine manufacturer community.

1. A-18-003: Establish and lead an industry group that evaluates current and enhanced technologies regarding their appropriateness and effectiveness for applications using nickel alloys, and use the results of this evaluation to issue guidance pertaining to the inspection process for nickel-based alloy for rotating engine components.
2. A-18-004: Require subsurface in-service inspection techniques, such as ultrasonic inspections, for critical high-energy, life-limited rotating parts for all engines.

We would like to collaborate with the Aerospace Industries Association (AIA), Civil Aviation Regulatory & Safety Committee (CARS), Propulsion Sub-Committee (PC) to address these two recommendations.

Safety Recommendation A-18-003 addresses the inspection of nickel rotor products within the supply chain, prior to them being shipped to the airline customer. Specific issues include:

- Benchmarking current practices for the inspection of billet, forgings, and finished parts before shipment to the airline customer.
- Developing information for best practices where the initial, prioritized implementation could begin in 1-2 years. This initiative should include best practices for anomaly evaluation protocols.
- Identifying improvements within a 3-5 year timeframe. This may include suggestions for industry-level development programs.

We estimate this task will take 1 year to provide the information, and 2 years to implement improvements.

Safety Recommendation A-18-004 addresses in-service inspection of these parts; affecting the airline customers and manufacturing repair and overhaul (MRO) networks. Specific issues include:

- Reviewing the current techniques for sub-surface inspection.
- Reviewing current in-service inspection protocols, prior studies, FAA guidance materials, etc., and proposing an approach where initial, prioritized implementation could begin within 1-2 years from proposal submittal.
- Identifying improvements within a 3-5 year timeframe. The proposal may include suggestions for industry-level development programs.

We estimate this task will take 1 year for the initial, prioritized implementation, and 2 years to implement improvements.

After an accident in 1989, teams were established to address a similar melt-related issue in titanium alloys. In 1991, the FAA issued a report titled "Titanium Rotating Component Review Team Report," which described the state of the industry at the time. The report made several suggestions that prompted work in material melting process development, raw material and forging inspection, and development of a probabilistic design methodology to address melt-related anomalies.

Two current and longstanding government/industry teams, the Aerospace Industries Association (AIA) Rotor Integrity Steering Committee (RISC) and Jet Engine Titanium Quality Committee (JETQC) have their genesis in the industry's response to this FAA report. Both have expressed their interest and willingness to support with us in addressing these safety recommendations.

These teams include U.S. and European companies, providing a broad view of the aviation industry, as did the original FAA titanium review team. The FAA would appreciate AIA's consideration of our request to continue working with the Aerospace and Defense Industries Association of Europe (ASD) to ensure we maintain this broad perspective.

We leave it to your discretion whether two working groups would be more convenient and productive than one. In either case, we very much appreciate your assistance and collaboration. Please send any comments or questions to Dr. Tim Mouzakis, AIR-6A1, via email at Timoleon.Mouzakis@faa.gov or by telephone at (781) 238-7114. We look forward to hearing from you soon.

Sincerely,

Dr. Michael C. Romanowski
Aviation Safety
Director, Policy and Innovation Division
Aircraft Certification Service

cc: Robert Ganley (AIR-6A0)

Tim Mouzakis (AIR-6A1)

Acknowledgements

Team AIA A-18-003 would like to express our sincere gratitude for the efforts and submissions made by the OEMs, which were instrumental in the successful completion of project AIA A-18-003. Your dedication and collaboration have been invaluable to our work, and we deeply appreciate your contributions.

We would like to specifically recognize the following individuals and organizations for their outstanding contributions:

GE Aerospace: Umar Shafique, Richard Klaassen, Patrick Howard,

Edward J Nieters

Rolls-Royce: Waled Hassan, Tim Barden, Rebecca Brooks Hardy, David Wright.

MTU Aero Engines: Ernst Rau, Frederik Elischberger

Safran: Richard Coulette, Patrick Lestoille, Etienne Juliac

Pratt & Whitney: Anton Lavrentyev, Kevin D. Smith (retired)

Honeywell Aerospace: Surendra Singh

Thank you for your commitment and support in making this project a success.

For inquiries related to this report, please reach out to

Umar Shafique at umar.shafique@geaerospace.com

Table of Contents

List of Figures

List of Tables

Chapter 1

1.1 Executive Summary

The aero gas turbine industry has collaborated with the Federal Aviation Administration (FAA) to study and provide guidance regarding the inspection process for the subsurface volume of critical nickel-based engine hardware, through the Aerospace Industries Association (AIA) team AIA A-18-003. Data from across a broad spectrum in the industry is needed for this work since the probability of an uncontained rotor event from any cause has proven to be extremely low. Following an uncontained event from a melt anomaly in a nickel high pressure turbine (HPT) disk in 2016, industry teams including this team AIA A-18-003, team AIA A-18-004, the AIA Jet Engine Nickel Quality Committee (JENQC), and the AIA Rotor Integrity Steering Committee (RISC) have collected data and considered ways to improve rotor damage tolerance through improvements in inspection technologies, melting and manufacturing practices, and part design and lifing. This report documents the findings from the evaluation of Ultrasonic (UT) forging inspections. The inspection guidance and recommendations provided here are integral components of a broader damage tolerance strategy for critical parts. A comprehensive damage tolerance strategy includes part manufacturing, service management, and engineering design characteristics to effectively minimize potential threats.

The position of AIA A-18-003 Team is that aircraft safety is enhanced by the inclusion of subsurface UT inspections. The most effective and desirable method to detect subsurface anomalies and remove defective material from the supply chain is through original equipment manufacturer (OEM) UT inspections of billets and forgings prior to finished part machining. Focusing on the UT inspection of forgings, anomaly detection capability could be enhanced

beyond the current baseline by adopting a Multi Zone Multi Angle (MZMA) inspection approach. Evaluation and recommendations for the UT inspection of billets will be addressed in a separate report to be published later.

Additionally, another opportunity to detect anomalies is visual inspection of the etched surface of forging and/or finish machined parts, as part of a series of inspection processes.

1.2 Background

Turbine engine rotating parts are high-energy components subject to strict regulatory oversight. The National Transportation Safety Board (NTSB) recently released its investigation report, NTSB/AAR-18-01, on the uncontained engine failure event of American Airlines Flight 383 on October 28, 2016. This report includes seven safety recommendations directed to the Federal Aviation Administration (FAA). Two of these recommendations are especially relevant to the engine manufacturing community.

1) A-18-003: Establish and lead an industry group that evaluates current and enhanced technologies regarding their appropriateness and effectiveness for applications using nickel alloys and use the results of this evaluation to issue guidance pertaining to the inspection process for nickel-based alloy for rotating engine components.
2) A-18-004: Require subsurface in-service inspection techniques, such as UT inspections, for critical high-energy, life-limited rotating parts for all engines.

Team A-18-004 issued a report titled “In-Service UT Inspections for Turbine Engine, Life Limited Rotating Parts” summarizing their recommendations for in-service inspection in July 2023 and this report is now being reviewed by the FAA for further policy recommendations.

This team (A-18-003) was tasked with evaluating inspection practices for nickel-based alloys materials, including billets and forgings. The tasking letter, attached in page III, outlines the team's specific requests as follows:

1) Benchmarking current practices for the inspection of billets, forgings, and finished parts before shipment to the airline customer.
2) Developing information on best practices, with the aim of initial, prioritized implementation within 1-2 years. This initiative should include best practices for anomaly evaluation protocols.
3) Identifying improvements within a 3-to-5-year timeframe which may include suggestions for industry-level development programs.

Due to the significant work scope of Team A-18-003, two sub-teams were formed. The first sub-team is dedicated to providing recommendations for billet material UT inspection and is working on generating a separate report on that topic. The second sub-team is focused on developing recommendations for best practices in Ultrasonic forging inspection. This report will focus only on recommendations for the improvement of Ultrasonic forging inspection.

1.3 Safety Through Improved Inspection Sensitivity

Nickel (Ni) alloys such as IN718 (cast/wrought), IN901 (cast/wrought), Waspaloy (cast/wrought), 720Li (cast/wrought), IN100 (powder metal), RR1000 (powder metal) and R88 (powder metal) are used extensively in high-temperature jet engine applications. Various melt anomaly types exist in cast and wrought alloys, including dirty white spots, clean white spots, less commonly positive

segregation (freckle), and slag from either primary Vacuum Induction Melting (VIM) or Secondary melting Electro Slag Remelting (ESR) processes and Vacuum Arc Melting (VAR). In powder alloys, inclusion types include ceramic particles, porosity, and powder lot anomalies [1] Typically dependent on alloy chemistry, dirty white spots contain a microstructure of Nb-lean alloy with fine oxides, nitrides, and carbonitrides. Freckle segregation consists of Nb-rich regions in billets that produce undesirable, brittle phases. Slag defects, which are Ca-rich ceramic phases, originate from either the Vacuum Induction Melting (VIM) or Electroslag Remelting (ESR) process and can result from inadequate ingot surface preparation.

On October 28, 2016, American Airlines flight 383, a Boeing 767-323, N345AN at Chicago O'Hare International Airport, Chicago, Illinois, experienced an uncontained engine failure in the right engine, leading to a subsequent fire. The uncontained engine failure resulted from a high-pressure turbine (HPT) stage 2 disk rupture. The HPT stage 2 disk initially separated into two fragments. Examination of the fracture surfaces in the forward bore region of the HPT stage 2 disk revealed dark gray subsurface material discontinuities with multiple cracks initiating along the edges, consistent with low-cycle fatigue. Additionally, a discrete region beneath the largest discontinuity appeared white compared to the surrounding material. Interspersed within this region were stringers (microscopic-sized oxide particles), collectively referred to as a "discrete dirty white spot."

The National Transportation Safety Board's (NTSB) investigation found that the discrete dirty white spot was likely undetectable during production and subsequent in-service inspections using the procedures available at the time. Following the incident (referred to as "the Chicago event") [2] and the subsequent investigation, the NTSB requested the FAA collaborate with the industry, via the AIA, to evaluate potential improvements in rotor forging UT inspection strategies. This

report documents those findings, specifically focusing on improvements to the current UT inspection techniques for aerospace industry forgings.

Improvements to the UT inspection of forgings can be achieved through the following proposed methods:

1) Adjusting UT technique set up parameters, including transducer frequency, focusing characteristics, and transducer water path.
2) Utilizing multiple incident angles for the UT beam instead of just normal-to-surface angle.
3) Implementing a Multi-Zone UT inspection, where the inspected volume of the material is divided into discrete zones, each inspected separately using different set up parameters.
4) Employing Multi-Mode UT inspections, including longitudinal, axial shear, and circumferential shear UT modes, using both direct reflection and tip diffraction methods.
5) Evaluating UT data with a dual accept/reject threshold, including both traditional UT amplitude and a Signal-to-Noise (SNR) criteria.

While exploring and evaluating improvements to UT inspection sensitivity for forgings, this team aimed to avoid unintended consequences that could adversely impact raw material availability, UT inspection capacity in the supply chain, and the potential increase in false call rates, which could significantly affect material availability. This report focuses on recommendations to enhance the safety and reliability of forgings for critical rotating components. It is the responsibility of the individual OEMs to determine the best implementations of these recommendations considering the specific nuances of their components.

1.4 Reference

[1] G. E. M. a. S. W. L. A. Jackman, "New Knowledge About 'White Spots' in Supperalloys," *Advance Materials & Processes,* vol. 5, pp. 18-25, May 1993.

[2] "Uncontained Engine Failure and Subsequent Fire American Airlines Flight 383 Boeing 767-323, N345AN Chicago, Illinois," 28 October 2016. [Online]. Available: https://www.ntsb.gov/investigations/AccidentReports/Reports/aar1801.pdf.

Chapter 2

2.1 Enhanced Inspection and Characterization

This chapter outlines the essential steps involved in detecting and evaluating UT indications, which could be classified as melt anomalies during the manufacturing process and describes observations made during a case study on a population of melt anomalies. The evaluation steps help determine whether the UT indication may be classified as a melt anomaly. Additionally, results from experimental scans are utilized prior to excising the indication for metallographic evaluation to identify and further develop the most suitable UT inspection method.

Not all anomalies are both detectable and rejectable. During the detection stage, ultrasound technology can identify indications of anomalies. Further ultrasonic or other evaluative techniques can then be employed to determine whether the indication is a genuine anomaly or a false call, such as an artifact resulting from the part's geometry, or an area of microstructural variations resulting from the forging process.

2.2 Ultrasonic Inspection for Initial Detection of Anomalies

An ultrasonic inspection is a method used to assess the material cleanliness and detect indications within the raw material and forging volume. In this method, a sound beam is transmitted into the material, and reflections (echoes) are measured, specifically the echo’s magnitude (amplitude) and time of occurrence. Factors affecting the detectability of anomalies include:

- Location: Distance from part surfaces and edges, as well as depth from the inspection surface.
- Orientation: Angle of anomaly surface facets relative to the sound beam.
- Nature of anomaly: Differences in modulus and density compared to the matrix, and whether the anomaly is voided or not. Size and shape: Includes particle density and whether it is continuous or a cluster of small artifacts.
- Background noise: Typically caused by the baseline material grain structure but could also be due to electrical noise in fine grain materials inspected at high amplifications.
- Inspection parameters: Includes transducer choice, water path, angle of incidence, volume coverage (gate selection), calibration, and reject limits in accordance with specifications.
- Forging process: Such as ring rolling and closed die forging.

The conventional ultrasonic inspection scans include:

- Scans with the sound beam perpendicular to the forging flow lines for detection of anomalies aligned parallel to the forging flow lines:
    - 10 MHz frequency, 0° longitudinal wave (LW)
    - 5 MHz frequency 45° axial/radial shear wave (SW)

- Flow line disoriented scans for increased detection of anomalies not aligned with forging flow lines.
    - 5 MHz frequency 45° circumferential shear wave (CS)

2.3 Evaluation of Detected Indications

After an indication is detected during UT inspection the following steps are applied by manufacturers to determine whether it is a true melt anomaly:

- Initial Detection: Use ultrasound to identify anomalies within the material and record indications that trigger the evaluation or rejection thresholds, as well as any other indications that warrant further investigation. At this stage, an indication may be dismissed as an “artifact” if determined to be caused by non-relevant conditions, such as known geometrical features or surface blemishes.
- Preliminary Analysis: Compare the indications against material inspection specification requirements and determine if further investigation is warranted. For example, an echo may be detected having an amplitude greater than the acceptance threshold, but if it is surrounded by similar echoes just below the threshold, the group may be determined to be caused by the grain structure of the metal.
- Experimental Scans (High-Resolution Scans): Conduct experimental scans to gather additional data on the anomaly. Use this information to determine the next steps in the evaluation process. Most defective conditions exhibit higher signal-to-noise responses in high resolution scans, which can offer improved size/location measurements and shape characteristics.
- Further Evaluation: Utilize additional ultrasonic evaluations or alternative methods. Depending on part and indication characteristics, NDE methods such as X-Ray, eddy current, and infrared can provide insight into the nature of the original indication. Data from high-resolution scans and alternative methods should be

used to determine whether the indication is a relevant anomaly or a false call. At this point, the part may be reduced to a smaller sample for improved inspection with high-resolution and alternative methods.

- Metallographic Evaluation: Perform a detailed metallographic evaluation to confirm the presence and nature of the anomaly.

2.4 Types of Anomalies

In Nickel-based alloys, such as those listed in section 1.3 and including cast and wrought alloys such as 718 (DM and TM) Waspaloy, 720Li and Rene 65, various anomalies have been observed following the final forging operation. The goal of the ultrasonic and surface inspection is to detect these anomalies, which originate from the manufacturing process of the raw material and the strain induced by the forging process. These anomalies vary in nature and can degrade the performance of the finished parts.

The following are several common types of anomalies identified in materials manufacturing by the cast and wrought process:

2.4.1 Clean void

A cavity may occur individually, in tight clusters, or in scattered populations. These cavities may contain vacuum, air, or other gases and typically form near the outer surface of a billet or from excess local strain during the forging operation. Figure 2.1 shows a metallographic image of a cluster of clean voids.

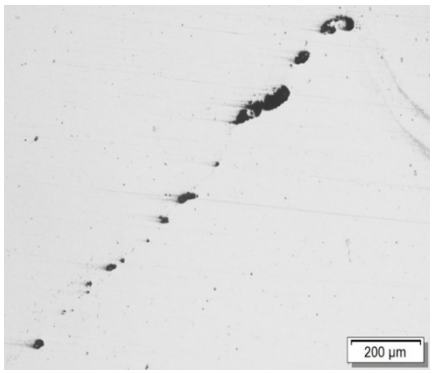

Figure 2.1 Clean voids.

2.4.2 OCNC

Oxide, Carbide, or Nitride clusters (OCNCs) combined with lighter elements such as Al, Mg, and Ca which may also become voided at the boundary with the matrix after the forging process. Figure 2.2 shows metallographic images of an OCNC observed in a ring rolled forging.

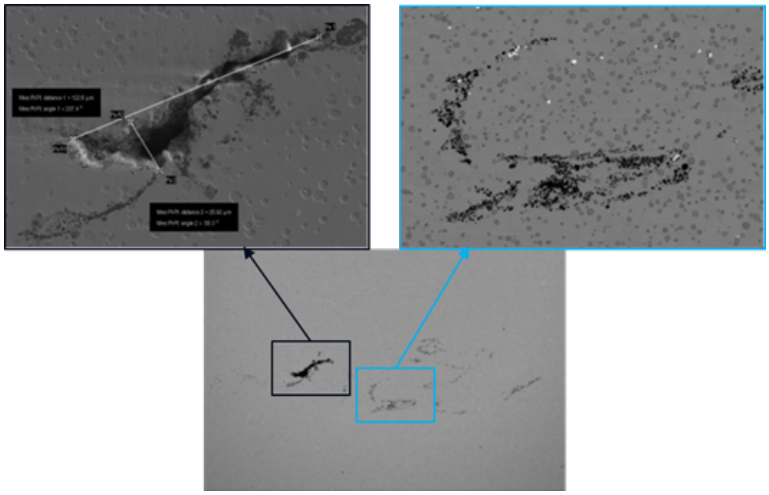

Figure 2.2 OCNC.

2.4.3 Dirty White Spot (DWS)

A region of segregation, typically characterized by a reduced content of the hardening element and an oxide layer (OCNC) surrounding the segregated volume. After etching, these regions typically appear whiter than the surrounding material (matrix) and depending on thermomechanical processing conditions, may show an area of grain coarsening. Voided areas may form at the boundary between the dirty zone and the matrix. Figure 2.3 is a metallographic image of a DWS found in ring-rolled forging.

Figure 2.3 . Dirty White Spot (DWS).

Note that the Information presented in the following section is a case study of actual indications found in nickel-based alloy forged parts during manufacturing. The examples shown are from forgings manufactured from Rene 65. Further similar examples are recorded in the JENQC database, which includes examples from 718(DM and TM), Waspaloy, 720Li and Rene 65 manufactured by the cast and wrought process. The concepts presented here form the foundation of the investigation of inspection techniques presented in Chapter 3.

2.5 Detection Sensitivity

Detection sensitivity threshold is a critical parameter in capturing anomalies in forgings. During a recent manufacturing process, several indications were detected below the reject

threshold. These indications were further investigated and confirmed through metallurgical evaluation. To capture these sub-threshold anomalies, the reject threshold levels were lowered. However, lowering the threshold value also increases the likelihood that noise (grain or electrical) will exceed the threshold, resulting in an increased false call rate.

To better distinguish indications corresponding to actual anomalies from false positives, the Signal-to Noise ratio (SNR) was calculated according to definition given in AMS2628 for the inspection of premium Titanium billets, with a reject threshold set at 2.5.

The outcome of this SNR study shows that for this population of parts, indications with an SNR lower than 2.2 were not associated with potential detrimental anomalies. For example, some low SNR indications were un-recrystallized (NRX) areas, which were determined to not affect the performance of the part being manufactured.

In this study, most of the anomalies were detected by at least 0° LW, often by both 0° LW and 45° CS methods, and sometimes by all inspection modes. It was also noted that several anomalies were only detected using the 45° CS method. Figure 4(a) illustrates the UT beam insertion with respect to flowlines and the response amplitude of the indication. Figure 2.4 (b) shows the metallographic image of the corresponding Dirty White Spot (DWS).

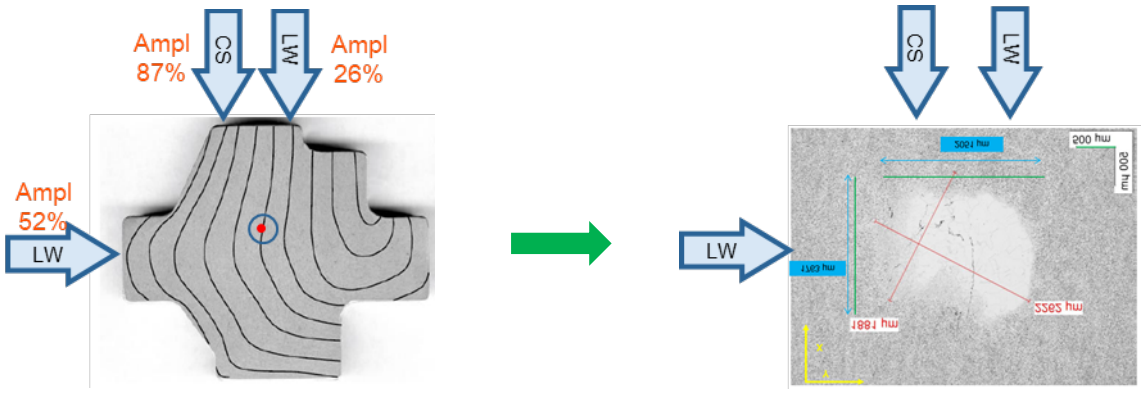

(a) (b)

Figure 2.4. Example of DWS detection.

2.6 Anomaly Characterization

Metallographic evaluation of an anomaly provides valuable information about its size and shape, but the impact on part performance must be inferred. An alternate approach is to incorporate the anomaly into a Low Cycle Fatigue (LCF) specimen when its location allows for sufficient material to create this larger specimen.

Figure 2.5 illustrates the process of sequentially cutting down several subsequent pieces in a part to ensure accurate placement of the anomaly in the center of the LCF specimen. The location of the anomaly at each step is determined using multiple high-resolution ultrasonic inspections.

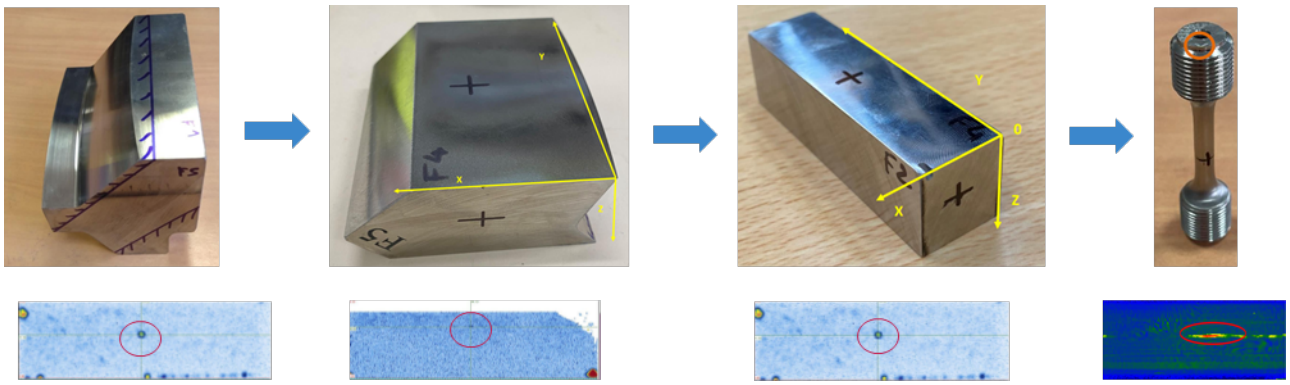

Figure 2.5. Example of detection and location of one anomaly (upper left 3 images) using ultrasound (lower left 3 images) after initial cut operation, prior placement into a test specimen. The LCF specimen is shown on the right with the ultrasonic image verifying proper anomaly placement in the gage section.

Prior to metallurgical evaluation and for a 3D characterization, an X-Ray computed tomography (CT) scan was performed. This CT scan is used to assess the size and nature of the anomaly, as shown in Figure 2.6 & Figure 2.7. The CT image is especially valuable when polishing into the anomaly, as it clearly reveals the location and extent of various types of anomalies, eliminating uncertainty about when to stop polishing. Polishing is typically stopped when the true nature and largest extent of the anomaly are observed. Without the CT data, it is challenging to determine whether the current polish plane meets those criteria, potentially leading to a lower 2D size being recorded or inaccurate characterizations of anomalies.

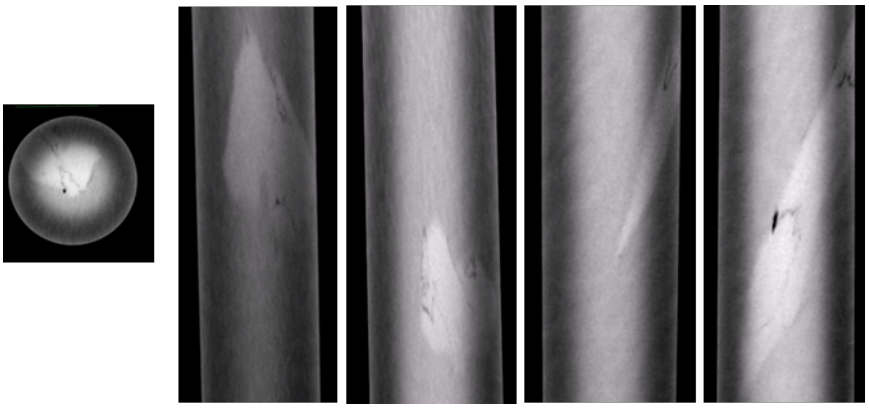

Figure 2.6. X-Ray CT results showing a Dirty White Spot (DWS) in the test specimen (five CT planes of the same anomaly shown).

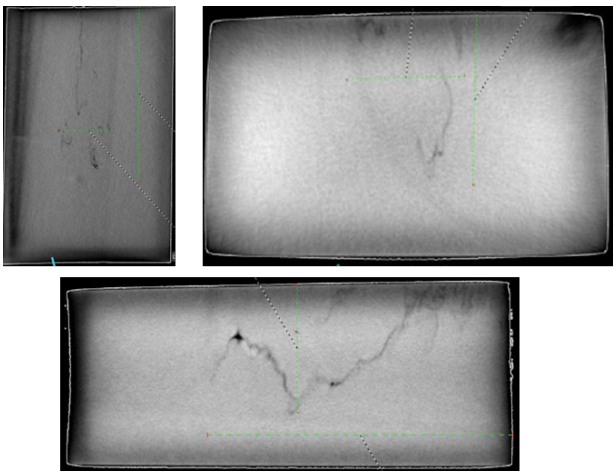

Figure 2.7 X-Ray CT results showing an OCNC in a test sample (three CT planes of observation shown).

Four anomalies used in this study are presented in Table 2.1. Each anomaly is represented by two rows of data: one for the full region of segregation, and one for the OCNC (“dirty”) zone. Note that the observed amplitudes do not correlate with the size of the anomaly but are instead linked to the different morphologies of these DWSs (Dirty White Spots).

Table 2.1. Indication types with corresponding sizes and UT amplitude response signal percentages.

Sample	Type	Feature (mils)			Size of the anomaly		Amplitude	Comment
Serial	*Nature*	*X (mils)*	*Y (mils)*	*Z (mils)*	*Area method (mm^2)*	*Area method ($mils^2$)*		
#1	DWS	172	252	55.1	**21.97**	**34047.3**	**16% LW**	**Low amplitude / low size of the oxyde layer**
#1	Dirty zone	63	78.7	90.6	**3.61**	**5599.9**		
#2	DWS	172	354.3	19.7	**30.89**	**47879.1**	**22% LW**	**Low amplitude / important oxyde layer**
#2	Dirty zone	172	354.3	3.9	**30.89**	**47879.1**		
#3	DWS	69.4	80.7	393.7	**16.11**	**24968.2**	**52% LW**	**High amplitude / important oxyde layer**
#3	Dirty zone	66.1	43.3	393.7	**13.19**	**20451.8**		
#4	DWS	275.6	63	165.7	**23.1**	**35858.2**	**12% LW / 100% CS**	**High amplitude / low size of the oxyde layer**
#4	Dirty zone	44.5	24.8	165.7	**3.8**	**5889.1**		

2.7 Effect of Forging Process on Detectability

The natural consequence of detecting and evaluating anomalies is the generation of new insights into the manufacturing process. One outcome of this particular case study was that the type of forging process used may correlate with the detection of anomalies. The parts containing the anomalies shown in Table 2.1 were manufactured from the same raw material source produced during the same time period but forged using two different processes: closed die and ring roll. They were inspected using the same ultrasonic technique. Fewer indications were observed in die-forged parts, while more indications were observed in ring-rolled parts. This observation suggests that the forging process influences the detectability of material anomalies.

A simulation performed for these forging processes, using a conservative approach with a hard inclusion within the billet material, verified the influence of the forging process on anomaly detectability. For the die forging process, the model shows that a void can be created

but is filled during the hold at the end of the operation due to material creep under compressive hydrostatic pressure. In contrast, for ring rolling, the result is different, with an increase of the void associated with the inclusion and less compressive hydrostatic pressure to fill it back. The increased presence of these voids, or potential cracking associated with the hard inclusion, leads to higher detectability during the ultrasonic inspection.

This Chapter provided an overview of the inspection-detection-evaluation process, which is instrumental to improving the quality of the raw material used to manufacture critical rotating parts. The following chapter summarizes conclusions drawn from multiple engine manufacturers who followed similar processes to define an improved inspection protocol.

Chapter 3

3.1 Studies

Engine manufacturers (OEMs) inspect life-limited Ni-based turbine rotating parts using specialized ultrasonic inspection techniques. While the exact methods vary, each OEM has developed and standardized their approach to effectively detect rejectable indications in Ni forgings. These techniques involve critical parameters such as transducer frequency, beam angle, scan direction, scan depth, and setup gains. Under the AIA charter of enhancing flight safety, these inspection techniques were evaluated for their effectiveness and additional techniques were proposed and evaluated to identify a set of optimized inspections for the detection of melt anomalies in new make Ni forgings.

A comprehensive list of ultrasonic inspection method parameters currently used by OEMs for inspecting Ni forgings was created and summarized in Table 3.1. In addition to setup parameters, the reporting requirements were captured and summarized in Table 3.2. Optimized setup parameters maximized the ability of the ultrasonic inspection to generate a signal response from anomalies in the raw material. Reporting requirements were selected as part of a procedure that ensures every inspector identified the relevant signals.

‘

Table 3.1 Survey of Inspection Approaches.

Inspection Approach	Permutations Used by One or More OEMs
Beam angles	0°, 5°, 7.5°, 10° and 20° incidence
Scan angles per surface	Up to 5 scans
Minimum scans per volume	1 to 4 scans per material volume
Zone depth per Surface	1” to 3” scan zone depth
Longitudinal/rad/ax shear scans	Apply both based on part geometry
Circumferential shear scans	Apply both clockwise and counterclockwise scan directions
Flow line-based beam insertion	For some OEMs, Sound beam is oriented perpendicular to inspection surface or to the direction the material flows during the forging operation
Frequency	5 and 10 MHz
Focal length & Water path	Focus at or just below surface
Dynamic or Static Calibration	Half use Dynamic and other used Static calibration
Scan Speed	Using dynamic calibration or up to 30"/sec (800 mm/sec)
Scan index	Based on effective beam width of the UT probe

Table 3.2 Reporting Requirements.

Reporting Requirements	Summary of Survey Response
Maximum-allowable noise level	0-4 dB below evaluation threshold
Criteria for targets under reject threshold	Repeatable, Under 3:1 Aspect Ratio
A-scan/strip chart/C-scan/Stop on indication	Primarily C-Scan
Time of Flight data	Used by a single OEM
SNR criteria	Used by a single OEM

The relative effectiveness of these approaches was tested by inspecting a titanium disk forging that contained a number of known indications. The results of this evaluation are described in the following section.

3.2 UT Inspection of a Forging Having Known Indications - Round Robin Disk

3.2.1 Background

The purpose of this exercise was to assemble a database of responses for the range of inspection processes applied by the industry. A forging known to contain several indications was used as a common test part in a round-robin exercise. The aim was to identify a set of core best practice approaches that could provide optimal detection of at least one type of anomaly. These results would then be extrapolated to other types of anomalies and tested for broader effectiveness.

Before starting, it was recognized that the forging shape had been designed with inspection criteria in mind. Such a part is designed to provide as many detection opportunities as reasonably possible by allowing ultrasonic access from as many directions as possible. This design-for-inspection philosophy ensures a range of independent normal-to-surface and angled radial-axial beams to cover the material that will ultimately become flight hardware.

The anticipated coverage is modelled in the form of a cross-section color map, where the color corresponds to the number of sound beams interacting with the specific volume of flight material. The results for this part are shown in Figure 3.1. Note that the color-bar maximum (blue) indicates four scans of coverage, but some of the blue regions may actually have a higher count.

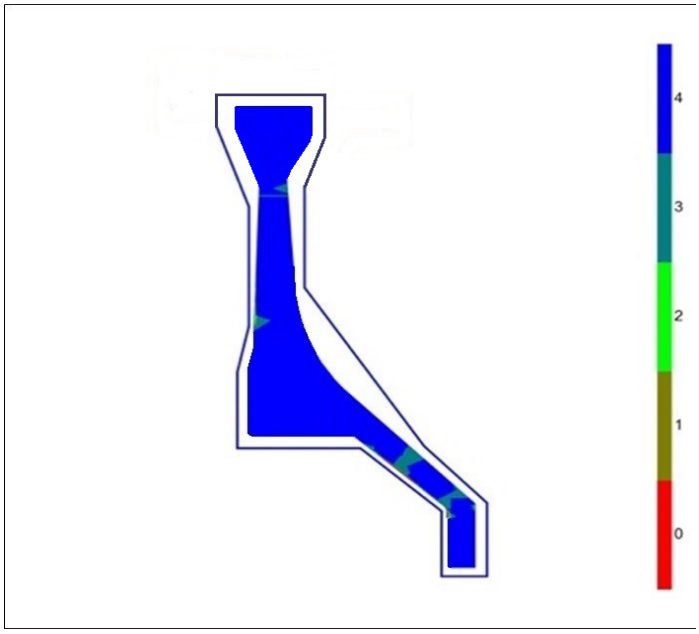

Figure 3.1. Coverage model of forging disk, with color map indicating the number of beams interacting with specific volumes of forging material. The finish part machining shape shown here is a generic representation, not the actual shape.

It was recognized that the forging provided was made of a Titanium alloy containing Tungsten based contaminants, while the purpose of this activity was the inspection of nickel-based alloys with varied types of anomalies. Due to the scarcity of alternate samples, this disk was used as an indicator of how ultrasonic inspections penetrate geometries and interact with inclusions.

Four engine manufacturers inspected the provided contaminated Titanium alloy forging using both their standard production inspection practices and experimental inspection practices. The inspections are summarized below and detailed in Appendix A Table A 4.1.

The indications in this disk are assumed to be Tungsten-related inclusions based on metallography done on a disk made from the same batch of raw material. No metallography was

performed on the indications in this disk. Although a direct linkage between signal strength and target specifics cannot be made, the ultrasonic responses can be compared to assess the effectiveness of the scans used. The amplitudes show which scan setups generated the strongest response for each indication, while the Signal-to-Noise Ratio (SNR) shows which inspection setups are able to detect the indication above the noise level. A weak signal in a low noise environment may be more detectable than a strong signal in a high noise environment. In a low noise environment, a procedure can be specified to add amplification and bring the signal above the evaluation threshold. Figure 3.2 illustrates four possible response categories for a given indication/inspection combination. Note that the best detection is possible for the cases in the top half of the graph, and inspections which show such a response for these indications are expected to be the most effective.

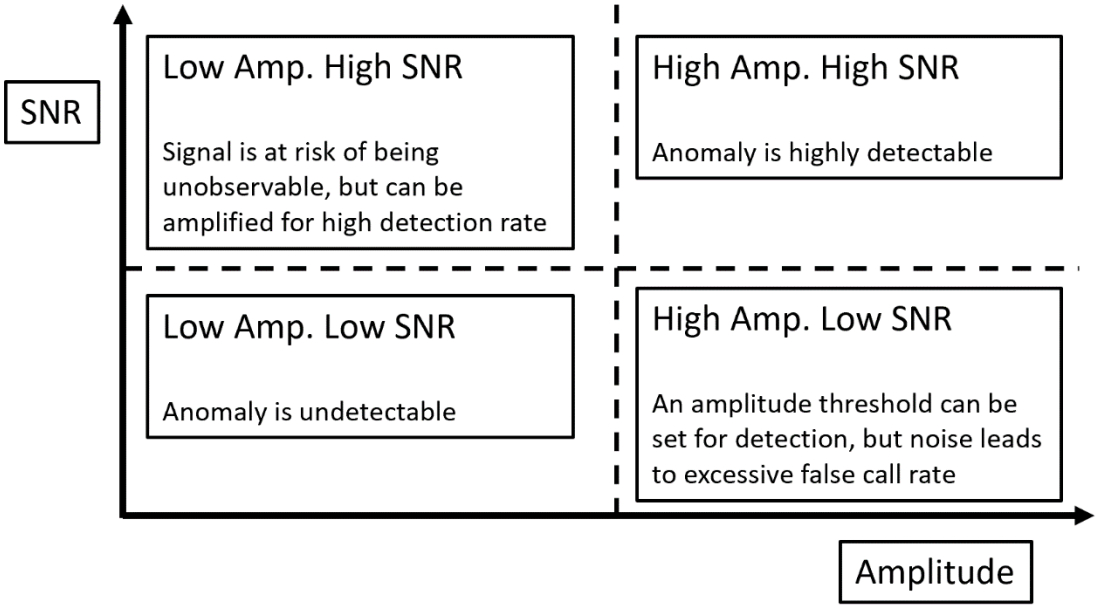

Figure 3.2. Implications of Amplitude and Signal-to-Noise Ratio (SNR) responses from anomalies.

3.2.2 Data Collection

After a thorough inspection of all surfaces and detailed correlation of detections from the various surfaces, the team concluded that the supplied forging contained six (6) indications. Figure 3.3(a) illustrate the circumferential arrangement of these indications, while Figure 3.3 (b) presents a cross-sectional view. The cross-sectional view also shows the inspection surfaces relevant to each indication, coded with unique colors for each indication. Each surface was inspected using the full set of scans, as listed in Table 3.3. Indications were commonly detected from multiple scans from each accessible surface.

Note that all longitudinal scans were calibrated to #1 Flat Bottom Hole (FBH) at 80%, and shear scans were calibrated to a 0.020" (.5mm) Side Drilled Hole (SDH) at 80%.

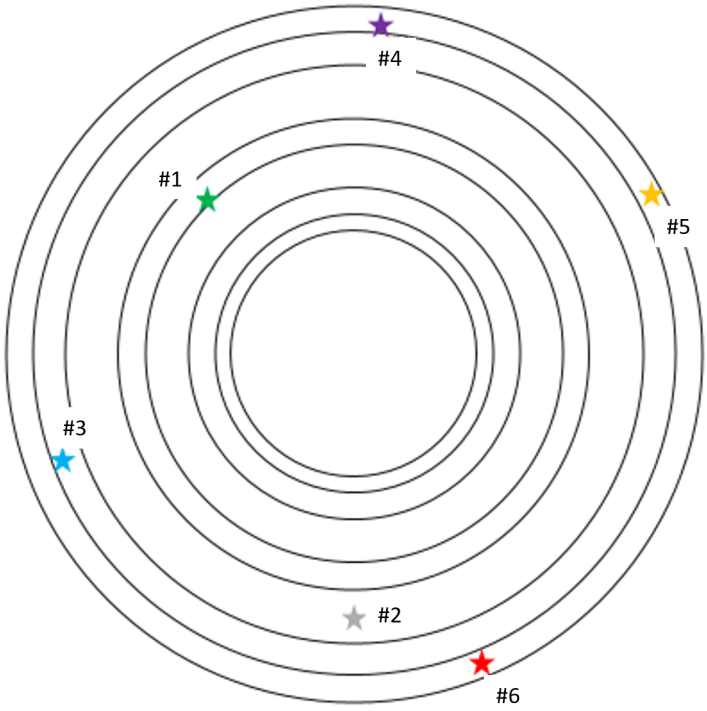

(a)

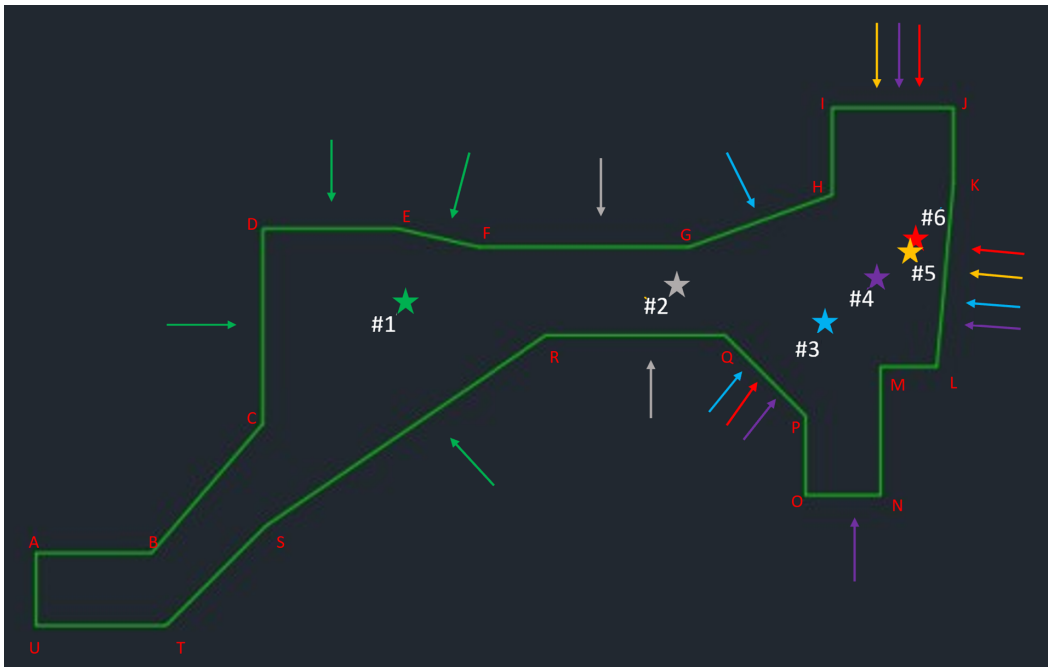

(b)

Figure 3.3 (a). Forging with six known indications and their locations, top view (b). Forging with six known indications and their locations, cross-section view. Arrows show inspection surfaces which offered detections of indications, with colors of arrows corresponding to colors of indications.

Table 3.3 List of inspections applied to each surface. Each scan was used to interrogate indications from each surface indicated by the arrows in Figure 3.3.

Frequency	Internal Angle	Direction	Mode	Focus
5MHz	0°		Long	Surface
5MHz	20°	+Rad/Ax	Long	Surface
5MHz	20°	-Rad/Ax	Long	Surface
5MHz	20°	+ Circ	Long	Surface
5MHz	20°	- Circ	Long	Surface
5MHz	45°	+ Circ	Shear	Surface
5MHz	45°	- Circ	Shear	Surface
10MHz	0°		Long	Surface
10MHz	0°		Long	Sub- Surface

3.2.3 Results Analysis

Table 3.4 describes the ultrasonic evaluations that provided maximum responses. The data clearly demonstrates that for this anomaly type, 5MHz longitudinal beams typically yield the maximum amplitude responses, while10MHz longitudinal beams provide the best SNR. Both 0° and 20° refracted longitudinal scans were effective configurations, but longitudinal scans consistently exhibited increased sensitivity compared to shear scans. Data collected during the round-robin study is given in Appendix A Table A 4.2.

Table 3.4 List of the ultrasonic evaluations providing maximum signal responses.

Maximum Acoustic Responses -			
Indication Number	**SNR Max**	**Amplitude Max**	**Max Combined Result**
#1	10MHz 20° radial axial longitudinal surface focus	5MHz 20° radial axial longitudinal surface focus	5MHz 20° radial axial longitudinal surface focus
#2	10MHz 0° longitudinal surface focus	5MHz -20° radial axial longitudinal surface focus	5MHz 20° radial axial longitudinal surface focus
#3	5MHz 0° longitudinal surface focus	10MHz 0° longitudinal sub-surface focus	5MHz 0° longitudinal surface focus
#4	10MHz 0° longitudinal surface focus	5MHz 20° radial axial longitudinal surface focus	5MHz 0° longitudinal surface focus

#5	5MHz 0° longitudinal surface focus	5MHz 0° longitudinal surface focus	5MHz 0° longitudinal surface focus
#6	10MHz 0° longitudinal sub-surface focus	5MHz 0° longitudinal surface focus	5MHz 0° longitudinal surface focus

While the longitudinal scans were clearly more effective than the shear scans for this anomaly type, there was no consistent pattern for which longitudinal angle or frequency performed best.

Figure 3.4 shows the detections of the indications from scans done by two inspection sources, viewed in a matrix parallel to the one shown in Figure 3.2. The plot is divided into quadrants by setting the SNR threshold to 3 and the amplitude threshold at -5 dB from a #1 FBH. These values are anecdotal, and a discussion about the selection of actual criteria can be found in Section 4.

In Figure 3.4, there are no clusters of points indicating that one target was more detectable than the others, nor is there a clear pattern showing that any particular target/inspection combination was repeatable between the two inspection sources. It should be noted that the two inspections sources did not intend to replicate each other's scan setups, nor did either complete all scan permutations.

To have a high chance of detecting anomalies of this type, the longitudinal scans are necessary. Additionally, it is evident that the maximum likelihood of detection is achieved by providing as many detection opportunities as possible through the use of multiple incidence angles and multiple inspection surfaces. Figure 3.5 and Figure 3.6 show two more examples of the variance

in scan results for a specific target, further demonstrating how multiple scans improve the odds of detection.

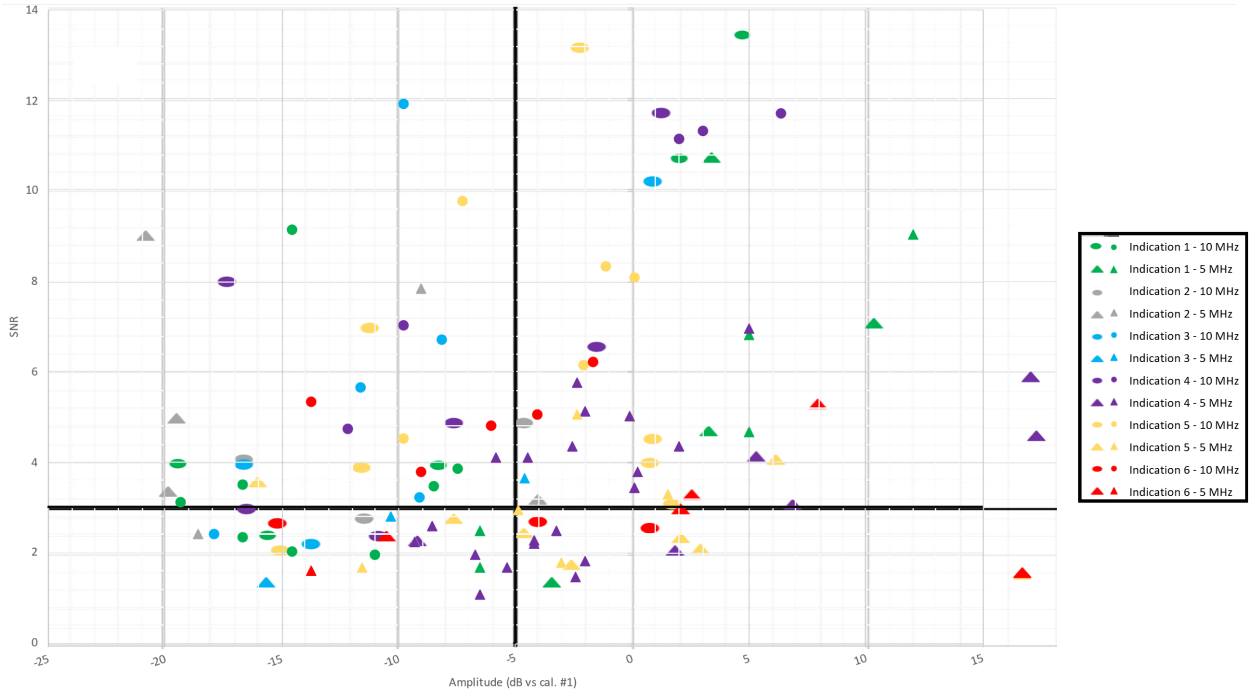

Figure 3.4 Amplitude vs. SNR evaluation of all indications, using inspection data from two OEMs (symbols from one OEM are elongated horizontally compared to the other).

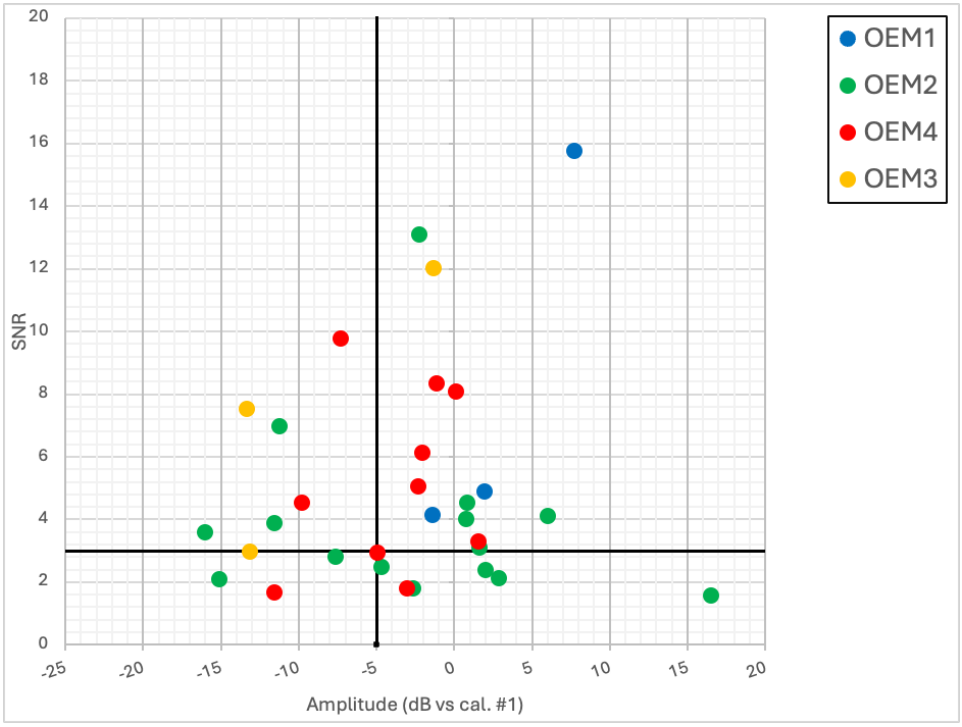

Figure 3.5 Amplitude vs. SNR plot of the indication #5 identified by four OEMs.

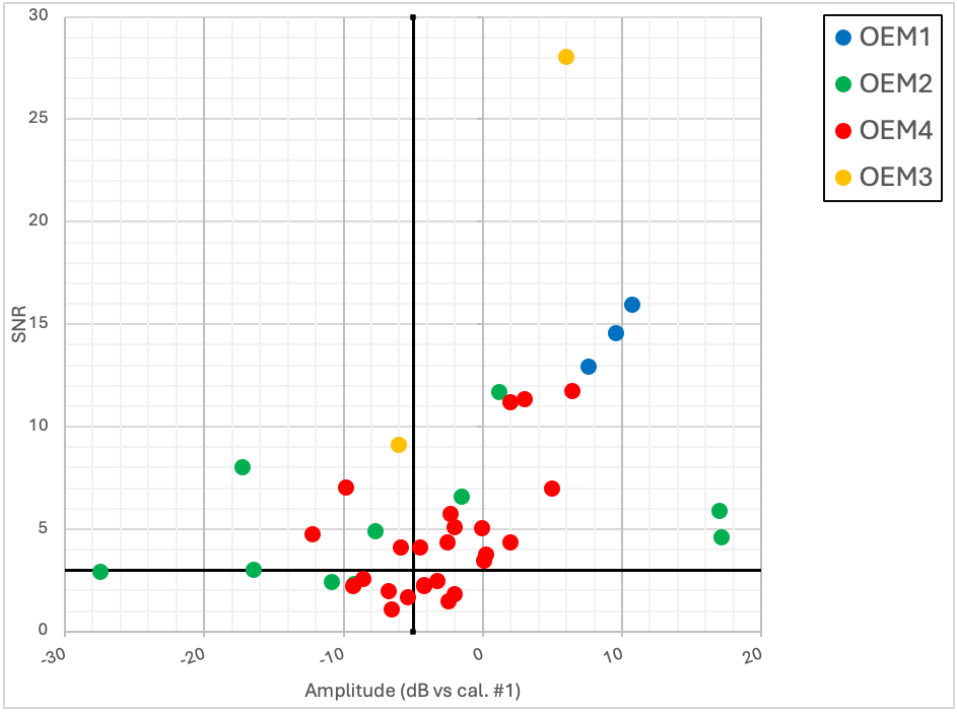

Figure 3.6 Amplitude vs. SNR plot of the indication #4 identified by four OEMs.

A subtle yet important observation made during this exercise was that the indications were elongated in the direction of the forging material flow. This characteristic was best observed from high-resolution ultrasonic inspections. The second major axis of the anomalies was arbitrarily rotated about the circumferential direction. Consequently, the largest area of each anomaly intersected the sound beam when the beam was perpendicular to the flow, with circumferential incidence angles occasionally offering superior beam alignment.

3.2.4 Round Robin Disk Conclusion

This exercise provided evidence that existing practices of all OEMs were sufficient to detect the anomalies in this particular disk. Specifically, for this type of anomaly- discrete inclusions - 5MHz longitudinal beams generally provided the maximum amplitude response, while 10MHz longitudinal beams yielded the best SNR. Both 0° and 20° refracted longitudinal scans were effective configurations, but longitudinal scans consistently offered increased sensitivity over shear scans. Additionally, due to the high degree of signal variability associated with target details and scan setup, the maximum likelihood of detection is achieved by inspecting from multiple angles and surfaces.

3.3 Definition of Standard for Investigative UT inspection of Forgings

Drawing on the lessons learned from the Round Robin Disk, the team collaboratively developed a standardized set of ultrasonic scans, as detailed in Table 3.5. These scans were applied to a series of Ni-alloy parts with known indications to determine the optimal inspection approaches for a wider variety of anomaly types. Once a part was identified as having an indication of interest, these scans were applied, data were recorded, and the indications were evaluated with

metallography to ascertain their nature. In some cases, additional scans were incorporated beyond the initial list. Note that a number of scans were carried out on parts during in service inspection, rather than at new make. As detailed in section 2.4 additional examples of anomalies similar to the 9 presented here are reported in the JENQC database.

Based on the results from multiple parts, a reduced set of scans (as detailed in Table 3.5) was selected as the recommended protocol for the production-level inspection of Nickel forgings.

Table 3.5 List of standard scans.

Depth	Frequency	Focal Length	Water path	Incidence Angle	Mode	Direction
0 to 2" (51mm) deep	5 MHz	6" (152mm)	6" (152mm)	0°	Long	None
				+/- 5°	Long	Rad/Ax
						Circ
				+/- 19°	Shear	Rad/Ax
						Circ
				+/- 26°	Shear	Circ
	10 MHz	3" (76mm)	3" (76mm)	0°	Long	None
				+/- 5°	Long	Rad/Ax
						Circ
				+/- 19°	Shear	Rad/Ax
						Circ
				+/- 26°	Shear	Circ
Only if <0.5" (12mm) deep	5 MHz	2" (51mm)	2" (51mm)	0°	Long	None
Only if >0.5" (12mm) deep	5 MHz	2" (51mm)	2" (51mm)	+/- 5°	Long	Rad/Ax
	10 MHz	8" (203mm)	Focus at ind. Depth	+/- 5°	Long	Circ
				+/- 19°	Shear	Rad/Ax
				+/- 19°	Shear	Circ
				0°	Long	None
	10 MHz	8" (203mm)	Same Wp as 0° scan	+/- 5°	Long	Circ
			4" (101mm)	+/- 19°	Shear	Circ

For all the scans listed in Table 3.5, the following inspection data were collected:

- Calibration:
  - Target type
  - Depth
  - Amplitude
  - Gain
- Record from C-scan:
  - Peak signal amplitude
  - Mean noise
  - Peak noise
  - Noise standard deviation

3.4 Ultrasonic Inspection of Disk 1

3.4.1 Background

One OEM identified Disk 1 as having an indication of interest, located as shown in Figure 3.7. The red circle marks the location of the indication and the relevant scan regions of the disk are labeled as “OD” (Outer Diameter) and “Rim”. The C-scan image of the indication is shown in Figure 3.8.

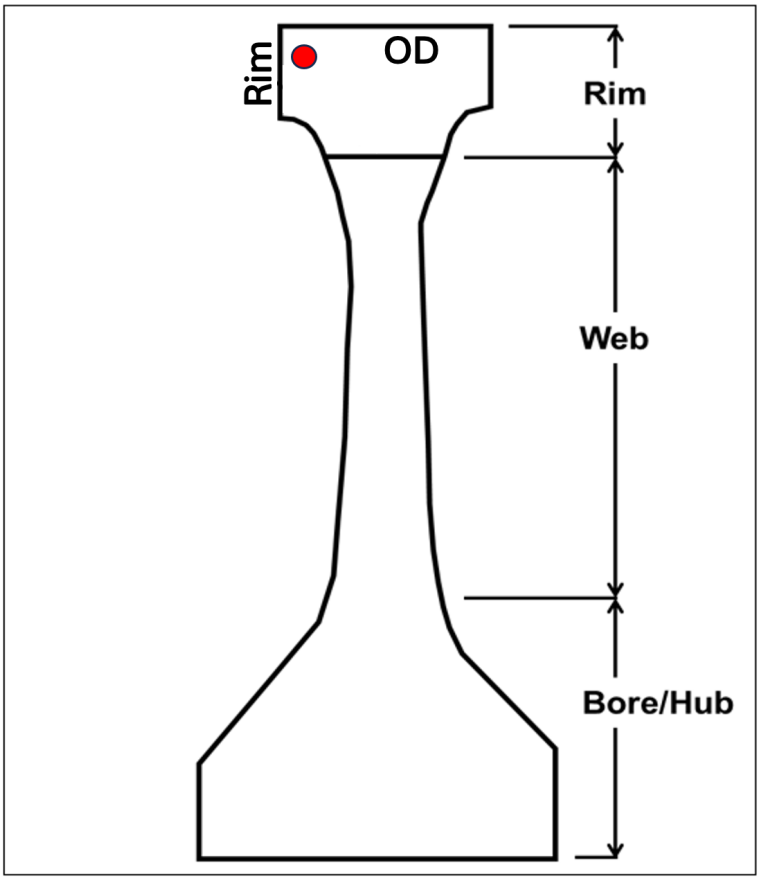

Figure 3.7. Disk 1 showing relevant UT scan regions (OD and Rim) and an indication at the approximate location marked by the red circle.

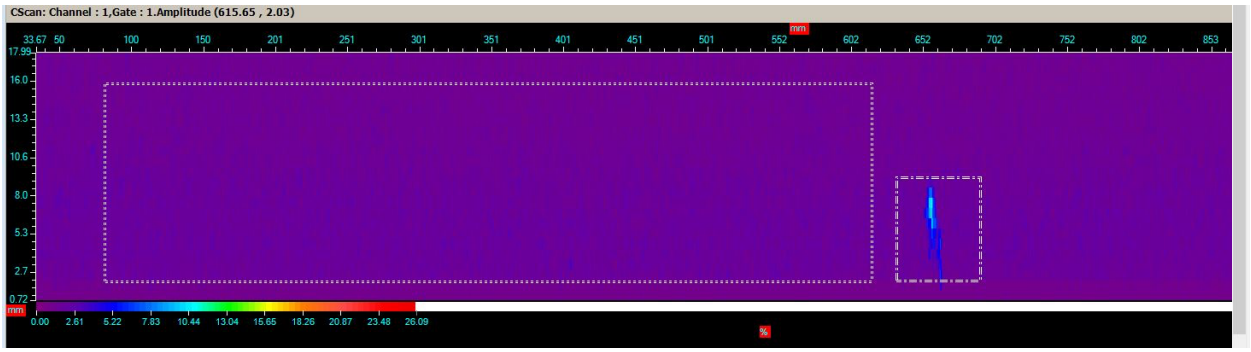

Figure 3.8 C- Scan image of the Disk 1 indication using 45° shear wave.

3.4.2 Results

Detailed results of the standard investigative scans of the OD region are given in the Appendix Table B-4.4 and the results of the five scans having the highest SNR and amplitude are shown in Table 3.6 and Table 3.7. Amplitudes are referenced to Calibrations of #1 FBH =80% for Longitudinal wave scans, and .020" (.5 mm) SDH =80% for shear wave scans.

Table 3.6 Disk 1, Surface Rim, Scan summary

Frequency	Angle	Mode	Direction	Focus	% Amp	Mean Noise	SNR
5 MHz	20°	Long	FWD	Surf	16%	3.4%	4.9
5 MHz	20°	Long	Aft	Surf	20%	3.4%	4.7
10 MHz	20°	Long	CW	Surf	13%	3.5%	2.8
10 MHz	20°	Long	CCW	Surf	13%	3.5%	2.6
5 MHz	45°	Shear	CW	Surf	3.5%	1.2%	2.5

Table 3.7 Disk 1, Surface OD, Scan summary

Frequency	Angle	Mode	Direction	Focus	% Amp	Mean Noise	SNR
10 MHz	45°	Shear	Rad/Ax	Surf	12%	1.7%	5.4
10 MHz	45°	Shear	CCW	Surf	6%	1.3%	5.3
10 MHz	45°	Shear	CW	Surf	5%	1.2%	5.0
5 MHz	45°	Shear	CCW	Surf	3.5%	1.2%	4.1
5 MHz	45°	Shear	CW	Surf	3.5%	1.2%	4.0

The location of this indication was pinpointed using a high-resolution UT scan. The disk was then cut into a cube and polished for a photomicrograph, as shown in Figure 3.9. This indication was determined to be a Coarse Grain Structure (CGS) area, approximately 0.12” X 0.12” X 0.08” (3mm x 3mm x 2mm), classified as ASTM Class 1.5.

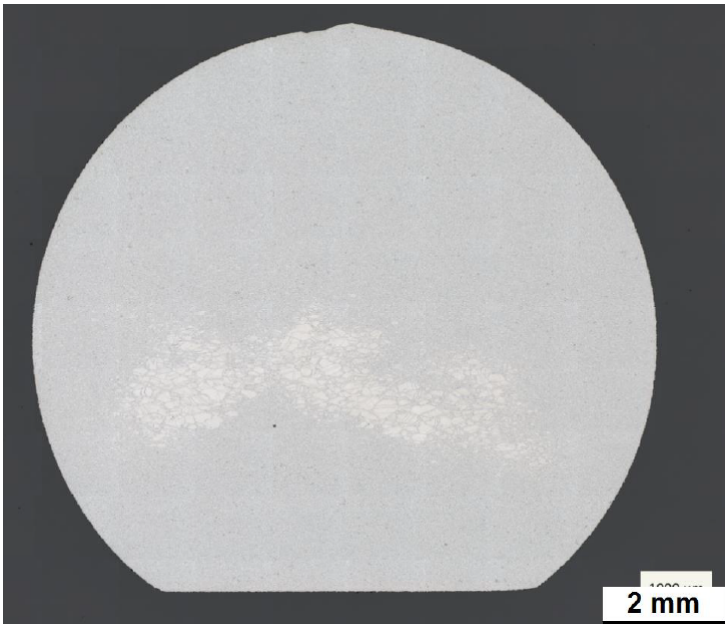

Figure 3.9 Photomicrograph of Disk 1 indication showing a cluster of large grains.

3.4.3 Conclusion

Disk 1 provided evidence that for this anomaly type, a cluster of large grains, 10 MHz and 5MHz, 20° Longitudinal and 45° shear inspections generally provided the maximum amplitude and SNR response.

3.5 Ultrasonic Inspection of Disk 2

3.5.1 Background

One OEM identified Disk 2 as having an indication of interest, located as shown in Figure 3.10. The red circle marks the location of the indication, and the relevant scan regions of the disk are labeled as B,C and D. The C-scan image of the indication is shown in Figure 3.11.

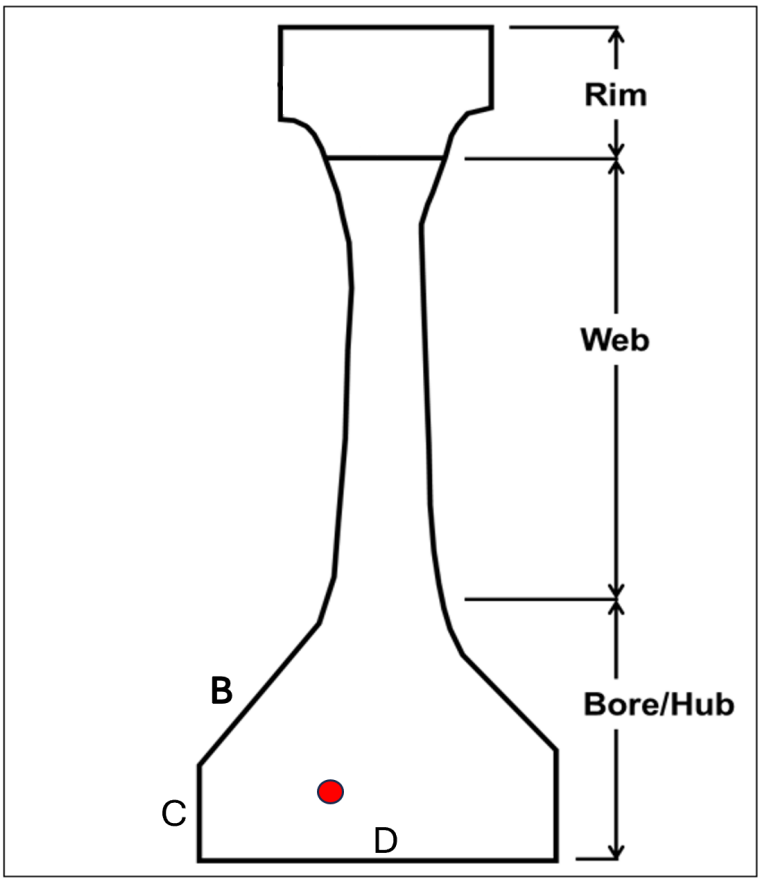

Figure 3.10 Disk 2 with relevant UT scan regions B, C, and D, showing an indication at the approximate location marked by the red circle.

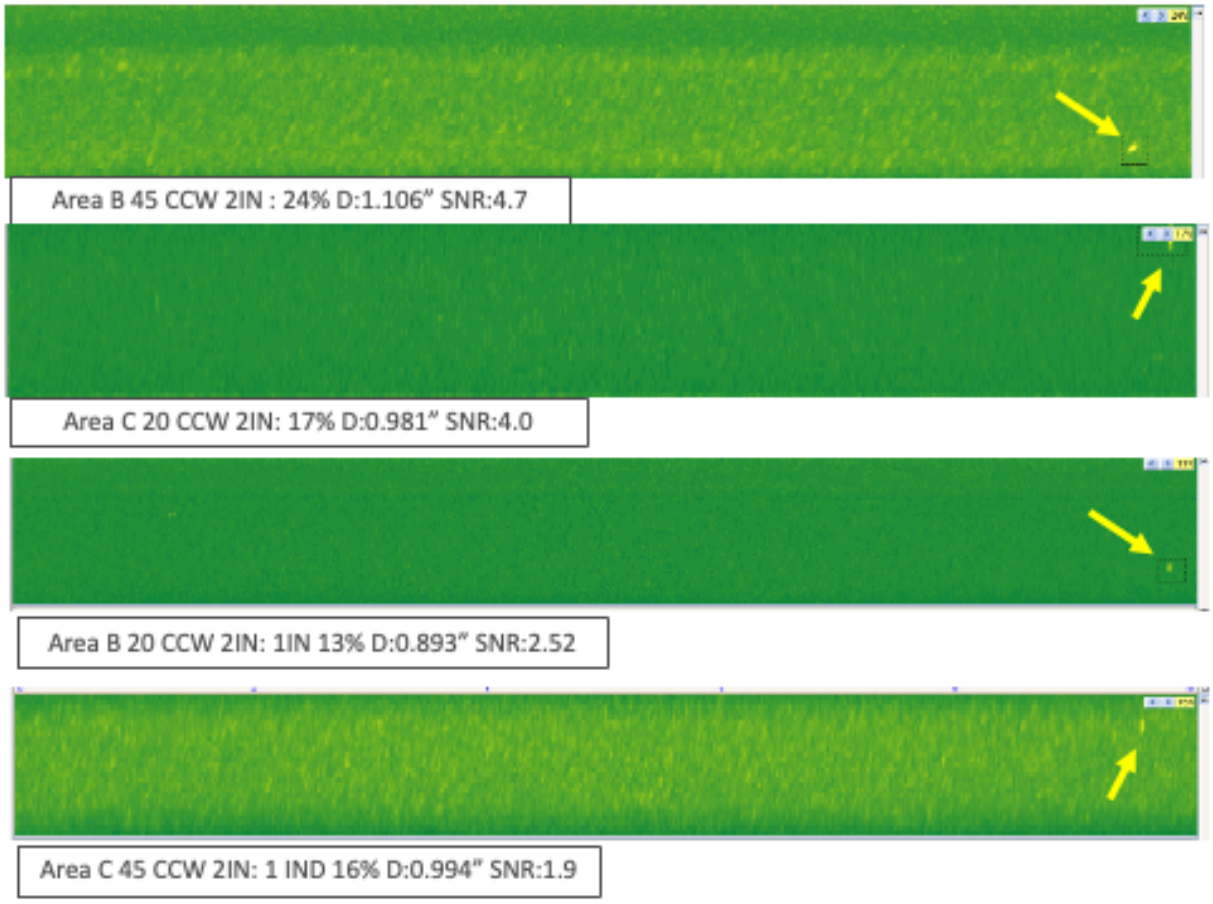

Figure 3.11 C- Scan images of the Disk 2 indication.

3.5.2 Results

The only scans which were able to detect this indication in Disk 2 are those shown in Figure 3.11, with the SNR values displayed within the figure. Amplitudes are referenced to Calibrations of #2 FBH =80% + 12 dB for Longitudinal wave scans (5 MHz, 20°), and .020" (.5 mm) SDH =80% + 12 dB for 45° shear wave scans.

The location of this indication was pinpointed using a high-resolution UT scan, as shown in Figure 3.12 (a). The disk was then cut into a cube and polished along the orange dashed line for a photomicrograph, shown in Figure 3.12 (b). The indication was determined to be a clean void.

(a)

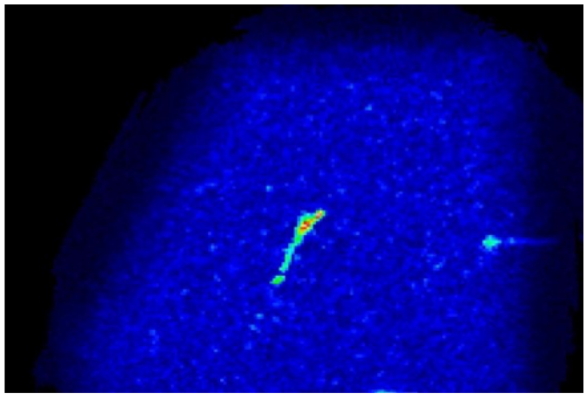

Polish plane is parallel to page

(b)

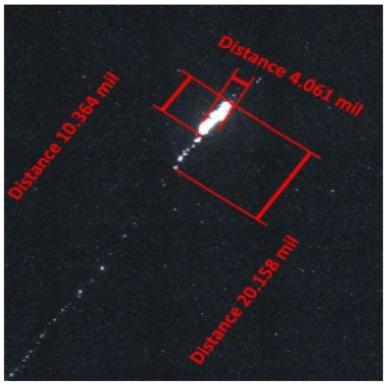

Clean Voids

Figure 3.12 High-resolution image of the Disk 2 indication (a). Polished indication showing a clean void (b).

3.5.3 Conclusion

Disk 2 provided evidence that for this anomaly type, a series of clean voids, 5MHz 45° shear and 20° longitudinal beams provided the maximum amplitude and SNR response.

3.6 Ultrasonic Inspection of Disk 3

3.6.1 Background

One OEM identified Disk 3 as having an indication of interest, located as shown in Figure 3.13. The red circle marks the location of the indication, and the relevant scan regions of the disk are labeled as “OD” and “Rim”. A C-scan image of the indication is shown in Figure 3.14.

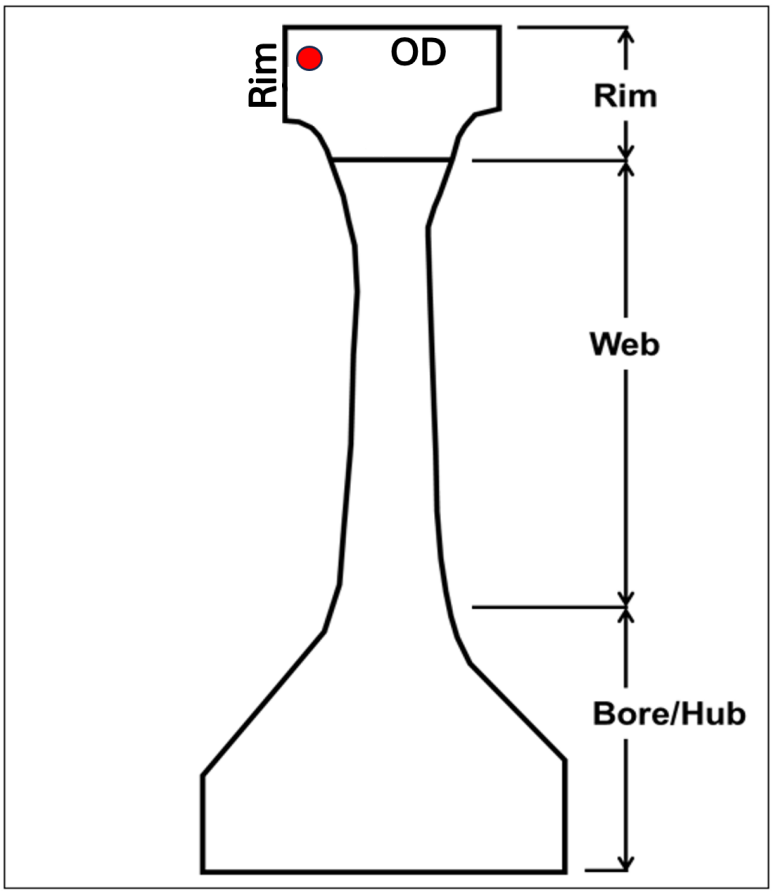

Figure 3.13 Disk 3 with relevant UT scan regions labeled as OD and Rim, showing an indication at the approximate location marked by the red circle.

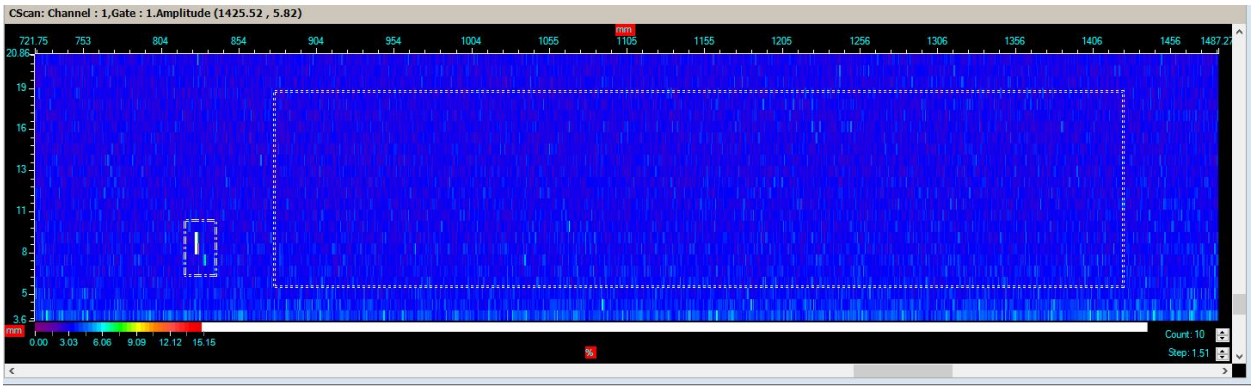

Figure 3.14 C- Scan images of the Disk 3 indication using 10 MHz, 0° longitudinal scan

3.6.2 Results

Detailed results of the standard investigative scans of region OD are provided in the Appendix Table B-4.5. The results of the five scans having the highest SNR and amplitude are summarized in Table 3.8 and Table 3.9. Amplitudes are referenced to Calibrations of #1 FBH =80% for Longitudinal wave scans and .020" (.5 mm) SDH =80% for shear wave scans.

Table 3.8 Scan summary for Disk 3 - Surface Rim.

Frequency	Angle	Mode	Direction	Focus	% Amp	Mean Noise	SNR
10 MHz	0°	Long	NA	Surf	27%	3.1%	11.0
10 MHz	20°	Long	CW	Surf	42%	3.3%	10.9
5 MHz	20°	Long	CW	Surf	18%	3.4%	5.6
10 MHz	20°	Long	CCW	Surf	41%	3.5%	5.2
10 MHz	45°	Shear	CW	Surf	9.4%	2.8%	2.7

Table 3.9 Scan summary for Disk 3 - Surface OD.

Frequency	Angle	Mode	Direction	Focus	% Amp	Mean Noise	SNR
10 MHz	0°	Long	NA	Surf	27%	5.5%	10.0
5 MHz	0°	Long	NA	Surf	27%	5.5%	10.0
5 MHz	20°	Long	CW	Surf	24%	3.4%	9.2
10 MHz	20°	Long	CW	Surf	24%	3.4%	7.3
5 MHz	20°	Long	CCW	Surf	27%	3.6%	6.9

The location of this indication was pinpointed using micro–CT X-Ray, as shown in Figure 3.15 (a). The disk was then cut into a cube and polished for a photomicrograph, shown in Figure 3.15 (b). The indication was determined to be a voided inclusion.

(a) (b)

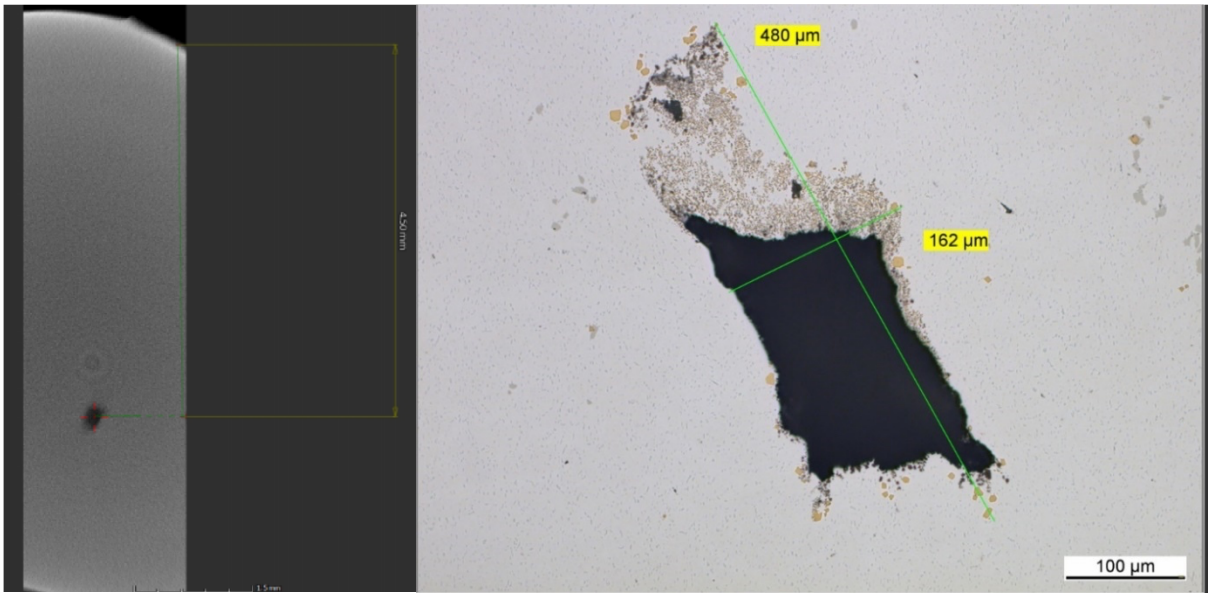

Figure 3.15 High-resolution image of the Disk 3 indication. (a) Micro-CT image of the indication showing void and (b) Metallography results, revealing a voided inclusion with void length of approximately 300µm.

3.6.3 Conclusion

Disk 3 provided evidence that for this anomaly type, a voided inclusion, 5 MHz and 10 MHz, 0° and 20° longitudinal inspections provided the maximum amplitude and SNR response.

3.7 Ultrasonic Inspection of Disk 4

3.7.1 Background

One OEM identified Disk 4 as having an indication of interest, located as shown in Figure 3.16. The pink cross marks the location of the indication, and the relevant scan regions of the disk are labeled as UA, UB, UC, and UE. The parameters used for the planned C-scans are shown in Table 3.10. Due to location of the indication and part geometry, not all scans could be performed. One Characteristic C-scan of this indication is shown in Figure 3.17.

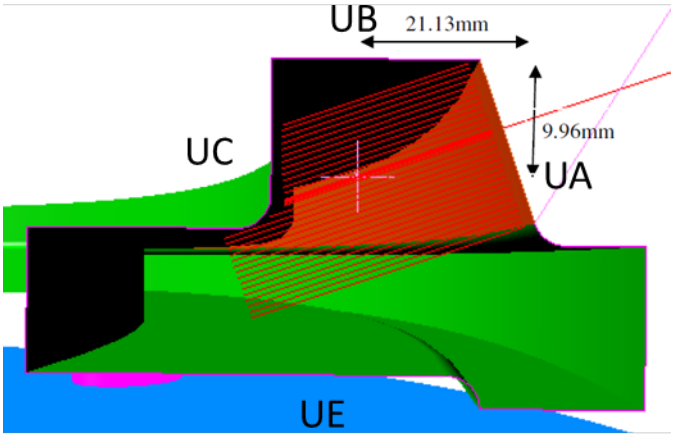

Figure 3.16 Cross-section of Disk 4. The relevant UT scan regions are UA, UB, UC, and UE. The pink cross shows the approximate location of the indication.

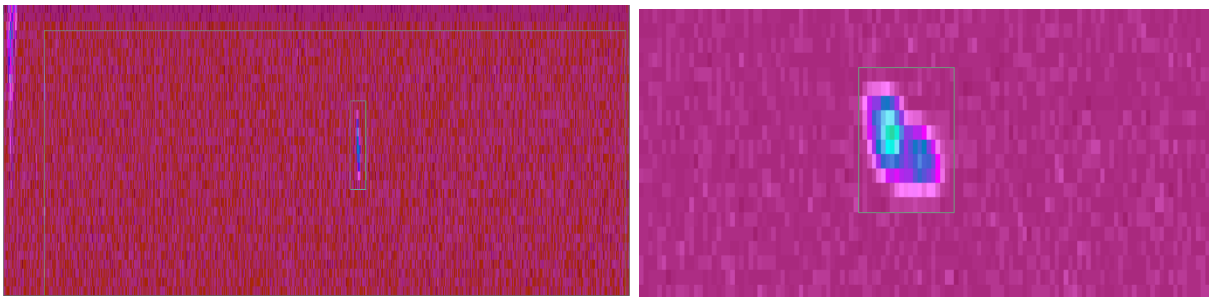

Figure 3.17 Disk 4, C-scan image of the indication detected from the UE region using 45-deg circumferential shear surface focusing using 10 MHz probe.

Table 3.10 Inspection conditions for UA, UB, UC, and UE regions.

Frequency, Water Path & focal Length	**Incidence Angle, Mode**	**Direction**	**NSR**	**UA**	**UB**	**UC**	**UE**	**Calibration**
				Depth	**Depth**	**Depth**	**Depth**	
10 MHz, 3.15" (80mm), 3" (76mm)	0°, Long	None	1.6mm	41.1mm	38.1mm	34mm	41.1mm	diam. 0.8 mm FBH
5 MHz, 4,72" (120mm), 6" (152mm)	+/- 19°, Shear	Rad/Ax					42mm	Gene diam 0.5 mm
		Circ	1.6mm	38.1mm	38.1mm	34mm	38.1mm	Gene diam 0.5 mm, +6dB

3.7.2 Results

Detailed results of the standard investigative scans of each region are provided in the Appendix Table B-4.6. The results of the scans with the highest SNR and amplitude for each region are shown in Table 3.11 through Table 3.14. Amplitudes are referenced to Calibrations of #2 FBH =80% for Longitudinal wave scans (5 & 10 MHz / 0° & 20°), .020" (.5 mm) SDH =80% for radial/axial shear wave scans (45°) and .020" (.5 mm) SDH =80% + 6dB for circumferential shear wave scans (45° & 65°). This indication was not metallographically evaluated, so the type of anomaly detected in this part remains unknown.

Table 3.11 Disk 4, UA Scan summary. The indication from this region is approximately 0.82" (21 mm) deep.

Frequency	Angle	Mode	Direction	Focus	% Amp	Mean Noise	SNR
10 MHz	20°	Long	CCW	Subs	280%	12.9%	35
5 MHz	20°	Long	CCW	Surf	96%	7.8%	21.3
5 MHz	45°	Shear	CCW	Subs	14%	2.0%	20.5
5 MHz	45°	Shear	CW	Subs	16%	2.4%	14.7
10 MHz	20°	Long	CW	Subs	120%	13.3%	13.4

Table 3.12 Disk 4, UB Scan summary. The indication from this region is approximately 0.67" (17 mm) deep.

Frequency	Angle	Mode	Direction	Focus	% Amp	Mean Noise	SNR
10 MHz	20°	Long	CCW	Subs	312%	18.8%	21.1
10 MHz	20°	Long	RI	Subs	144%	12.6%	17.0
5 MHz	20°	Long	CCW	Surf	89%	10.6	13.5
5 MHz	0°	Long	NA	Subs	34%	7.5%	10.8
10 MHz	45°	Shear	CCW	Surf	52%	9.4%	9.9

Table 3.13 Disk 4, UC Scan summary.

Frequency	Angle	Mode	Direction	Focus	% Amp	Mean Noise	SNR
5 MHz	20°	Long	CCW	Surf	71%	4.3%	40.5
5 MHz	20°	Long	CW	Surf	58%	6.7%	17.4
10 MHz	20°	Long	CCW	Surf	42%	6.7%	11.4
10 MHz	65°	Shear	CCW	Surf	18%	5.1%	7.9
5 MHz	0°	Long	NA	Surf	56%	14.1%	6.3

Table 3.14 Disk 4, UE Scan summary. The indication from this region is approximately 1.02" (26 mm) deep.

Frequency	Angle	Mode	Direction	Focus	% Amp	Mean Noise	SNR
5 MHz	45°	Shear	CCW	Subs	27%	3.1%	45.9
5 MHz	20°	Long	CCW	Subs	42%	3.3%	40.2
5 MHz	20°	Long	CCW	Surf	18%	3.4%	32.4
5 MHz	20°	Long	RO	Subs	41%	3.5%	20.4
10 MHz	45°	Shear	CCW	Surf	9.4%	2.8%	18.4

3.7.3 Conclusion

Disk 4 provided evidence that for this unknown anomaly type, a 5 MHz 20° longitudinal beam yielded the maximum amplitude and SNR response overall. However, various other scan configurations were highly effective when used from the four scan surfaces.

3.8 Ultrasonic Inspection of Disk 5

3.8.1 Background

One OEM identified Disk 5 as having an indication of interest, located as shown in Figure 3.18. The cross marks the location of the indication, and the relevant scan regions of the disk are labeled as UI, UJ, and UK. The C-scan image of the indication is presented in Figure 3.19 C-scan images of the Disk 5 indication from surface UI using a 0-deg longitudinal surface focusing using 10 MHz probe C-scan images of the Disk 5 indication from surface UI using a 0-deg longitudinal surface focusing using 10 MHz probe. The parameters used for the planned C-scans are detailed in Table 3.15.

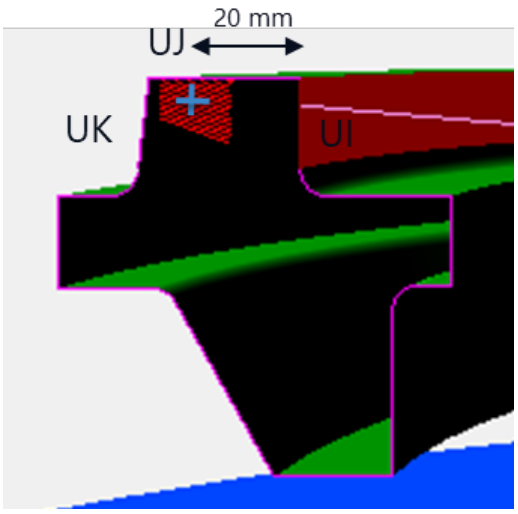

Figure 3.18 Disk 5 with relevant UT scan regions UI, UJ, and UK, showing an indication at the approximate location marked by the blue cross.

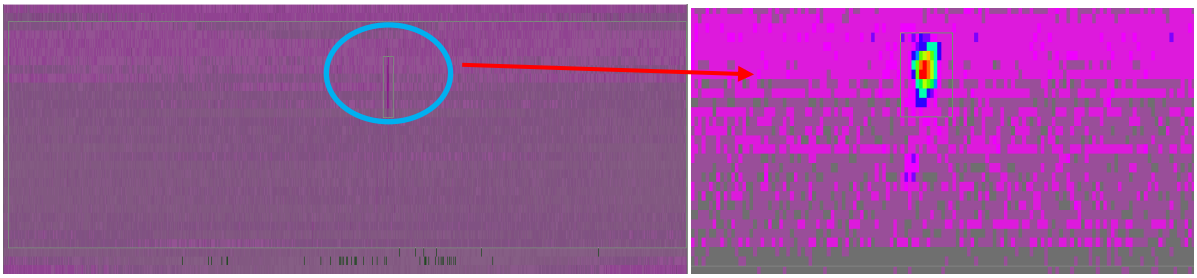

Figure 3.19 C-scan images of the Disk 5 indication from surface UI using a 0-deg longitudinal surface focusing using 10 MHz probe.

Table 3.15 Inspection conditions for UI, UJ, and UK regions.

Frequency, Water Path, Focal Length	Incidence Angle, Mode	Direction	UI		UJ		UK		Calibration
			NSR	Depth	NSR	Depth	NSR	Depth	
10 MHz, 3.15" (80mm), 3" (76mm)	0°, Long	None			1.6mm	38.1mm			diam. 0.8 mm FBH
	1.5°, Long	Rad/Ax	2.5mm	39mm			1.6mm	28.6mm	diam. 0.8 mm FBH +1dB

	5°, Long	Rad/Ax			2.5mm	44.5mm			diam. 0.8 mm FBH + 3dB
5 MHz, 4,72" (120mm), 6" (152mm)	+/- 19°, Shear	Rad/Ax							diam 0.5 mm
		Circ	1.6mm	38.1mm	1.6mm	38.1mm	1.6mm	38.1mm	diam 0.5 mm, +6dB

3.8.2 Results

The indication was detected only from surface UI. Detailed results of the standard investigative scans of region UI are provided in Appendix Table B-4.7, and the results of the four scans with the highest SNR and amplitude are shown in Table 3.16. Amplitudes are referenced to Calibrations of #2 FBH =80% for Longitudinal wave scans (5 & 10 MHz / 0° & 20°), .020" (.5 mm) SDH =80% for radial/axial shear wave scans (45°) and .020" (.5 mm) SDH =80% + 6dB for circumferential shear wave scans (45° & 65°).This indication was not metallographically evaluated, so the type of anomaly detected in this part remains unknown.

Table 3.16 Disk 5, UI Scan summary. The indication from this region is approximately 0.79" (20 mm) deep.

Frequency	Angle	Mode	Direction	Focus	% Amp	Mean Noise	SNR
10 MHz	0°	Long	NA	Surf	16.9%	4.3%	4.5
10 MHz	6°	Long	Aft	Surf	14.9%	3.4%	3.1
5 MHz	0°	Long	NA	Surf	12.2%	4.9	2.5
5 MHz	0°	Long	NA	Subs	21.2%	7.1%	2.3

3.8.3 Conclusion

Disk 5 provided evidence that for this unknown anomaly type, a 5 and 10 MHz 0° longitudinal beam provided the maximum amplitude and SNR response overall. The 20° longitudinal and 45° shear scans were unable to detect this indication.

3.9 Ultrasonic Inspection of Disk 6

3.9.1 Background

One OEM identified Disk 6 as having an indication of interest, with its C-scan image shown in Figure 3.20. The yellow box marks the location of the indication and only this surface (surface 1) was inspected.

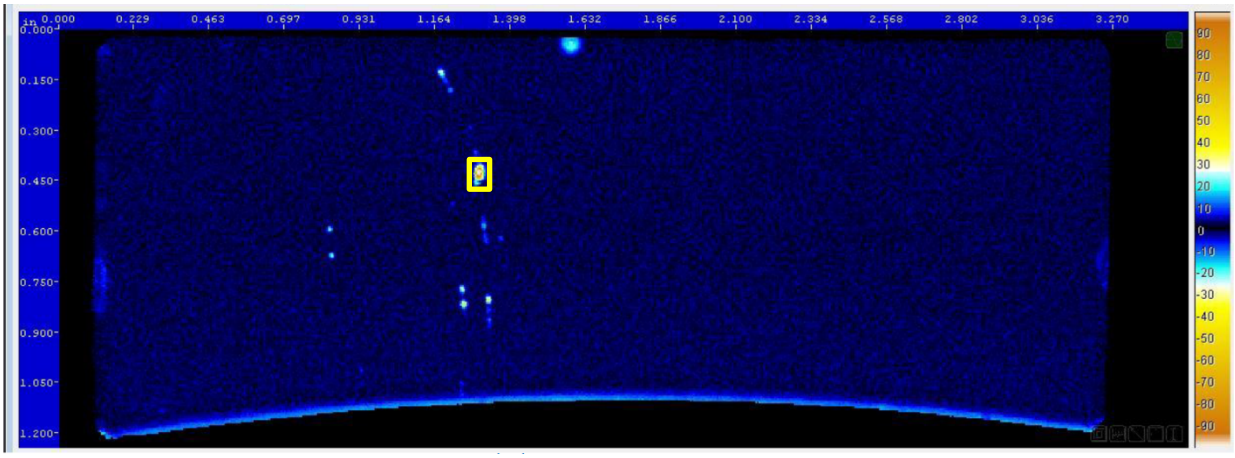

Figure 3.20 High-resolution C- Scan images of the Disk 6 indication: 50MHz PVDF ultrasonic probe with 50mm focal length and a diameter of 6.0 mm. The probe has an effective beam diameter of 0.075mm. Note that only the indication in the yellow box was detectable with any of the scans in the Tables in the Appendix.

3.9.2 Results

The indication was only inspected from surface 1, but multiple OEMs performed these inspections. Detailed results from the two OEMs who performed the most exhaustive set of scans are provided in Appendix Table B-4.8. The results of the three scans with the highest SNR and amplitude for both OEMs are shown in Table 3.17. For OEM 4 scans, amplitudes are referenced to Calibrations of #1 FBH =80% for Longitudinal wave scans, and .020" (.5 mm) SDH =80% for shear wave scans.

A high-resolution CT X-Ray was performed on this sample, and a high-density indication was detected, as shown in Figure 3.21. This indication was not metallographically evaluated, so the type of anomaly detected in this part remains unknown.

Table 3.17 Disk 6, Surface 1 scan summary.

Frequency	Angle	Mode	Direction	Focus	% Amp	Mean Noise	SNR
OEM 1							
10 MHz	20°	Long	CCW	Surf	41%	3.7%	13.7
5 MHz	20°	Long	CCW	Subs	25%	3.7%	6.4
5 MHz	20°	Long	Rad In	Surf	32%	4.5%	5.4
OEM 4							
5 MHz	0°	Long	NA	Surf	65%		6.5
10 MHz	20°	Long	CW	Surf	40%		4.8
5 MHz	45°	Shear	CCW	Surf	44%		4.3

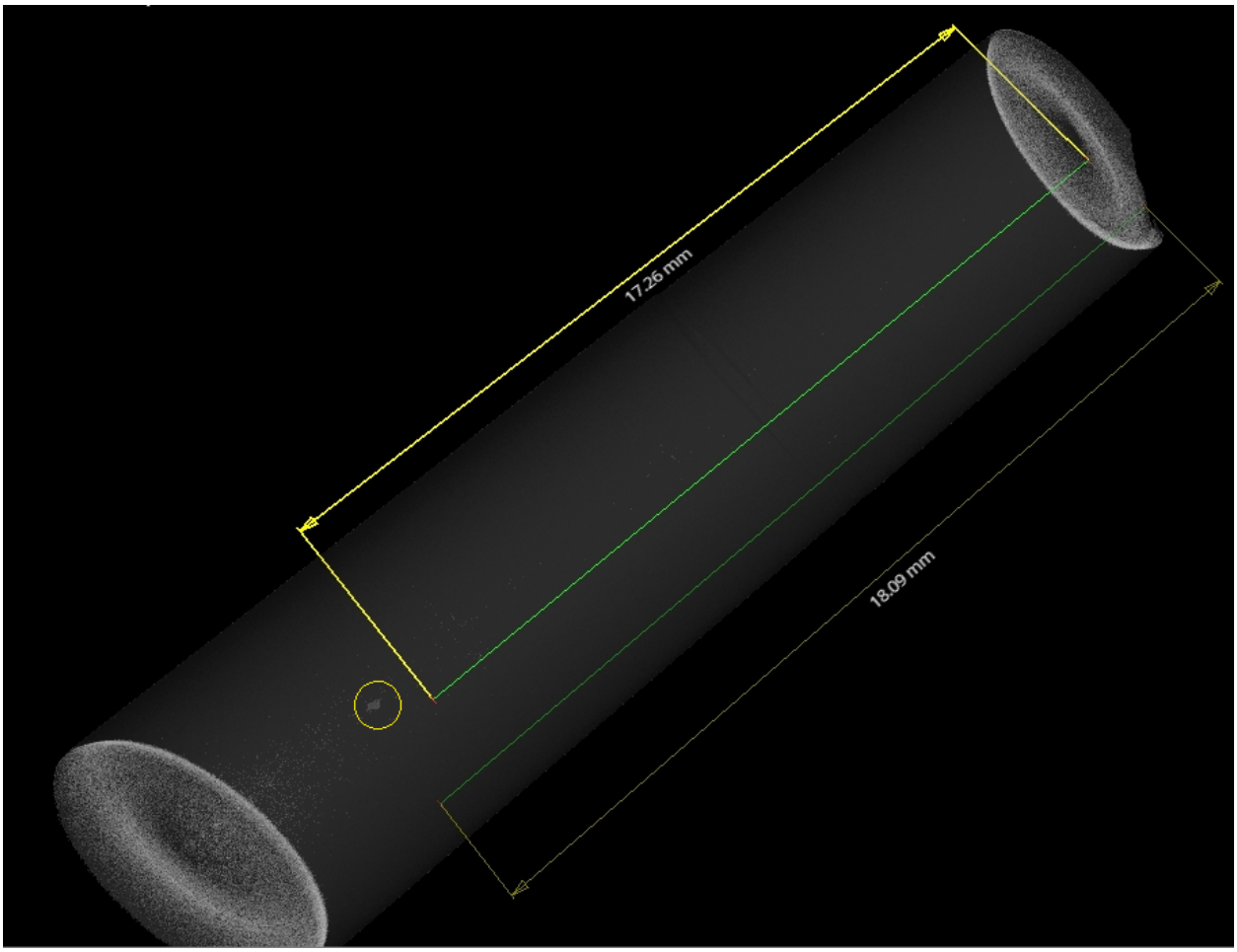

Figure 3.21 CT X-Ray of indication in Disk 6. The indication is highlighted within the yellow circle.

3.9.3 Conclusion

Disk 6 provided evidence that for this unknown anomaly type, 5 and 10 MHz 20° longitudinal beams yielded the maximum amplitude and SNR response overall.

3.10 Ultrasonic Inspection of Disk 7

3.10.1 Background

One OEM identified Disk 7 as having an indication of interest, located in the disk web, approximately 0.25 inches (6mm) beneath the nearest web surface. Figure 3.22 shows a basic schematic of Disk 7, with the red circle showing the location of the indication.

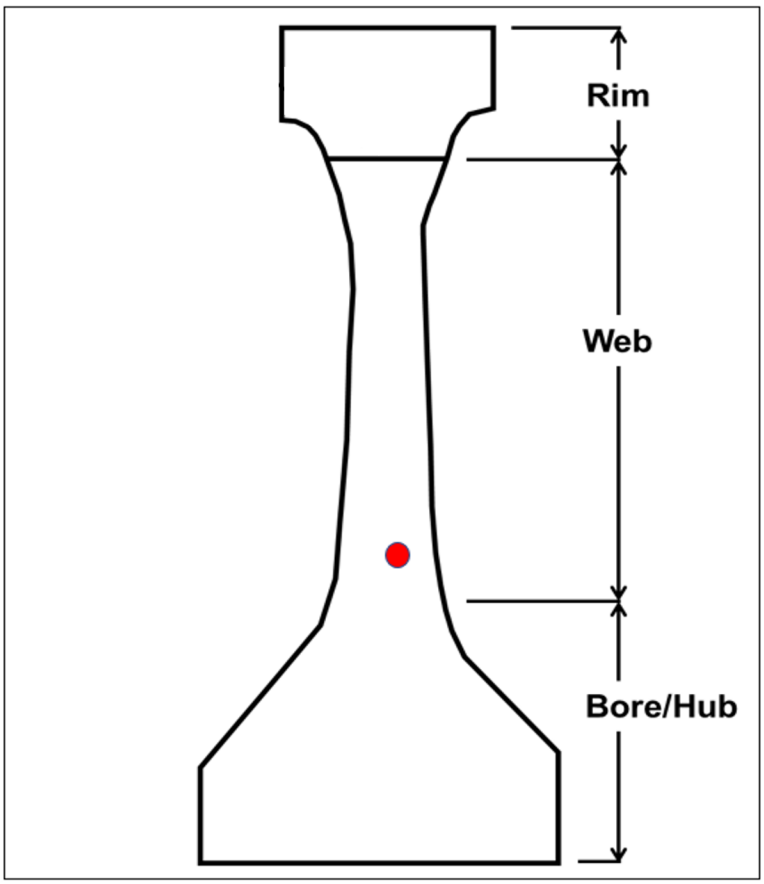

Figure 3.22 Disk 7 with UT scan region labeled "Web" and an indication at the approximate location marked by the red circle.

The indication was originally detected using a 5 MHz probe with a 6" (152mm) focal length, 0.75" (19mm) diameter, 6" (152mm) water path. The sound beam used was a 45° refracted shear wave

oriented in a circumferential direction. The ultrasonic amplitude of the indication was 13%, based on the following calibration: 0.020" (0.5mm) Side Drilled Hole (SDH) = 80%, then add 12dB. Figure 3.23 shows the C scan image of the indication.

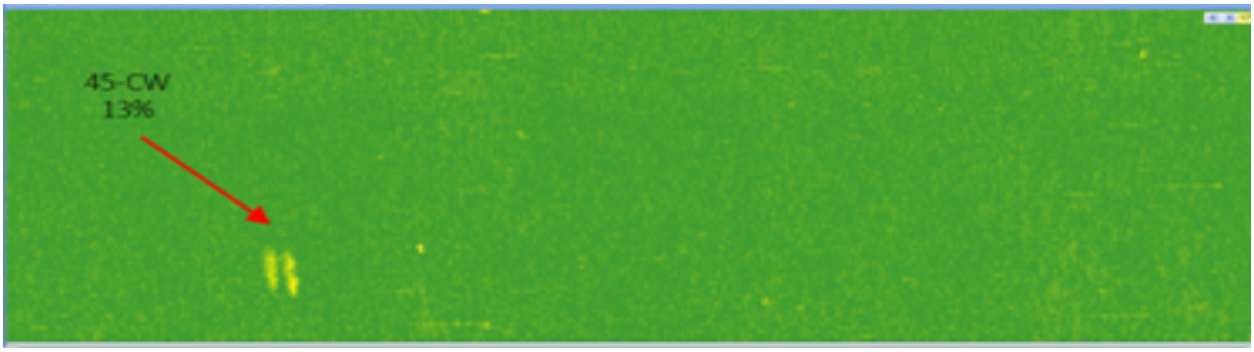

Figure 3.23 C-Scan image of the indication in Disk 7.

3.10.2 Results

The results of the standard investigative scans of the web region of Disk 7 were ranked for effectiveness based on the SNR, which was calculated using the following equation:

$$SNR = \frac{Peak\ Signal - Mean\ noise}{Peak\ noise - Mean\ noise}$$

Table 3.18 shows the results of the scans, representative of the full set. Amplitudes are referenced to Calibrations of #2 FBH =80% for Longitudinal wave scans (5 & 10 MHz / 0° & 20°), and .020" (.5 mm) SDH =80% + 6dB for 45° shear wave scans.

It is clear that the 45° shear scans, both at 5 and 10 MHz, offered superior detection, while the longitudinal scans offered significantly weaker responses.

Table 3.18 Highlighted Disk 7 scans ranked using SNR criteria.

Frequency	Incident Angle	Refracted Angle	Mode	Direction	SNR
10 MHz	20	45	Shear	RO	16.84
5 MHz	20	45	Shear	RI	12.51
10 MHz	5	20	Long	UNK	6.52
5 MHz	10	45	Long	CCW	4.61
5 MHz	10	45	Long	RI	2.37

The results from the full set of scans of Disk 7 are provided in Appendix B, Table B-4.9.

The Disk 7 indication was cut through its center and polished. The photomicrograph, shown in Figure 3.24., reveals the indication characterized as an uncracked/un-voided Dirty White Spot in Inconel 718 material. The dimensions of this plane of the indication are 397.52 by 73.01 mils, (10.1 mm by 1.9 mm).

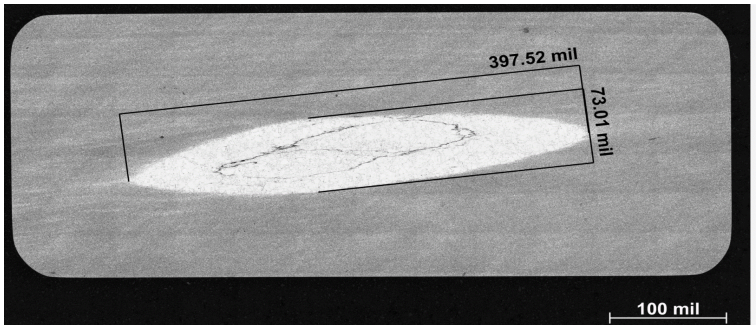

Figure 3.24 Photomicrograph of Disk 7 indication, showing an uncracked and un-voided Dirty White Spot.

3.10.3 Conclusion

This exercise provided evidence that, for this anomaly type, an uncracked/un-voided dirty white spot, 10 MHz and 5MHz 45° shear inspections yielded the maximum amplitude and SNR response.

3.11 Ultrasonic Inspection of Disk 8

3.11.1 Background

One OEM identified Disk 8 as having an indication of interest, located as shown in Figure 3.25. The red circle marks the location of the indication, and the scan regions of the disk are labeled as B, C1, C2, and D. The C-scan image of the indication is shown in Figure 3.26.

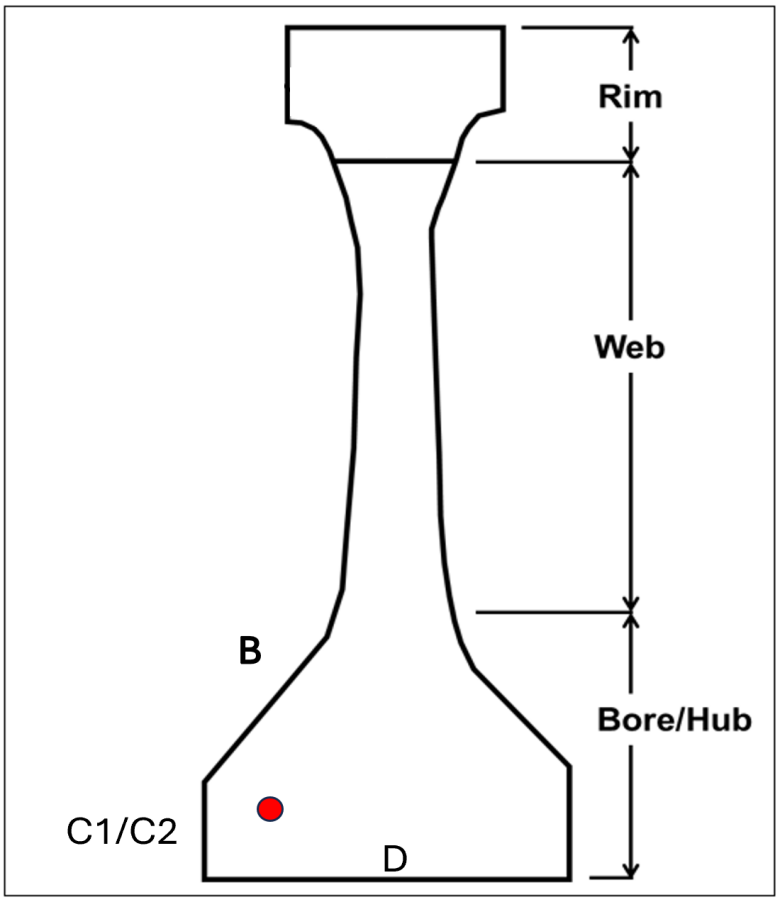

Figure 3.25 Disk 8 with UT scan regions B, C1, C2, and D, showing an indication at the approximate location marked by the red circle.

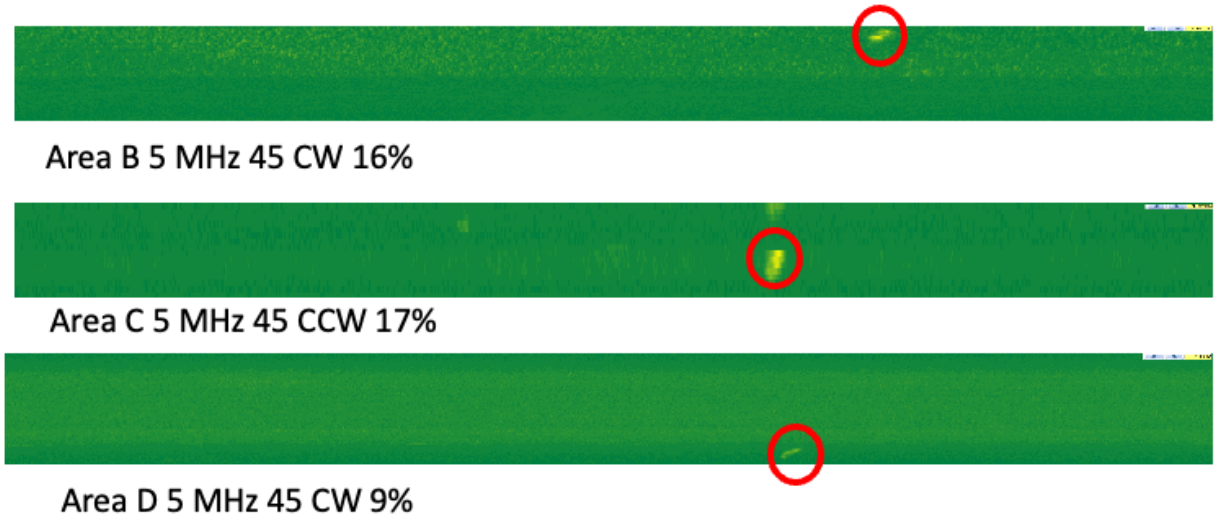

Figure 3.26 C- Scan images of the Disk 8 indication.

3.11.2 Results

Detailed results of the standard investigative scans of each region B, C1, C2, and D are given in Appendix Table B-4.10. The results of the five scans with the highest SNR and amplitude are shown in Table 3.19 to Table 3.22. Amplitudes are referenced to Calibrations of #2 FBH =80% for Longitudinal wave scans (5 & 10 MHz / 0° & 20°), and .020" (.5 mm) SDH =80% + 6dB for 45° shear wave scans.

Table 3.19 Disk 8, Surface B - Scan summary.

Frequency	Angle	Mode	Direction	Focus	AMP %	Max Noise	Noise avg.	Noise Std.	SNR
10 MHz	45	Shear	CCW	Subs	26	4	2.8	0.5	19.3
5 MHz	45	Shear	RI	Surf	10	2	1.4	0.5	14.3
5 MHz	45	Shear	CW	Subs	12	2	1.1	0.3	12.1
5 MHz	45	Shear	CCW	Subs	10	2	1.1	0.3	9.9
10 MHz	45	Shear	CW	Subs	23	5	2.9	0.5	9.6

Table 3.20 Disk 8, Surface C1 - Scan summary.

Frequency	Angle	Mode	Direction	Focus	AMP%	Max Noise	Noise avg.	Noise Std.	SNR
5 MHz	45	Shear	CCW	Subs	9	2	1	0.1	8
5 MHz	45	Shear	CW	Subs	8	2	1	0.1	7
10 MHz	0	Long		Subs	26	9	5.6	1.3	6
10 MHz	45	Shear	CCW	Surf	12	5	3.5	0.6	5.7
10 MHz	20	Long	CW	Surf	6	3	2	0.2	4

Table 3.21 Disk 8, Surface C2 - Scan summary.

Frequency	Angle	Mode	Direction	Focus	AMP%	Max Noise	Noise avg.	Noise Std.	SNR
10 MHz	45	Shear	CCW	Subs	48	5	2.9	0.5	21.5
5 MHz	45	Shear	CCW	Subs	17	2	1.1	0.2	17.7
5 MHz	45	Shear	CW	Subs	13	2	1.1	0.2	13.2
10 MHz	20	Long	CW	Subs	24	5	3.3	0.5	12.2
10 MHz	45	Shear	CW	Subs	46	7	3.2	0.7	11.3

Table 3.22 Disk 8, Surface D - Scan summary.

Frequency	Angle	Mode	Direction	Focus	AMP%	Max Noise	Noise avg.	Noise Std.	SNR
5 MHz	45	Shear	Aft	Surf	18	3	1.8	0.4	13.5
10 MHz	45	Shear	Aft	Surf	15	4	2.7	0.5	9.5
10 MHz	20	Long	CW	Surf	15	8	5.3	0.7	3.6
10 MHz	20	Long	CCW	Surf	15	9	6.5	0.8	3.4
10 MHz	45	Shear	CCW	Surf	8	4	2	0.3	3.0

The location of this indication was pinpointed using a high-resolution UT scan as shown in Figure 3.27(a). The disk was then cut into a cube and polished for a photomicrograph, shown in Figure 3.27(b). Metallurgical analysis showed that the indication is a Dirty White Spot (DWS) with dimensions approximately 0.65” X 0.08“ (16.3 mm X 2 mm).

(a) (b)

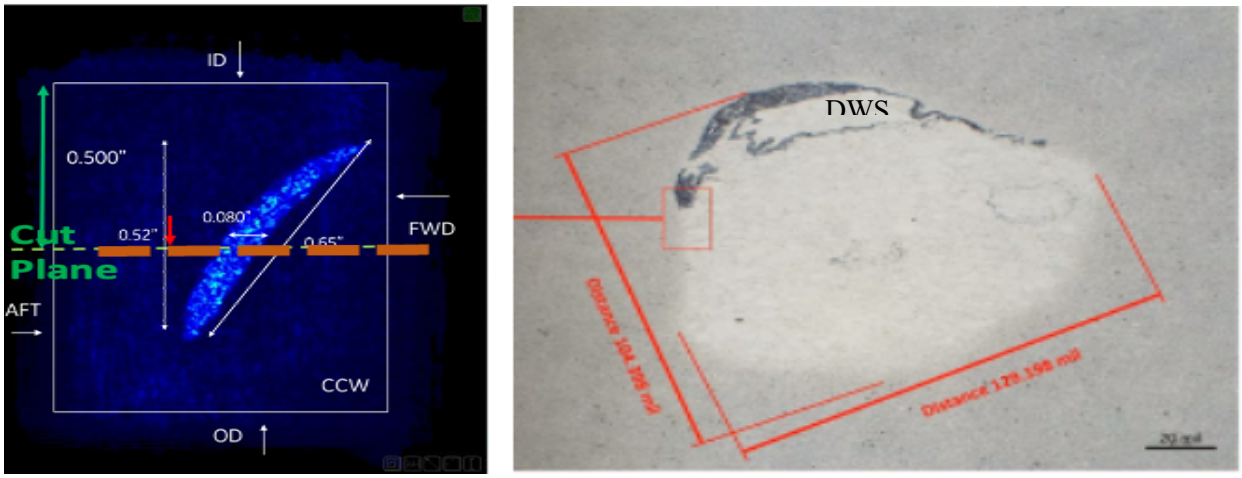

Figure 3.27 High-resolution image of the Disk 8 indication (a). After cutting and polishing along the orange dotted line, the photomicrograph (b) reveals that this is a dirty white spot in In718.

3.11.3 Conclusion

Similar to the results for Disk 7, Disk 8 provided evidence that for this anomaly - an uncracked/unvoided Dirty White Spot - 10 MHz and 5MHz 45° shear inspections generally yielded the maximum amplitude and SNR response.

3.12 Ultrasonic Inspection of Disk 9 Indication #1

3.12.1 Background

One OEM identified Disk 9 as having an indication of interest, located as shown in Figure 3.28. The red circle represents the location of the indication, and the relevant scan regions of the disk are labeled as D and E. The C-scan image of the indication is shown in Figure 3.29.

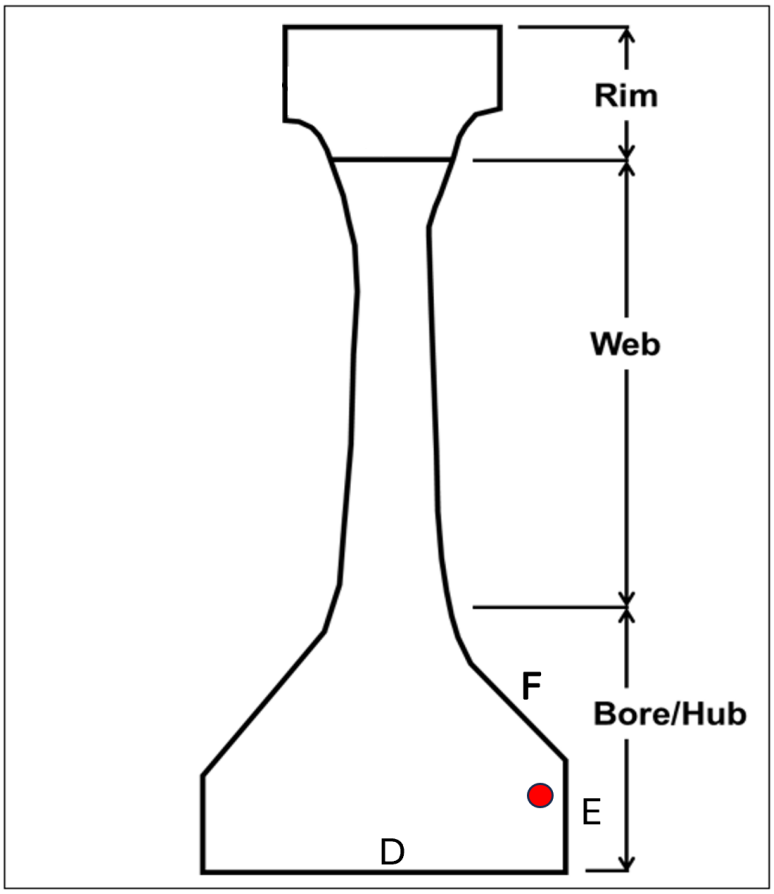

Figure 3.28 Disk 9 showing relevant UT scan regions D and E, with an indication at the approximate location marked by the red circle.

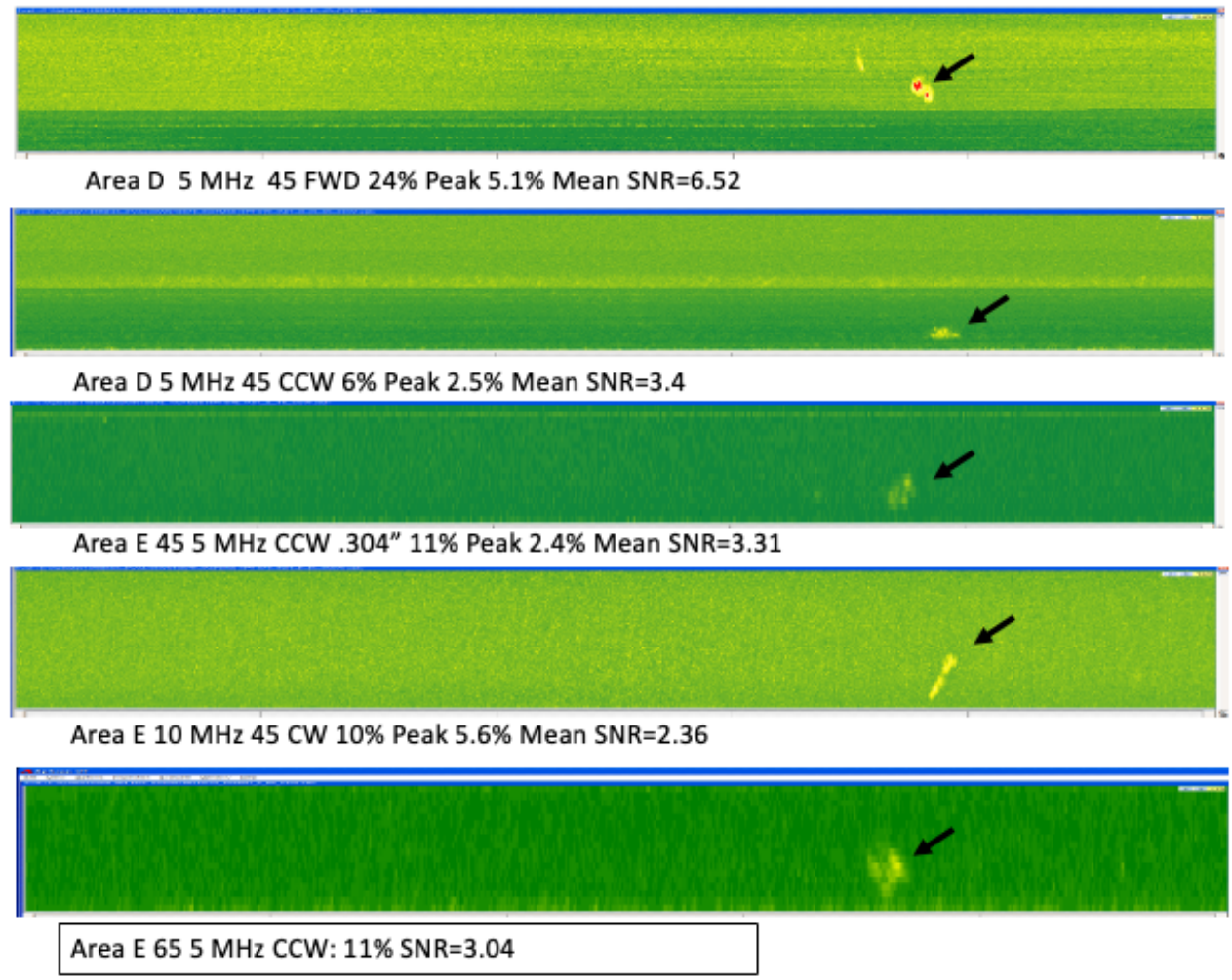

Figure 3.29 C- Scan images of the Disk 9 indication.

3.12.2 Results

Detailed results of the standard investigative scans of each region D and E are provided in Appendix Table B-4.11, with the highest SNR results summarized in Table 3.23 and Table 3.24 below. As with previous parts, the results are sorted by SNR. Amplitudes are referenced to calibrations of #2 FBH =80% for Longitudinal wave scans (5 & 10 MHz / 0° & 20°), and 0.020" (.5 mm) SDH =80% + 6dB for 45° shear wave scans.

Table 3.23 Scan summary for Disk 9 Surface D.

Frequency	Angle	Mode	Direction	Focus	% Amp	Mean Noise	SNR
5 MHz	45	Shear	FWD	Surf	24%	5.10%	6.52
5 MHz	45	Shear	Aft	Surf	20%	3.20%	4.42
5 MHz	45	Shear	CW	Surf	13%	2.20%	3.86
5 MHz	45	Shear	CCW	Surf	6%	2.50%	3.4
10 MHz	20	Long	CW	Surf	9%	2.60%	1.88

Table 3.24 Scan summary for Disk 9 Surface E.

Frequency	Angle	Mode	Direction	Focus	% Amp	Mean Noise	SNR
5 MHz	65	Shear	CW	Surf	12%	2.10%	3.41
10 MHz	65	Shear	CCW	Surf	24%	4.00%	3.33
5 MHz	45	Shear	CCW	Surf	11%	2.40%	3.31
5 MHz	65	Shear	CCW	Surf	11%	1.70%	2.82
10 MHz	65	Shear	CW	Surf	19%	3.40%	2.79

The location of this indication was pinpointed using a high-resolution UT scan as shown in Figure 3.30(a). The disk was then cut into a cube and polished along the orange dashed line for a photomicrograph, shown in Figure 3.30 (b). Metallurgical analysis showed that the indication is a Dirty White Spot (DWS).

(a)

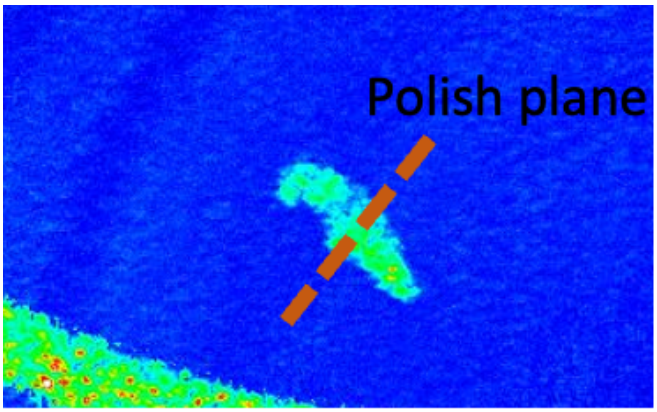

(b)

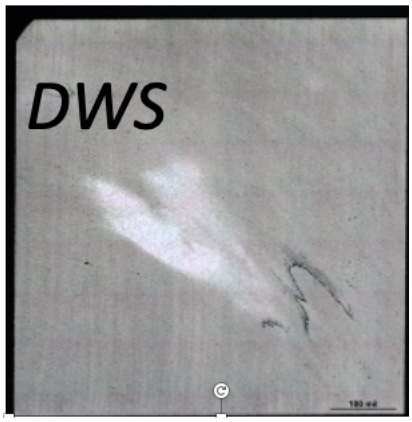

Figure 3.30 High-resolution image of the Disk 9 indication (a), and metallographic view identifying the indication as a diffuse dirty white spot (b).

3.12.3 Conclusion

Similar to the results from Disk 7 and 8, Disk 9 provided evidence that for this anomaly type, an uncracked/un-voided dirty white spot, 10 MHz and 5MHz 45° shear inspections generally yielded the maximum amplitude and SNR response.

3.13 Ultrasonic Inspection of Disk 9 Indication #2

3.13.1 Background

One OEM identified Disk 9 as having a second indication of interest, located as shown in Figure 3.31. This indication is very close to disk 9 indication#1 and can be seen in first C-scan image Figure 3.29. Similarly, both indications are seen in figure 3.32. The red circle represents the location of the indication and the relevant scan regions of the disk are labeled as D and E. All the C-scan images which show the indication are in Figure 3.32.

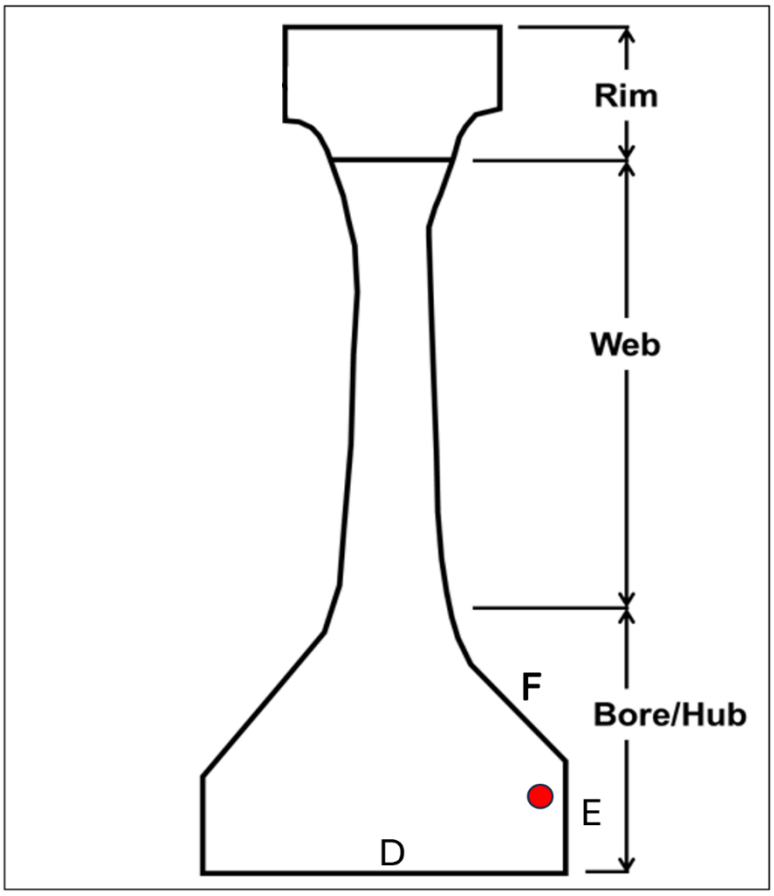

Figure 3.31 Disk 9, having relevant UT scan regions D and E and a second indication at the approximate location of the red circle

3.13.2 Results

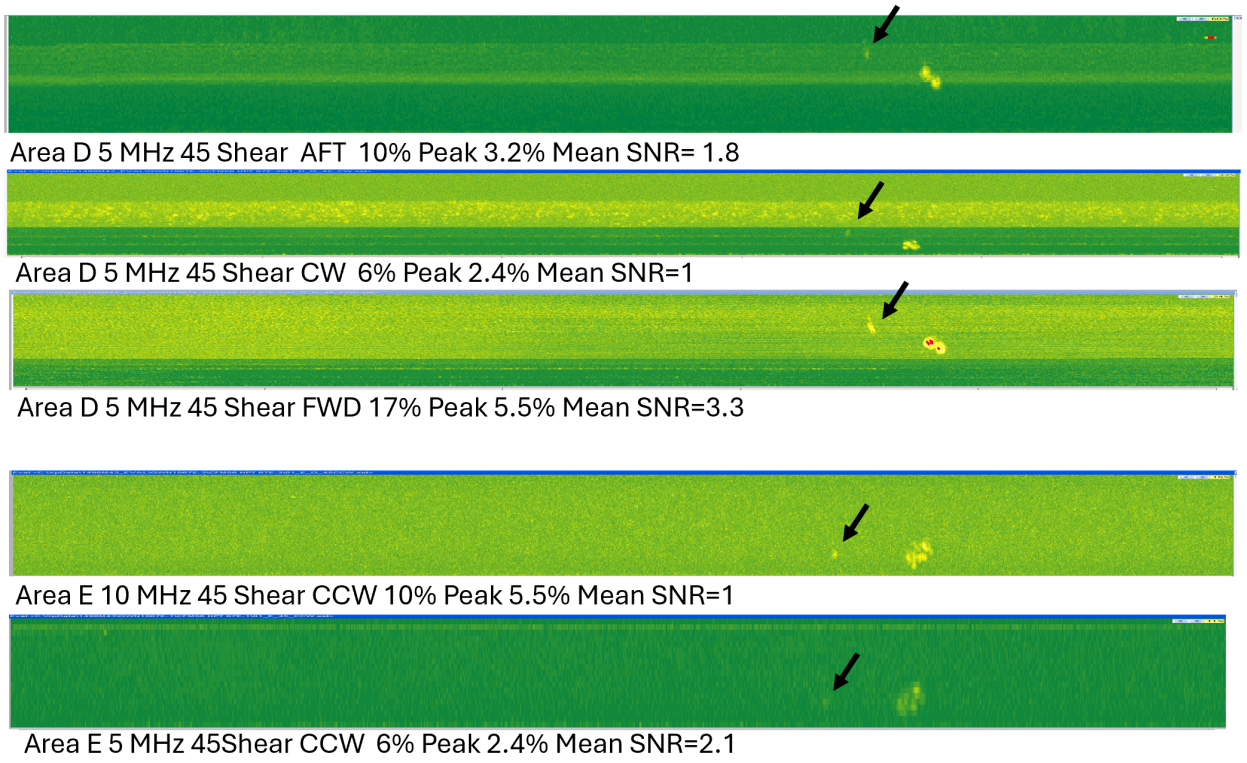

Figure 3.32 Scan images of the second indication in Disk 9.

Detailed results of the standard investigative scans of each region D and E are given in Table 3.25 and Table 3.26. Unlike previous parts, the results are sorted by the inspection angle. Amplitudes are referenced to Calibrations of #2 FBH =80% for Longitudinal wave scans (5 & 10 MHz / 0° & 20°), and .020" (.5 mm) SDH =80% + 6dB for 45° shear wave scans. These Tables show that none of the longitudinal scans were able to detect this anomaly, and Figure 3.33 shows all the longitudinal images which were attempted and found to be ineffective.

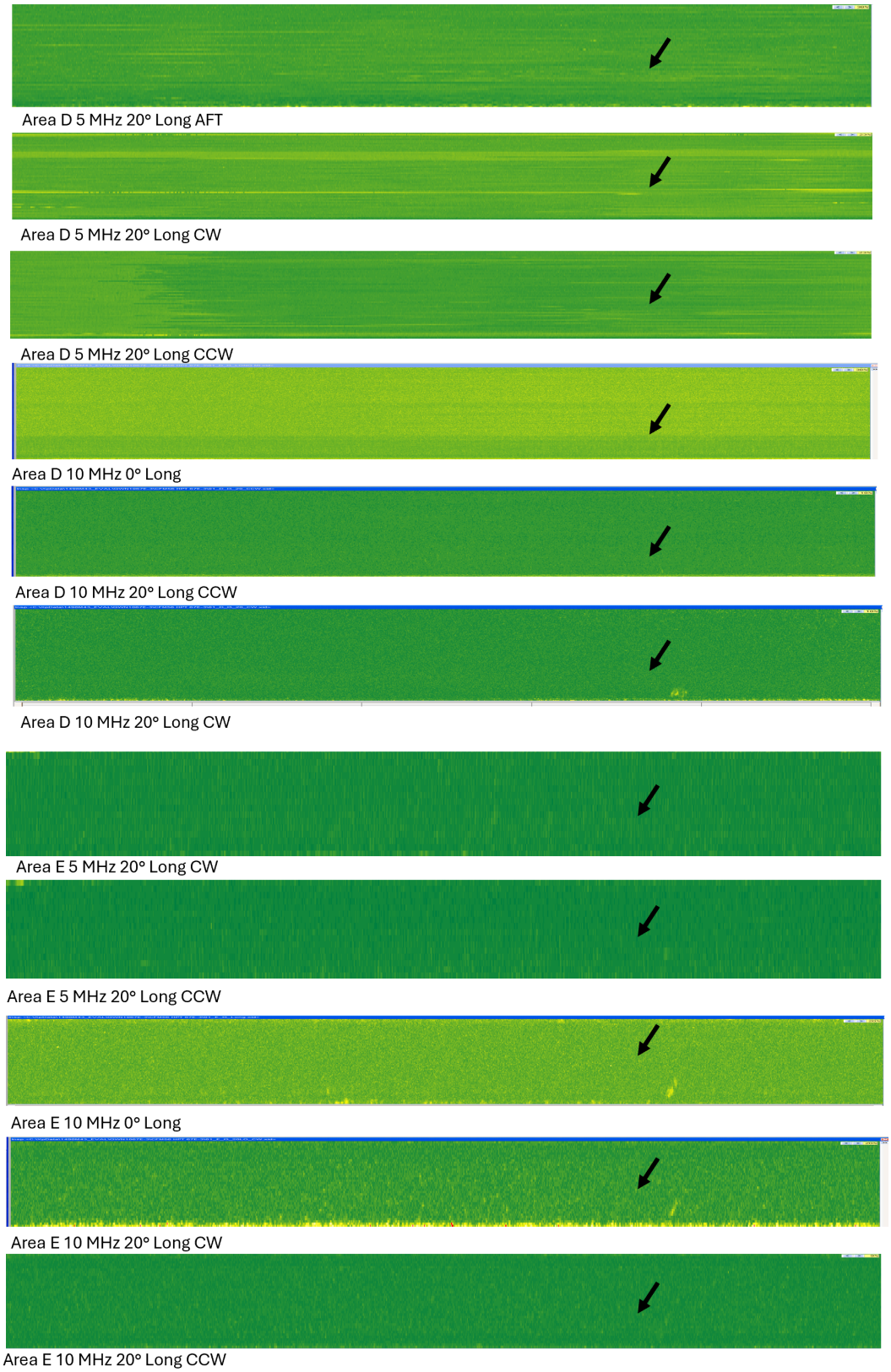

Figure 3.33 Longitudinal scans demonstrating lack of detection for this anomaly

Table 3.25 Disk 9, Surface D, Scan summary

Region	Frequency	Angle	Mode	Direction	Focus	% Amp	Mean Noise	SNR
D	5 MHz	0	Long	NA	Surf	ND		
D	5 MHz	20	Long	CW	Surf	ND		
D	5 MHz	20	Long	CCW	Surf	ND		
D	5 MHz	45	Shear	FWD	Surf	17%	5.50%	3.29
D	5 MHz	45	Shear	Aft	Surf	10%	3.20%	1.83
D	5 MHz	45	Shear	CW	Surf	6%	2.40%	1
D	5 MHz	45	Shear	CCW	Surf	ND		
D	10 MHz	0	Long	NA	Surf	ND		
D	10 MHz	20	Long	CW	Surf	ND		
D	10 MHz	20	Long	CCW	Surf	ND		
D	10 MHz	45	Shear	CW	Surf	ND		
D	10 MHz	45	Shear	CCW	Surf	ND		

Table 3.26 Disk 9, Surface E, Scan summary

Region	Frequency	Angle	Mode	Direction	Focus	% Amp	Mean Noise	SNR
E	5 MHz	20	Long	CW	Surf	ND		
E	5 MHz	20	Long	CCW	Surf	ND		
E	5 MHz	45	Shear	CCW	Surf	6%	2.10%	2.18
E	5 MHz	45	Shear	CW	Surf	ND		
E	10 MHz	0	Long	NA	Surf	ND		
E	10 MHz	20	Long	CW	Surf	ND		
E	10 MHz	20	Long	CCW	Surf	ND		
E	10 MHz	45	Shear	CW	Surf	ND		
E	10 MHz	45	Shear	CCW	Surf	10%	5.50%	1

The location of this indication was pinpointed using a high-resolution UT scan as shown in Figure 3.34(a). The disk was then cut into a cube and polished along the orange dashed line for a photomicrograph, shown in Figure 3.34(b). Metallurgical analysis showed that the indication is a Dirty White Spot (DWS).

(a) (b)

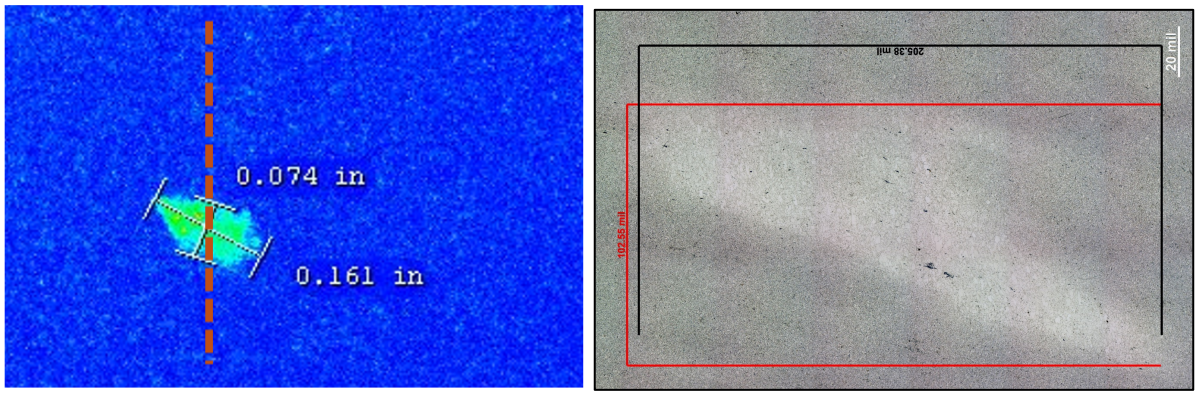

Figure 3.34 High resolution image of the Disk 9 second indication (a), and metallographic view of indication, identifying it as a diffuse white spot (b).

3.13.3 Conclusion

Similar to Disk 7 and 8 results, Disk 9 provided evidence that for this anomaly type, an uncracked/unvoided white spot, 10 MHz and 5MHz 45° shear inspections provided the only detectable response.

3.14 Summary of Anomaly Detections

The scan results of the nine anomaly disks, along with the round robin disk, show that all three scan angles offer significant opportunities to detect anomalies. The strongest detections are summarized in Table 3.27. It is apparent that for the voided or un-voided inclusions, the 0° longitudinal scan generally provided the best detection. For anomalies primarily associated with enlarged grain structures, such as white spots, the 45° shear scan outperformed the longitudinal scans. The angle that offered the most detections overall was the 20° longitudinal scan. Note that these detections were ranked based on SNR, as, even without an SNR criterion, high SNR responses allow for an amplitude threshold to be set to reject the anomaly without a high false positive rate.

Because anomalies in forged nickel rotors are relatively rare, Table 3.27 offers only a glimpse of the range of anomaly types and severities. For example, only three Dirty White Spots are evaluated in this document, which does not allow for a statistically valid analysis. Adding data from additional Nickel forging anomalies would be beneficial to guide further optimization of the protocol. It is the recommendation of this AIA team to encourage the submission of Nickel forging findings to an industry consortium, including inspection parameters, inspection results, and anomaly metallographic details. In the interest of safety, the learnings from this effort should be implemented according to the individual OEM's best judgment until further clarity is established.

Although this report primarily focusses on UT inspection, it is recognized that visual inspection of etched surfaces of forgings and finish machined parts is also successful in identifying melt anomalies, including dirty white spots, of which there are multiple examples in the JENQC database.

Table 3.27 summarize the most effective scan (dark green) and second most effective scan (light green) for the 9 disks assessed, ranked by the number of detections at each angle. Values in the cells represent the maximum SNR exhibited at that angle.

Table 3.27 Most effective scans from the 9 disks assessed

				Most Effective Scans' SNR					
				Surface Focus Scans			SubSurface Focus Scans		
Disk	Anomaly Type	Scan Surface	Depth	0 Long	20 Long	45 shear	0 Long	20 Long	45 shear
Round Robin	Unvoided Inclusion #1	CD		2.4	5.5			2.5	
		DE		NA	7	7.1	NA	NA	NA
		EF		4	9.1		NA	NA	NA
		RS		26	4.7			6.8	
Round Robin	Unvoided Inclusion #2	FG		7.6	4.1	19.1	NA	NA	NA
		QR		5.7	7.8	1.8	NA	NA	NA
Round Robin	Unvoided Inclusion #3	GH		10.2	11.3				
		KL		4	2.8				
		PQ			3.6				
Round Robin	Unvoided Inclusion #4	IJ		2	5.8	6.8		4.4	
		KL		28.1	14.6	5.2		3.5	
		NO		4.9	4.4			2.5	
		PQ		11.7	5			3.8	
Round Robin	Unvoided Inclusion #5	IJ		13.1	5.1	2		3.3	
		KL		15.7	9.8	6	NA	NA	NA
		PQ		3.9					
Round Robin	Unvoided Inclusion #6	IJ		4.5	1.6	2.1			
		KL		10	8.3	7.8	NA	NA	NA
		PQ		2.7					
Disk 1	Unvoided Cluster of Large Grains	Rim		ND	4.9	2.5	NA	NA	NA
		OD		2.2	1.7	5.4	NA	NA	NA
DIsk2	String of Clean Voids	B	1.0" (25 mm)	ND	ND	ND	ND	2.5	4.7
		C	1.0" (25 mm)	ND	ND	ND	ND	4.0	1.9
Disk 3	Voided Inclusion	Rim		11.0	10.9	2.7	NA	NA	NA
		OD		10.1	9.2	ND	NA	NA	NA
Disk 4	Unknown	UA	0.82" (21 mm)	3.7	21.3	6.5	7.3	35	20.5
		UB	0.67" (17 mm)	6.2	13.5	9.9	10.8	21.1	4.9
		UC	0.43" (11mm)	6.3	40.5	6.6	NA	NA	NA
		UE	1.02" (26 mm)	6.3	32.3	18.4	4.1	40.2	45.9
Disk 5	Unknown	UI	0.79" (20 mm)	4.5	ND	ND	2.3	ND	ND
Disk 6	Unknown	1	0.12" (3 mm)	6.5	13.7	7.1	NA	NA	NA
Disk 7	Unvoided Discrete Dirty White Spot	Web	.25" (6mm)	4	6.5	16.8	NA	NA	NA
Disk 8	Unvoided Discrete Dirty White Spot	B	0.6" (15mm)	2.8	5	14.3	3.9	5	19.3
		C1	0.8" (20 mm)	ND	4	5.7	6	3	8
		C2	0.8" (20 mm)	4.7	9.8	5.1	4.3	12.2	21.5
		D	0.4" (10 mm)	1.7	3.6	13.5	NA	NA	NA
Disk 9	Unvoided Diffuse Dirty White Spot	D	0.7" (18mm)	ND	1.9	6.5	NA	NA	NA
		E	0.25" (6 mm)	1.6	1.6	3.4	NA	NA	NA
Disk 9 Indication 2	uncracked/unvoided white spot	D		ND	ND	3.29	NA	NA	NA
		E		ND	ND	2.18	NA	NA	NA

Chapter 4 Down select protocol.

4.1 Recommendations for Inspection Parameters

From the data presented in Chapter 3, it is apparent that some anomalies are better detected with a particular angle such as 45° shear beams, while other anomalies are detected using different angles, such as 20° longitudinal beams. To assure a high rate of detection for a large variety of anomaly types, multiple angles of sound beams and multiple modes of transmission are recommended. It has also been demonstrated that anomalies are best detected when a sound beam is focused at a depth close to that of the anomaly, so multiple depth zones are recommended.

One parameter which did not appear to be significant variable in the detection of these anomalies was the frequency of the sound beam. The 5 MHz and 10 MHz inspections demonstrated similar detection rates. Furthermore, when employing multiple scans, anomalies were generally detected with each frequency in at least one scan, so there is no recommendation for a specific frequency. Given that the depth of field of a 5 MHz transducer is longer than that of a 10 MHz transducer having the same focal properties, 5 MHz could be preferred to minimize the number of scans needed for full volume coverage. For inspections with high sensitivity requirements, such as #1/2 FBH, the use of 10 MHz probes could be preferred.

While different combinations of frequencies and sound beam angles can be effective, one protocol is described below which is known to be effective and is recommended for the

ultrasonic inspection of Nickel turbine disk forgings. This recommendation does not exclude the use of alternative scan selections; however, choosing such alternatives may require additional sensitivity validation. Alternative inspections are in fact warranted for several special cases, including inspection through curved surfaces, interrogating material very near the surface of the part, and very high sensitivity inspections.

Based on the results shown in Chapter 3 plus the team's historic knowledge of ultrasonic inspection, the recommended ultrasonic inspection protocol is:

1. Each volume element in forging which will end in the finished part should be scanned from multiple surfaces and/or using multiple refracted angles, including some or all of 0° longitudinal, +/-20° longitudinal and +/-45° shear. It is recommended that each volume element receive at least four (4) scan angles unless otherwise agreed by the OEM's design authority.
2. Refracted angles should be selected based on the type of anomalies anticipated in the material being inspected. The preferred refracted angles are 0° and +/-20° longitudinal for materials at risk of containing voids or discrete inclusions. The preferred angles are +/-45° shear for materials that may contain anomalies such as enlarged grains and/or cracks perpendicular to the scan surface in the axial/radial plane.
3. To minimize the number of depth zones, the baseline transducer should operate at 5 MHz with a 6-inch (152 mm) focal length and 0.75-inch (19 mm) diameter.
4. Material with a depth of less than 0.75 to 1.0 inch (19mm to 25mm) should be inspected with scans using the 5 MHz transducer with a 6 inch (152 mm) water path.

5. Material with a depth of 0.75 to 1.0 inch (19mm to 25mm) to 1.75 to 2.25 inches (44mm to 57mm) should be inspected scans using the 5 MHz transducer with a 2-inch (51 mm) water path.
6. Beyond 1.75 to 2.25 inches (44mm to 57mm), the volume should receive a minimum of 3 scan angles including 0° longitudinal, +/-20° longitudinal. Each OEM will determine what is necessary and effective.
7. For depths beyond 1.5 to 3 inches, the sensitivity of shear wave is not proven during this study. Each OEM will determine appropriate scans to use.

A sketch for the above protocol is shown in Figure 4.1. In this figure, each yellow oval represents a sound beam from a 5 MHz transducer, focussed at the location of the corresponding black circle. All angles shown can be in either the circumferential or radial/axial direction, or both. Note that for improved near surface resolution, the 0° longitudinal scan might be performed with a 10 MHz transducer. In that case, the zone depths would need to be adjusted according to the transducer's depth of field. 10 MHz transducer can be also beneficial for high-sensitivity inspection, e.g. FBH #1/2 equivalent.

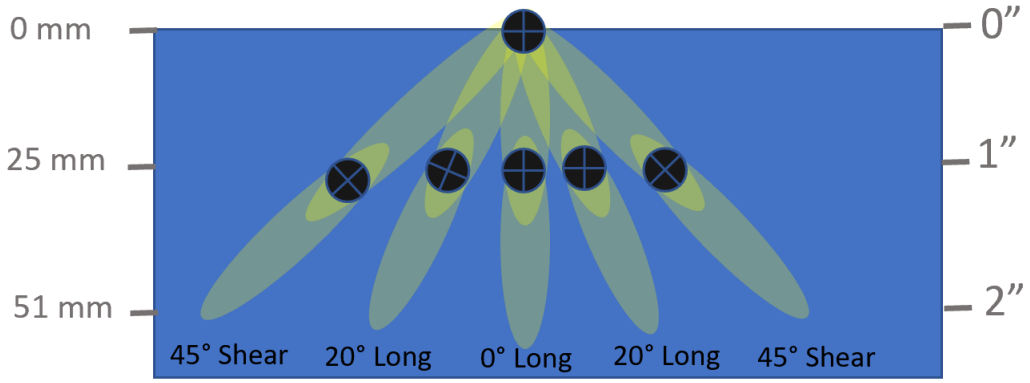

Figure 4.1 The recommended inspection protocol. Each yellow oval represents the inspection volume of a sound beam, and the black circle represents the focal position for each yellow beam. Note that Deep zones are shown, with the focus approximately 1.0” deep, inspecting to a depth of 2” or greater. The depths are perpendicular to the surface, not to the sound travel paths.

4.2 Threshold Setting Strategy

The inspection protocol described in Section 4.1 was chosen to maximize the response and detectability of anomalies. The next critical decision is the selection of accept/reject criteria. Common types of criteria are based on the maximum allowed signal amplitude or maximum allowed Signal-to-Noise Ratio (SNR). Indications that fall below the acceptance threshold will not be flagged for evaluation, meaning that an optimized inspection will be ineffective if the thresholds are set too high.

Nickel turbine disk designs specify an operational life determined by several factors, including material properties such as crack initiation or damage tolerance, operational parameters such as temperature and stress, and inspection sensitivity and reliability. Since all these factors

interact as a system, tradeoffs between design parameters (stress, material selection, etc.), inspection sensitivity/reliability, and lifespan are made to meet the overall requirements of a given engine. As such, some highly stressed components may require a very high sensitivity inspection to meet life requirements, while others, lower-stress components, even those made from the same material for the same engine, may require a less sensitive inspection. Consequently, engines designed by different OEMs and of different thrust classes or certification requirements can also have different inspection sensitivity and inspection requirements.

In few cases Accept/Reject criteria based on the maximum allowed signal amplitude can be directly related to the maximum allowed flaw size through the concept referred to as the “Area-Amplitude” relationship. That size is tied to the required component life (measured in flight cycles) after inspection (with a predefined probability of detection). For some OEMs the inspection Accept/Reject criteria are derived directly from the part design requirements, which may include the required life of the part. For example, one can estimate the maximum allowed flaw size based on required life, location within the part, and expected operational conditions/stress map. If sufficient information is available, zoned accept/reject criteria can be also established for a given part, with zones correlating with part stress maps.

Design and inspection scenarios are not always ideal and alternative accept/reject criteria, such as the maximum allowed Signal-to-Noise Ratio (SNR), may be used. This can be beneficial when inspecting materials where the microstructure is not uniform throughout the part volume due to specific manufacturing practices, such as extrusion, forging, or heat treatment. Microstructural non-uniformity results in variations in sound interactions leading to

variations in observed grain scattering noise and attenuation. Higher attenuation (and resulting lower signal amplitude) is often associated with lower grain noise levels, while lower attenuation (higher signal amplitude) is associated with higher grain noise levels. These variations often depend on circumferential position on the part. Therefore, inherent microstructural variations result in variations in observed signal amplitudes. An SNR approach accommodates such variations and maximizes the inspection sensitivity across all regions of a part.

Ultimately, the decision on which type of accept/reject criteria to use is directly linked to the sensitivity needed for the specific part and location within that part. Because the corresponding factors may differ significantly between different OEMs, a single accept/reject strategy and threshold cannot be defined for all Nickel turbine rotors.

4.3 Evaluation Criteria: Amplitude and Signal-to-Noise Ratio (SNR)

As an initial assessment of desirable amplitude thresholds, Table 4.2 and Table 4.3 indicate that an amplitude threshold of 25% FSH is required to call out the indications described in Chapter 3 of this report. Note that 25% FSH is nominally relative to the calibration target being set to 80%, and the calibration target for longitudinal scans being a #1 flat bottom hole and for shear scans being a .020” (.5mm) side-drilled hole. Given the statistically small number of samples with indications, which were only available due to prior detection by a previous inspection, it is recommended to use this 25% FSH value only as a preliminary guideline. Each OEM is advised to develop their own thresholds based on the specific Nickel material being inspected and its design/life needs, consistent with the discussion in Section 4.2.

For the most demanding inspection requirements, there is a risk that stealthy anomalies exhibit signal strengths not proportional to their size. This makes amplitude-based life assessments inaccurate and necessitates the use of the lowest possible amplitude threshold. Since every type of material generates an ultrasonic noise floor corresponding to its grain structure, it is crucial that the threshold be defined as close to the noise floor as possible, without generating false positives. This can be achieved by using an SNR threshold, which dynamically adjusts the amplitude threshold as the noise floor fluctuates. Consequently, an SNR criterion flags all indications above the noise floor, making them detectable by the inspection protocol without generating false positives in high-noise parts.

One drawback of an SNR criterion is that high-noise parts can push the amplitude threshold to a high level that renders the inspection ineffective. To ensure the minimum effectiveness of the inspection, an absolute maximum amplitude threshold should be used in conjunction with the SNR threshold. Scans with high noise level exceeding this maximum amplitude threshold should be considered un-inspectable due to their high noise level, rather than defective.

When applying an SNR criterion, there may be implications for the inspection protocol. For example, the ultrasonic inspections described in Chapter 3 utilized transducers with frequencies of 5MHz and 10MHz. The 10 MHz transducers often produce higher amplitudes from anomalies but, depending on the grain structure, can also exhibit higher noise. These increased amplitudes combined with higher noise levels may produce lower SNRs compared to the 5 MHz inspection.

4.4 Discussion of the risk for potential False-Positives

When selecting the rejection criteria, it's important to consider the false alarm rate. Low thresholds in amplitude and/or SNR criteria can increase false call rates. The goal is to detect critical anomalies in rotor material while minimizing the impact on production output.

Although the data in this report shows that an SNR threshold of 4.0 would have detected all anomalies, the collective experience of the team suggests that a lower threshold can be used without significantly affecting production output. SNR thresholds of 3.0, or even as low as 2.2, have been recommended for some specific applications. However, an SNR threshold lower than 2.2 is expected to result in a significant increase in false positives.

4.5 Implications of Flow Lines in Forgings

Inherent to the forging process is the occurrence of flow lines. As a material is forged from one shape to another, especially during the conversion from ingot to billet and also during the part forging process, the grain features and anomalies often become elongated and align parallel to the flow direction. Anomalies are most easily detected when the sound beam is perpendicular to the anomaly surface with the largest area. Since anomalies in new forgings are expected to lie parallel to the flow lines, it is advantageous to scan perpendicular to these lines. This can be achieved by obtaining the nominal flow line map from the forging process model, correlate with the forging flow lines measured and then selecting the sound beam incident angle in the radial/axial plane to ensure refracted angle in the part is normal to the flow lines. This setup should be added to the 0° scan in the protocol.

The protocol recommended in Section 4.1 specifies the addition of 20° longitudinal and 45° shear angles. These scan angles should be set with respect to the part surface and not linked to the flow lines. If two incident angles are added to accommodate flow line angles plus circumferential orientation, the total resulting refracted angle should be calculated. It is important to avoid compound incidence angles because sensitivity drops off rapidly at angles greater than the 20° refracted longitudinal. Likewise, shear wave sensitivity decreases at angles below 45°. If other angles are used, sensitivity should be verified.

4.6 Recommendation for "Design for Inspection Coverage"

For the purposes of this report, the principal target of ultrasonic inspection of forgings during new manufacture is 3-dimensional melt anomalies. To maximize the probability of detecting such anomalies, it is recommended that the material be inspected from as many different directions as reasonably practicable. This requires a design for inspection approach, which includes modelling sound paths and determining the number of scan angles at any point in the volume. The forging shape can be optimized to achieve the required number of scan angles, thereby maximizing the likelihood of detecting potential melt anomalies.

The unique geometry of a forging can make certain scans impossible, and some surfaces may only receive a subset of the recommended number of scans. The design of the forging shape for ultrasonic inspection should consider the factors given in the Table 4.1 below.

Table 4.1 Design of the forging shape for ultrasonic inspection requirements

Requirements	Justification / reasoning
Maximize the forging volume coverage using a 0° longitudinal beam or the beam angled normal to material flow.	Anomalies present in the material during the forging process are likely to be flattened parallel to the direction of the forging flow.
Ensure a specified minimum number of scan angles for each volume element, as agreed upon by the Company's Materials and Design community. It is recommended to have at least 4 scans for each volume element.	A standard is required for all forging shapes to maximize the opportunity for Anomalies detection.
Regions of under-inspected material (fewer scans than agreed-upon standard) should only be permitted by exception and with the agreement of the appropriate Materials and Design experts for the specific part.	Flexibility is necessary for each specific part.

Table 4.2 Summary of mean data values across all virtual round robin samples over frequency.

Wave Type	Frequency [MHz]	Peak Amp [% FSH]	Avg Noise [% FSH]	Standard Deviation Peak Amp [% FSH]	SNR
Long	5	29.20	4.49	1.35	7.22
Long	10	35.50	4.53	1.66	5.64
Shear	5	25.74	2.51	0.72	7.10
Shear	10	26.05	4.63	2.79	6.28

Table 4.3 Summary of mean data values across all virtual round robin samples by refracted angle.

Wave Type	Refracted Angle [°]	Peak Amp [% FSH]	Avg Noise [% FSH]	Standard Deviation Peak Amp [% FSH]	SNR
Long	0	27.11	6.20	0.91	4.55
Long	20	34.99	3.95	1.61	6.98
Long	45	26.32	5.82	2.47	4.60
Shear	45	25.84	3.62	1.98	7.0
Shear	65	26.27	3.68	1.05	4.33

4.7 Recommendations for future technology improvements in Ultrasonic Testing (UT).

4.7.1 Supplemental Topics

There are two key topics related to the ultrasonic inspection of Nickel turbine disks that are particularly relevant for future advancements in inspection techniques.

The first topic addresses the industry's capacity to implement the recommendations outlined in Chapter 4. One potential approach is to utilize phased array technology, which allows for the collection of greater volume of inspection data within the same timeframe as the current inspection methods.

The second topic is the recommendation to capture waveform data during ultrasonic inspections. This data will be invaluable as artificial intelligence capabilities advance, given that experts rely on waveform data to evaluate ultrasonic indications. By starting to collect waveform data now, a comprehensive library of both indications and indication-free data can be established.

The following content reflects the consensus view of the AIA NDE Team.

4.7.2 Enhancing Capacity with Phased-Array Technology

Upon implementation of the recommendations in Chapter 4, ultrasonic inspection is anticipated to become an even greater bottleneck in the manufacturing process for Nickel turbine disks. The total scan time may increase by 3 to 5 times, depending on the number of scans used in the previous protocol and the part geometry. The inspection supply chain is currently unable to expand quickly enough to accommodate this increase in demand and is already at maximum capacity.

Phased Array Ultrasonic Testing (PAUT) is an advanced ultrasonic inspection technique that uses the same physical principles as conventional ultrasound to detect anomalies in materials. Due to this overlap, PAUT can be developed as a direct replacement for conventional ultrasound. The benefit of PAUT lies in its capability to acquire data over a larger volume of material within the same timeframe.

PAUT utilizes a grid of small transducers (called elements) that function similarly to a larger, single element transducer. By adjusting the timing of the excitation and reception of these individual elements (a timing configuration known as a delay law), the array can simulate the characteristics of several different types of single element transducers simultaneously. For example, one delay law may perform a 0-degree longitudinal near surface scan, while the next delay law could perform a 20-degree longitudinal deep-focus scan.

Initial demonstrators of PAUT technology are already available on the market, with a small number of applications in production. These applications indicate a path to full-scale

implementation, though each new application still requires significant validation effort. For PAUT to be applied to this protocol, testing would be needed to:

- Demonstrate anomaly detection comparable to single-element inspections
- Show favorable total inspection time and coverage
- Establish reasonable controls for instrument certification and calibration

Multiple solutions exist within PAUT, including beam forming, plane wave imaging (PWI), and the total focusing method (TFM). The benefit of beam forming is that it closely mimics single element inspections, making it easier to demonstrate equivalent sensitivity. PWI offers the benefit of being the fastest and least computationally intense approach, though it may suffer from reduced near-surface resolution. TFM provides the best sensitivity but can be slower due to intense data handling requirements.

PAUT presents an attractive solution to the capacity challenge, but its implementation will require careful selection of the best configuration or combination of configurations. Significant effort will also be needed to scale the infrastructure, including defining requirements for instrument certification and daily calibration or other process checks.

4.7.3 Recommendations for Waveform Data Capture

Similar to phased array technology, the adoption of full ultrasonic waveform data collection in rotor material inspection has been slow. Although managing and analyzing large volumes of waveform data is complex, it offers a much richer dataset for characterizing anomalies, and the surrounding material compared to traditional C-scan amplitude and time-of-flight data.

Since the advent of computers, various analysis techniques have been tested on A-scan and C-scan data to improve differentiation of anomalies from background noise. Traditional signal processing techniques have shown value in a few applications. As computing power increases, other promising techniques, such as multi-gate analysis, are becoming more viable. In multi-gate analysis, waveform data is used to create multiple c-scan images from a single data set. Comparing C-scan analysis data across this collection of images can improve material and anomaly characterization.

The collection of waveform data also allows for the application of machine learning and artificial intelligence technologies to ultrasonic data. These advanced methods may identify characterization information that traditional analysis methods have missed.

As the cost of computational power and data storage continue to decrease, the collection and analysis of waveform ultrasonic data will play a crucial role in improving detection and characterization capabilities for ultrasonic testing. Given the rarity of anomalies and the intensive data needs for training machine learning algorithms, large-scale waveform capture should begin as soon as possible.

Appendix A

Table A 4.1 Summary of Ultrasonic Testing (UT) Inspections

Inspection Employed				
OEM	Frequency	Focus	Employed Beam Angles	Calibration
1	4-6MHz (5.5MHz for the data presented)	Surface	0 degree and 5-degree incident radial axial longitudinal	0.025-inch diameter flat bottomed hole @ 80% screen height
2	5MHz & 10MHz	Surface & Multizone	0 degree and 5-degree incident radial axial longitudinal 45 degree circumferential shear wave	Longitudinal - #1 flat bottom hole @ 80% screen height Shear - 1mm side drilled hole
3	10MHz	Surface & multizone	0 degree and radial-axial longitudinal (as defined by scan coverage)	#1 flat bottom hole @ 80% screen height
4	5MHz & 10MHz	Surface and Multizone	longitudinal - 0 degree, radial-axial, Circumferential	#1 flat bottom hole @ 80% screen height

Table A 4.2 Ultrasonic Testing (UT) Scan results of round robin disk

Indication	OEM	Surface	Depth	Frequency	Angle	Amplitude	SNR
1	OEM1	FG	Surface	5	0	1.40	7.61
1	OEM1	FG	Z1	5	-20	3.28	4.05
1	OEM1	QR	Surface	5	0	1.40	5.71
1	OEM1	QR	Z1	5	-20	6.13	6.56
1	OEM2	FG	Surface	5	0	-19.83	3.40
1	OEM2	FG	Surface	10	0	-16.61	4.10
1	OEM2	FG	Z1	5	45	-35.82	19.40
1	OEM2	FG	Z1	5	-20	-20.72	9.00
1	OEM2	QR	Surface	5	0	-31.41	3.20

Indication	OEM	Surface	Depth	Frequency	Angle	Amplitude	SNR
1	OEM2	QR	Surface	10	0	-11.44	2.80
1	OEM2	QR	Surface	10	0	-4.62	4.90
1	OEM2	QR	Z1	5	-20	-4.02	3.20
1	OEM2	QR	Z1	5	-45	19.90	1.80
1	OEM3	QR	Z1	5	20	-18.59	2.42
1	OEM3	QR	Z1	5	-20	-9.04	7.84
1	OEM4	GF	Surface	5	0	-6.82	7.30
1	OEM4	QR	Surface	5	0	-8.69	4.45
1	OEM4	QR	Z1	5	-20	-14.60	11.46
2	OEM1	KL	Surface	5	0	7.72	15.75
2	OEM1	KL	Z1	5	20	-1.40	4.14
2	OEM1	KL	Z1	5	-20	1.98	4.88
2	OEM2	IJ	Surface	5	0	-7.60	2.81
2	OEM2	IJ	Surface	10	0	-11.21	6.99
2	OEM2	IJ	Surface	10	0	-2.21	13.10
2	OEM2	IJ	Z1	5	45	-23.44	1.99
2	OEM2	KL	Surface	5	0	-16.00	3.60
2	OEM2	KL	Surface	5	0	16.54	1.57
2	OEM2	KL	Surface	10	0	0.75	4.00
2	OEM2	KL	Surface	10	0	0.83	4.54
2	OEM2	KL	Surface	10	0	1.63	3.10
2	OEM2	KL	Z1	5	20	-4.64	2.50
2	OEM2	KL	Z1	5	20	2.90	2.14
2	OEM2	KL	Z1	5	45	-17.49	2.64
2	OEM2	KL	Z1	5	45	-13.05	6.04
2	OEM2	PQ	Surface	5	0	-32.29	1.86
2	OEM2	PQ	Surface	10	0		1.90
2	OEM2	PQ	Surface	10	0	-15.08	2.10
2	OEM2	PQ	Surface	10	0	-11.54	3.90
2	OEM3	8/KL	Surface	5	0	-1.16	8.34
2	OEM3	26/KL	Z1	5	1.5	-2.07	6.14
2	OEM3	IJ	Surface	5	0	-4.90	2.93
2	OEM3	IJ	Surface	5	0	-3.03	1.80
2	OEM3	IJ	Z2	5	-20	1.56	3.29
2	OEM3	KL	Surface	5	0	0.08	8.09

Indication	OEM	Surface	Depth	Frequency	Angle	Amplitude	SNR
2	OEM3	KL	Z1	5	20	-9.80	4.53
2	OEM3	KL	Z1	5	-20	-7.30	9.77
2	OEM4	IJ	Surface	5	0	-13.30	7.52
2	OEM4	IJ	Surface	5	0	-13.15	2.98
2	OEM4	KL	Surface	5	0	-1.34	12.04
3	OEM1	KL	Surface	5	0	4.62	10.02
3	OEM1	KL	Z1	5	20	-1.00	5.77
3	OEM2	IJ	Z1	5	45	-23.38	2.07
3	OEM2	KL	Surface	5	0	-10.47	2.40
3	OEM2	KL	Surface	5	0	16.54	1.60
3	OEM2	KL	Surface	10	0	-4.08	2.74
3	OEM2	KL	Surface	10	0	0.70	2.60
3	OEM2	KL	Z1	5	45	-16.08	2.56
3	OEM2	KL	Z1	5	45	-11.64	7.83
3	OEM2	PQ	Surface	5	0	-33.74	1.45
3	OEM2	PQ	Surface	10	0	-15.14	2.70
3	OEM3	8 / K L	Surface	5	0	-6.02	4.82
3	OEM3	26 / K L	Z1	5	5	-1.67	6.24
3	OEM3	K_L	Surface	5	0	-4.05	5.07
3	OEM3	K_L	Z1	5	20	-9.04	3.78
3	OEM3	K_L	Z1	5	-20	-13.73	5.33
3	OEM4	IJ	Surface	5	0	-9.66	4.46
3	OEM4	IJ	Surface	5	0	-7.31	15.00
3	OEM4	KL	Surface	5	0	-3.04	9.89
3	OEM4	KL	Z1	5	20	-6.82	8.30
4	OEM1	KL	Surface	5	0	10.74	15.94
4	OEM1	KL	Z1	5	20	9.54	14.57
4	OEM1	KL	Z1	5	-20	7.57	12.91
4	OEM2	IJ	Z1	5	45	-19.20	6.82
4	OEM2	KL	Surface	10	0	-10.80	2.40
4	OEM2	KL	Surface	10	0	-1.54	6.56
4	OEM2	KL	Z1	5	20	17.01	5.90
4	OEM2	KL	Z1	5	20	17.15	4.60
4	OEM2	KL	Z1	5	45	-20.66	1.82
4	OEM2	KL	Z1	5	45	-17.74	5.20

Indication	OEM	Surface	Depth	Frequency	Angle	Amplitude	SNR
4	OEM2	NO	Surface	10	0	-7.69	4.90
4	OEM2	PQ	Surface	5	0	-27.49	2.90
4	OEM2	PQ	Surface	5	0	-9.24	2.30
4	OEM2	PQ	Surface	10	0	-17.25	8.00
4	OEM2	PQ	Surface	10	0	-16.44	3.00
4	OEM2	PQ	Surface	10	0	1.19	11.70
4	OEM3	8/KL	Surface	5	0	3.00	11.35
4	OEM3	26/KL	Z1	5	1.5	6.40	11.72
4	OEM3	IJ	Surface	5	0	-6.73	1.96
4	OEM3	IJ	Surface	5	0	-6.55	1.08
4	OEM3	IJ	Z2	5	20	2.00	4.37
4	OEM3	IJ	Z2	5	-20	-4.19	2.22
4	OEM3	KL	Surface	5	0	2.00	11.17
4	OEM3	KL	Surface	5	0	5.00	6.96
4	OEM3	KL	Z1	5	20	-12.21	4.76
4	OEM3	KL	Z1	5	-20	-9.80	7.05
4	OEM3	KL	Z2	5	20	-5.36	1.69
4	OEM3	KL	Z2	5	-20	0.08	3.45
4	OEM3	NO	Z2	5	-20	-3.27	2.48
4	OEM3	PQ	Surface	5	0	-4.19	2.28
4	OEM3	PQ	Surface	5	0	-2.44	1.46
4	OEM3	PQ	Z2	5	20	0.25	3.78
4	OEM3	PQ	Z2	5	-20	-2.00	1.83
4	OEM4	KL	Surface	5	0	6.02	28.07
4	OEM4	KL	Z1	5	20	-6.02	9.09
5	OEM1	RS	Surface	5	0	10.84	26.05
5	OEM2	CD	Surface	5	0	-30.14	2.00
5	OEM2	CD	Surface	10	0	-38.28	1.50
5	OEM2	CD	Surface	10	0	-19.34	4.00
5	OEM2	CD	Surface	10	0	-15.58	2.44
5	OEM2	CD	Z1	5	20	-32.30	2.00
5	OEM2	DE	Z1	5	45	-12.08	7.10
5	OEM2	EF	Surface	10	0	-8.23	3.98
5	OEM2	RS	Surface	5	0	3.34	10.70
5	OEM2	RS	Surface	10	0	1.94	10.70

Indication	OEM	Surface	Depth	Frequency	Angle	Amplitude	SNR
5	OEM2	RS	Surface	10	0	4.61	13.38
5	OEM2	RS	Z1	5	20	-3.50	1.40
5	OEM2	RS	Z1	5	20	3.22	4.70
5	OEM3	1/CD	Surface	5	0	-11.01	1.96
5	OEM3	2/DE	Surface	5	0	-14.60	2.04
5	OEM3	3/EF	Surface	5	0	-16.65	2.36
5	OEM3	13/Rs	Surface	5	0		7.52
5	OEM3	17/DE	Z1	5	20	-8.52	3.46
5	OEM3	21/RS	Z1	5	20	-7.50	3.88
5	OEM3	CD	Surface	5	0	-6.55	1.67
5	OEM3	CD	Z2	5	-20	-6.55	2.49
5	OEM3	EF	Surface	5	0	-16.65	3.50
5	OEM3	EF	Z1	5	20	-14.60	9.14
5	OEM3	EF	Z1	5	-20	-19.34	3.14
5	OEM3	RS	Surface	5	0	12.00	9.03
5	OEM3	RS	Z2	5	20	5.00	6.82
5	OEM3	RS	Z2	5	-20	5.00	4.66
6	OEM1	GH	Surface	5	0	-2.74	4.29
6	OEM2	GH	Surface	10	0	0.83	10.20
6	OEM2	KL	Surface		0		1.94
6	OEM2	KL	Surface	5	0	-31.51	1.30
6	OEM2	KL	Surface	10	0	-16.62	3.99
6	OEM2	KL	Surface	10	0	-13.71	2.23
6	OEM2	KL	Z1	5	20	-15.63	1.40
6	OEM3	5/GH	Surface	5	0	-9.12	3.24
6	OEM3	18/GH	Z1	5	20	-11.62	5.66
6	OEM3	GH	Surface	5	0	-8.13	6.72
6	OEM3	GH	Z1	5	20	-9.80	11.94
6	OEM3	GH	Z1	5	-20	-17.89	2.41
6	OEM4	GH	Surface	5	0	-9.43	5.19
6	OEM4	GH	Z1	5	20	-2.79	11.37

Appendix B

Table B-4.4 UT Scan results for disk 1

Surface	Frequency	Incident Angle	Mode	Direction	Peak Amplitude	SNR	Average noise
Flat	5	0	Long	-	-	-	-
Flat	5	5	Long	CCW	19,53	4,7	3,4
Flat	5	5	Long	CW	16,4	4,86	3,37
Flat	5	5	Long	Rad/Ax in	-	-	-
Flat	5	5	Long	Rad/Ax out	n/a	n/a	n/a
Flat	5	19	Shear	CCW	6,05	2,02	1,82
Flat	5	19	Shear	CW	3,52	2,48	1,22
Flat	5	19	Shear	Rad/Ax in	-	-	-
Flat	5	19	Shear	Rad/Ax out	n/a	n/a	n/a
Flat	5	26	Shear	CCW	-	-	-
Flat	5	26	Shear	CW	-	-	-
Flat	5	26	Shear	Rad/Ax in	-	-	-
Flat	5	26	Shear	Rad/Ax out	n/a	n/a	n/a
Flat	10	0	Long	-	-	-	-
Flat	10	5	Long	CCW	12,5	2,55	3,50
Flat	10	5	Long	CW	13,28	2,76	3,50
Flat	10	5	Long	Rad/Ax in	-	-	-
Flat	10	5	Long	Rad/Ax out	n/a	n/a	n/a
Flat	10	19	Shear	CCW	5,86	1,46	2,15
Flat	10	19	Shear	CW	6,45	2,18	2,12
Flat	10	19	Shear	Rad/Ax in	n/a	n/a	n/a
Flat	10	19	Shear	Rad/Ax out	6,64	1,88	20,6
Flat	10	26	Shear	CCW	-	-	-
Flat	10	26	Shear	CW	-	-	-
Flat	10	26	Shear	Rad/Ax in	n/a	n/a	n/a
Flat	10	26	Shear	Rad/Ax out	n/a	n/a	n/a
OD							
OD	5	0	Long	-	11,13	2,24	4,79
OD	5	5	Long	CCW	-	-	-
OD	5	5	Long	CW	7,03	1,15	4,09
OD	5	5	Long	Rad/Ax in	-	-	-
OD	5	5	Long	Rad/Ax out	8,2	1,59	4,01

Surface	Frequency	Incident Angle	Mode	Direction	Peak Amplitude	SNR	Average noise
OD	5	19	Shear	CCW	3,52	4,11	1,19
OD	5	19	Shear	CW	3,52	3,95	1,16
OD	5	19	Shear	Rad/Ax in	n/a	n/a	n/a
OD	5	19	Shear	Rad/Ax out	-	-	-
OD	5	26	Shear	CCW	-	-	-
OD	5	26	Shear	CW	-	-	-
OD	5	26	Shear	Rad/Ax in	-	-	-
OD	5	26	Shear	Rad/Ax out	-	-	-
OD	10	0	Long	-	6,64	1,48	3,07
OD	10	5	Long	CCW	6,45	1,66	3,01
OD	10	5	Long	CW	6,84	0,90	3,08
OD	10	5	Long	Rad/Ax in	-	-	-
OD	10	5	Long	Rad/Ax out	5,86	1,25	2,94
OD	10	19	Shear	CCW	5,86	5,30	1,29
OD	10	19	Shear	CW	4,88	5,07	1,23
OD	10	19	Shear	Rad/Ax in	-	-	-
OD	10	19	Shear	Rad/Ax out	11,52	5,43	1,71
OD	10	26	Shear	CCW	-	-	-
OD	10	26	Shear	CW	-	-	-
OD	10	26	Shear	Rad/Ax in	n/a	n/a	n/a
OD	10	26	Shear	Rad/Ax out	n/a	n/a	n/a

Table B-4.5 UT Scan results for disk 2

Surface	Frequency	Incident Angle	Refracted Angle	Mode	Direction	Peak Amplitude	SNR	Average noise	Standard Dev.
Flat	5	0	0	Long	-	10,74	2,55	4,0	0,65
Flat	5	5	20	Long	CCW	6,84	1,20	3,44	0,53
Flat	5	5	20	Long	CW	18,36	5,57	3,37	0,50
Flat	5	5	20	Long	Rad/Ax in	16,8	2,59	3,77	1,01
Flat	5	5	20	Long	Rad/Ax out	n/a	n/a	n/a	n/a
Flat	5	19	45	Shear	CCW	-	-	-	-
Flat	5	19	45	Shear	CW	-	-	-	-
Flat	5	19	45	Shear	Rad/Ax in	-	-	-	-
Flat	5	19	45	Shear	Rad/Ax out	n/a	n/a	n/a	n/a
Flat	5	26	65	Shear	CCW	-	-	-	-
Flat	5	26	65	Shear	CW	4,69	2,36	1,64	0,23
Flat	5	26	65	Shear	Rad/Ax in	n/a	n/a	n/a	n/a
Flat	5	26	65	Shear	Rad/Ax out	n/a	n/a	n/a	n/a
Flat	10	0	0	Long	-	26,9	11,0	3,1	0,41
Flat	10	5	20	Long	CCW	41,0	5,15	3,45	0,52
Flat	10	5	20	Long	CW	41,6	10,9	3,32	0,49
Flat	10	5	20	Long	Rad/Ax in	22,7	3,0	6,23	1,02
Flat	10	5	20	Long	Rad/Ax out	n/a	n/a	n/a	n/a
Flat	10	19	45	Shear	CCW	-	-	-	-
Flat	10	19	45	Shear	CW	9,38	2,67	2,83	0,38
Flat	10	19	45	Shear	Rad/Ax in	-	-	-	-
Flat	10	19	45	Shear	Rad/Ax out	n/a	n/a	n/a	n/a
Flat	10	26	65	Shear	CCW	-	-	-	-
Flat	10	26	65	Shear	CW	-	-	-	-
Flat	10	26	65	Shear	Rad/Ax in	n/a	n/a	n/a	n/a
Flat	10	26	65	Shear	Rad/Ax out	n/a	n/a	n/a	n/a
OD	5	0	0	Long	-	26,76	9,96	5,48	0,53
OD	5	5	20	Long	CCW	27,15	6,92	3,64	0,53
OD	5	5	20	Long	CW	24,22	9,23	3,41	0,51
OD	5	5	20	Long	Rad/Ax in	19,73	3,54	3,95	1,0
OD	5	5	20	Long	Rad/Ax out	n/a	n/a	n/a	n/a
OD	5	19	45	Shear	CCW	-	-	-	-
OD	5	19	45	Shear	CW	-	-	-	-

Surface	Frequency	Incident Angle	Refracted Angle	Mode	Direction	Peak Amplitude	SNR	Average noise	Standard Dev.
OD	5	19	45	Shear	Rad/Ax in	-	-	-	-
OD	5	19	45	Shear	Rad/Ax out	n/a	n/a	n/a	n/a
OD	5	26	65	Shear	CCW	-	-	-	-
OD	5	26	65	Shear	CW	-	-	-	-
OD	5	26	65	Shear	Rad/Ax in	n/a	n/a	n/a	n/a
OD	5	26	65	Shear	Rad/Ax out	n/a	n/a	n/a	n/a
OD	10	0	0	Long	-	26,76	10,07	5,51	0,52
OD	10	5	20	Long	CCW	-	-	-	-
OD	10	5	20	Long	CW	24,22	7,30	3,40	0,50
OD	10	5	20	Long	Rad/Ax in	-	-	-	-
OD	10	5	20	Long	Rad/Ax out	n/a	n/a	n/a	n/a
OD	10	19	45	Shear	CCW	-	-	-	-
OD	10	19	45	Shear	CW	-	-	-	-
OD	10	19	45	Shear	Rad/Ax in	-	-	-	-
OD	10	19	45	Shear	Rad/Ax out	n/a	n/a	n/a	n/a
OD	10	26	65	Shear	CCW	-	-	-	-
OD	10	26	65	Shear	CW	-	-	-	-
OD	10	26	65	Shear	Rad/Ax in	n/a	n/a	n/a	n/a
OD	10	26	65	Shear	Rad/Ax out	n/a	n/a	n/a	n/a

Table B-4.6 UT Scan results for disk 4

Surface	Frequency	Angle	Mode	Direction	Focus	Amp %	SNR	Peak noise%	Noise Av %	Max noise %
UA	5 MHz	0°	Long		Subs	29,41	7,31	6,67	3,06	6,67
UA	5 MHz	0°	Long		Surf	30,98	3,73	14,51	8,47	15,69
UA	5 MHz	20°	Long	AFT	Subs	NA	NA	NA	NA	NA
UA	5 MHz	20°	Long	AFT	Surf	69,41	12,5	8,63	3,34	8,63
UA	5 MHz	20°	Long	CCW	Subs	46,67	21,07	3,53	1,38	3,92
UA	5 MHz	20°	Long	CCW	Surf	96,08	21,3	7,84	3,49	7,84
UA	5 MHz	20°	Long	CW	Subs	16,47	8,3	3,14	1,31	3,53
UA	5 MHz	20°	Long	CW	Surf	32,94	10,6	5,88	3,07	5,88
UA	5 MHz	20°	Long	FWD	Subs	13,33	3,32	5,49	2,11	5,49
UA	5 MHz	20°	Long	FWD	Surf	23,14	4,23	7,84	3,1	7,84
UA	5 MHz	45°	Shear	AFT	Subs	NA	NA	NA	NA	NA
UA	5 MHz	45°	Shear	AFT	Surf	NA	NA	NA	NA	NA
UA	5 MHz	45°	Shear	CCW	Subs	14,12	20,46	1,96	1,34	1,96
UA	5 MHz	45°	Shear	CCW	Surf	25,49	6,52	5,1	1,41	5,1
UA	5 MHz	45°	Shear	CW	Subs	16,08	14,71	2,35	1,35	2,35
UA	5 MHz	45°	Shear	CW	Surf	25,1	5,78	5,49	1,39	5,49
UA	5 MHz	45°	Shear	FWD	Subs	NA	NA	NA	NA	NA
UA	5 MHz	45°	Shear	FWD	Surf	NA	NA	NA	NA	NA
UA	5 MHz	65°	Shear	CCW	Surf	NA	NA	NA	NA	NA
UA	5 MHz	65°	Shear	CW	Surf	NA	NA	NA	NA	NA
UA	10 MHz	0°	Long		Subs	59,61	6,74	13,33	5,27	14,51
UA	10 MHz	0°	Long		Surf	20	3,7	8,63	4,42	9,02
UA	10 MHz	20°	Long	AFT	Subs	108	9,56	16,08	5,34	21,57
UA	10 MHz	20°	Long	AFT	Surf	37,65	10,03	6,67	3,24	8,63
UA	10 MHz	20°	Long	CCW	Subs	280	35	12,94	5,16	14,12
UA	10 MHz	20°	Long	CCW	Surf	64,31	12,94	8,63	3,97	8,63
UA	10 MHz	20°	Long	CW	Subs	120	13,4	13,33	4,72	14,12
UA	10 MHz	20°	Long	CW	Surf	24,31	5,41	7,84	4,11	8,63
UA	10 MHz	20°	Long	FWD	Subs	104	10,7	14,12	4,82	14,9

Surface	Frequency	Angle	Mode	Direction	Focus	Amp %	SNR	Peak noise%	Noise Av %	Max noise %
UA	10 MHz	20°	Long	FWD	Surf	18,82	2,93	9,41	4,53	9,41
UA	10 MHz	45°	Shear	AFT	Subs	NA	NA	NA	NA	NA
UA	10 MHz	45°	Shear	AFT	Surf	NA	NA	NA	NA	NA
UA	10 MHz	45°	Shear	CCW	Subs	14,9	5,01	5,1	2,65	6,67
UA	10 MHz	45°	Shear	CCW	Surf	21,57	4,99	7,84	4,4	8,63
UA	10 MHz	45°	Shear	CW	Subs	23,53	8,35	5,1	2,59	5,1
UA	10 MHz	45°	Shear	CW	Surf	27,06	5,2	8,63	4,24	9,41
UA	10 MHz	45°	Shear	FWD	Subs	NA	NA	NA	NA	NA
UA	10 MHz	45°	Shear	FWD	Surf	NA	NA	NA	NA	NA
UA	10 MHz	65°	Shear	CCW	Surf	NA	NA	NA	NA	NA
UA	10 MHz	65°	Shear	CW	Surf	NA	NA	NA	NA	NA
UB	5 MHz	0°	Long		Subs	34,12	10,82	7,45	4,74	7,45
UB	5 MHz	0°	Long		Surf	29,41	6,19	9,41	5,56	9,41
UB	5 MHz	20°	Long	CCW	Subs	65,49	9,31	12,55	6,18	12,55
UB	5 MHz	20°	Long	CCW	Surf	89,4	13,5	10,59	4,2	14,51
UB	5 MHz	20°	Long	CW	Subs	18,43	3,2	11,37	8,17	11,37
UB	5 MHz	20°	Long	CW	Surf	29,41	4,29	9,41	3,33	10,59
UB	5 MHz	20°	Long	RI	Subs	40	7,16	10,59	5,81	11,37
UB	5 MHz	20°	Long	RI	Surf	45,88	6,19	10,59	3,79	10,98
UB	5 MHz	20°	Long	RO	Subs	43,53	6,83	12,55	7,24	14,12
UB	5 MHz	20°	Long	RO	Surf	45,48	4,97	12,16	3,67	12,16
UB	5 MHz	45°	Shear	CCW	Subs	30,98	4,92	7,45	1,45	8,63
UB	5 MHz	45°	Shear	CCW	Surf	49,8	7,59	7,84	1,48	10,2
UB	5 MHz	45°	Shear	CW	Subs	12,94	1,91	7,45	1,44	7,84
UB	5 MHz	45°	Shear	CW	Surf	17,65	3,64	5,88	1,42	6,67
UB	5 MHz	45°	Shear	RI	Subs	NA	NA	NA	NA	NA
UB	5 MHz	45°	Shear	RI	Surf	NA	NA	NA	NA	NA
UB	5 MHz	45°	Shear	RO	Subs	NA	NA	NA	NA	NA
UB	5 MHz	45°	Shear	RO	Surf	NA	NA	NA	NA	NA
UB	5 MHz	65°	Shear	CCW	Surf	NA	NA	NA	NA	NA
UB	5 MHz	65°	Shear	CW	Surf	NA	NA	NA	NA	NA
UB	10 MHz	0°	Long		Subs	67,84	6,56	14,12	4,46	14,51
UB	10 MHz	0°	Long		Surf	16,08	3,35	8,63	5,45	8,63
UB	10 MHz	20°	Long	CCW	Subs	312	21,12	18,82	4,26	25,49
UB	10 MHz	20°	Long	CCW	Surf	37,65	7,67	8,63	4,28	9,41

Surface	Frequency	Angle	Mode	Direction	Focus	Amp %	SNR	Peak noise%	Noise Av %	Max noise %
UB	10 MHz	20°	Long	CW	Subs	78,04	6,55	15,69	4,45	16,47
UB	10 MHz	20°	Long	CW	Surf	15,69	1,81	10,59	4,29	11,37
UB	10 MHz	20°	Long	RI	Subs	144	17,01	12,55	4,34	12,94
UB	10 MHz	20°	Long	RI	Surf	29,02	4,81	9,41	4,26	9,41
UB	10 MHz	20°	Long	RO	Subs	100	11,67	12,55	4,35	13,33
UB	10 MHz	20°	Long	RO	Surf	20,39	3,17	9,41	4,36	10,59
UB	10 MHz	45°	Shear	CCW	Subs	29,02	4,49	9,41	3,77	10,59
UB	10 MHz	45°	Shear	CCW	Surf	52,16	9,91	9,41	4,61	10,59
UB	10 MHz	45°	Shear	CW	Subs	23,92	4,12	8,63	3,73	9,41
UB	10 MHz	45°	Shear	CW	Surf	22,15	4,42	8,63	4,62	11,37
UB	10 MHz	45°	Shear	RI	Subs	NA	NA	NA	NA	NA
UB	10 MHz	45°	Shear	RI	Surf	NA	NA	NA	NA	NA
UB	10 MHz	45°	Shear	RO	Subs	NA	NA	NA	NA	NA
UB	10 MHz	45°	Shear	RO	Surf	NA	NA	NA	NA	NA
UB	10 MHz	65°	Shear	CCW	Surf	NA	NA	NA	NA	NA
UB	10 MHz	65°	Shear	CW	Surf	NA	NA	NA	NA	NA
UC	5 MHz	0°	Long		Surf	55,69	6,32	14,12	6,3	14,51
UC	5 MHz	20°	Long	AFT	Surf	58,43	6,8	14,51	6,94	16,47
UC	5 MHz	20°	Long	CCW	Surf	71,37	40,46	4,31	2,61	5,49
UC	5 MHz	20°	Long	CW	Surf	57,65	17,42	6,67	3,56	7,06
UC	5 MHz	20°	Long	FWD	Surf	NA	NA	NA	NA	NA
UC	5 MHz	45°	Shear	AFT	Surf	Not detected	Not detected	Not detected	Not detected	Not detected
UC	5 MHz	45°	Shear	CCW	Surf	25,49	6,55	5,1	1,43	10,2
UC	5 MHz	45°	Shear	CW	Surf	19,61	3,18	7,45	1,88	9,02
UC	5 MHz	45°	Shear	FWD	Surf	NA	NA	NA	NA	NA
UC	5 MHz	65°	Shear	CCW	Surf	10,59	3,06	4,31	1,26	4,31
UC	5 MHz	65°	Shear	CW	Surf	8,63	3,93	3,14	1,27	5,1
UC	10 MHz	0°	Long		Surf	31,37	6,12	9,41	5,12	10,2
UC	10 MHz	20°	Long	AFT	Surf	20,39	4,51	7,45	3,77	7,45
UC	10 MHz	20°	Long	CCW	Surf	41,57	11,36	6,67	3,3	6,67

Surface	Frequency	Angle	Mode	Direction	Focus	Amp %	SNR	Peak noise%	Noise Av %	Max noise %
UC	10 MHz	20°	Long	CW	Surf	24,31	4,67	7,84	3,35	9,41
UC	10 MHz	20°	Long	FWD	Surf	NA	NA	NA	NA	NA
UC	10 MHz	45°	Shear	AFT	Surf	23,53	5,6	7,84	4,43	8,63
UC	10 MHz	45°	Shear	CCW	Surf	27,45	5,73	7,84	3,7	9,02
UC	10 MHz	45°	Shear	CW	Surf	25,88	4,75	8,63	4,02	9,41
UC	10 MHz	45°	Shear	FWD	Surf	NA	NA	NA	NA	NA
UC	10 MHz	65°	Shear	CCW	Surf	17,65	7,85	5,1	3,27	5,49
UC	10 MHz	65°	Shear	CW	Surf	18,43	6,96	5,49	3,32	5,49
UC	Freq.	Angle	Mode	Direction	Focus	AMP %	SNR	Peak noise%	Noise Av %	Max noise %
UE	5 MHz	0°	Long		Subs	23,14	3,71	8,63	3,28	9,41
UE	5 MHz	0°	Long		Surf	23,92	1,25	22,35	15,99	22,35
UE	5 MHz	20°	Long	CCW	Subs	61,18	40,2	3,53	2,06	4,31
UE	5 MHz	20°	Long	CCW	Surf	91,37	32,35	7,45	4,77	8,63
UE	5 MHz	20°	Long	CW	Subs	15,69	8,11	3,92	2,27	4,31
UE	5 MHz	20°	Long	CW	Surf	22,35	6,41	7,45	4,69	7,45
UE	5 MHz	20°	Long	RI	Subs	19,61	2,53	10,98	5,35	11,37
UE	5 MHz	20°	Long	RI	Surf	30,59	6,54	11,37	7,9	11,37
UE	5 MHz	20°	Long	RO	Subs	43,14	20,4	4,31	2,31	4,31
UE	5 MHz	20°	Long	RO	Surf	58,82	13,39	7,45	3,31	8,63
UE	5 MHz	45°	Shear	CCW	Subs	47,45	45,88	2,35	1,35	2,35
UE	5 MHz	45°	Shear	CCW	Surf	59,61	10,28	7,06	1,4	9,02
UE	5 MHz	45°	Shear	CW	Subs	18,04	7,71	3,53	1,37	4,31
UE	5 MHz	45°	Shear	CW	Surf	24,31	3,79	7,45	1,42	10,98
UE	5 MHz	45°	Shear	RI	Subs	NA	NA	NA	NA	NA
UE	5 MHz	45°	Shear	RI	Surf	NA	NA	NA	NA	NA
UE	5 MHz	45°	Shear	RO	Subs	NA	NA	NA	NA	NA
UE	5 MHz	45°	Shear	RO	Surf	NA	NA	NA	NA	NA
UE	5 MHz	65°	Shear	CCW	Surf	NA	NA	NA	NA	NA
UE	5 MHz	65°	Shear	CW	Surf	NA	NA	NA	NA	NA
UE	10 MHz	0°	Long		Subs	28,63	4,14	9,02	2,78	9,41
UE	10 MHz	0°	Long		Surf	25,1	6,29	8,63	5,51	9,41

Surface	Frequency	Angle	Mode	Direction	Focus	Amp %	SNR	Peak noise%	Noise Av %	Max noise %
UE	10 MHz	20°	Long	CCW	Subs	61,96	14,44	6,67	2,55	6,67
UE	10 MHz	20°	Long	CCW	Surf	37,65	10,34	7,45	4,22	7,84
UE	10 MHz	20°	Long	CW	Subs	14,51	2,89	6,67	2,52	6,67
UE	10 MHz	20°	Long	CW	Surf	10,98	2,1	7,45	4,23	8,63
UE	10 MHz	20°	Long	RI	Subs	17,65	4,84	5,88	2,82	7,06
UE	10 MHz	20°	Long	RI	Surf	22,35	3,98	9,41	5,06	10,2
UE	10 MHz	20°	Long	RO	Subs	35,69	6,6	7,84	2,87	9,02
UE	10 MHz	20°	Long	RO	Surf	27,06	3,98	10,59	5,06	17,65
UE	10 MHz	45°	Shear	CCW	Subs	79,61	9,06	12,94	4,67	13,33
UE	10 MHz	45°	Shear	CCW	Surf	60,39	18,37	7,45	4,4	9,02
UE	10 MHz	45°	Shear	CW	Subs	21,57	2,66	10,98	4,59	12,55
UE	10 MHz	45°	Shear	CW	Surf	21,57	5,61	7,45	4,39	8,63
UE	10 MHz	45°	Shear	RI	Subs	NA	NA	NA	NA	NA
UE	10 MHz	45°	Shear	RI	Surf	NA	NA	NA	NA	NA
UE	10 MHz	45°	Shear	RO	Subs	NA	NA	NA	NA	NA
UE	10 MHz	45°	Shear	RO	Surf	NA	NA	NA	NA	NA
UE	10 MHz	65°	Shear	CCW	Surf	NA	NA	NA	NA	NA
UE	10 MHz	65°	Shear	CW	Surf	NA	NA	NA	NA	NA

Table B-4.7 UT Scan results for disk 5

Surface	Frequency	Angle	Mode	Direction	Focus	Amp %	SNR	Peak noise%	Noise Av %	Max noise %
UI	5 MHz	0°	Long		Subs	21.18	2.26	7.12	13.33	13.33
UI	5 MHz	0°	Long		Surf	12.16	2.45	4.86	7.84	12.55
UI	5 MHz	20°	Long	AFT	Subs	Not detected	Not detected	Not detected	Not detected	Not detected
UI	5 MHz	20°	Long	AFT	Surf	Not detected	Not detected	Not detected	Not detected	Not detected
UI	5 MHz	20°	Long	CCW	Subs	Not detected	Not detected	Not detected	Not detected	Not detected
UI	5 MHz	20°	Long	CCW	Surf	Not detected	Not detected	Not detected	Not detected	Not detected
UI	5 MHz	20°	Long	CW	Subs	Not detected	Not detected	Not detected	Not detected	Not detected
UI	5 MHz	20°	Long	CW	Surf	Not detected	Not detected	Not detected	Not detected	Not detected
UI	5 MHz	20°	Long	FWD	Subs	NA	NA	NA	NA	NA
UI	5 MHz	20°	Long	FWD	Surf	NA	NA	NA	NA	NA
UI	5 MHz	45°	Shear	AFT	Subs	NA	NA	NA	NA	NA
UI	5 MHz	45°	Shear	AFT	Surf	NA	NA	NA	NA	NA
UI	5 MHz	45°	Shear	CCW	Subs	NA	NA	NA	NA	NA
UI	5 MHz	45°	Shear	CCW	Surf	Not detected	Not detected	Not detected	Not detected	Not detected
UI	5 MHz	45°	Shear	CW	Subs	NA	NA	NA	NA	NA
UI	5 MHz	45°	Shear	CW	Surf	Not detected	Not detected	Not detected	Not detected	Not detected
UI	5 MHz	45°	Shear	FWD	Subs	NA	NA	NA	NA	NA
UI	5 MHz	45°	Shear	FWD	Surf	NA	NA	NA	NA	NA

Surface	Frequency	Angle	Mode	Direction	Focus	Amp %	SNR	Peak noise%	Noise Av %	Max noise %
UI	5 MHz	65°	Shear	CCW	Surf	NA	NA	NA	NA	NA
UI	5 MHz	65°	Shear	CW	Surf	NA	NA	NA	NA	NA
UI	10 MHz	0°	Long		Subs	Not detected	Not detected	Not detected	Not detected	Not detected
UI	10 MHz	0°	Long		Surf	16.86	4.52	4.27	7.06	7.06
UI	10 MHz	6°	Long	AFT	Surf	14.9	3.14	3.39	7.06	7.06
UI	10 MHz	6°	Long	FWD	Surf	Not detected	Not detected	Not detected	Not detected	Not detected
UI	10 MHz	20°	Long	AFT	Subs	Not detected	Not detected	Not detected	Not detected	Not detected
UI	10 MHz	20°	Long	AFT	Surf	Not detected	Not detected	Not detected	Not detected	Not detected
UI	10 MHz	20°	Long	CCW	Subs	Not detected	Not detected	Not detected	Not detected	Not detected
UI	10 MHz	20°	Long	CCW	Surf	Not detected	Not detected	Not detected	Not detected	Not detected
UI	10 MHz	20°	Long	CW	Subs	Not detected	Not detected	Not detected	Not detected	Not detected
UI	10 MHz	20°	Long	CW	Surf	Not detected	Not detected	Not detected	Not detected	Not detected
UI	10 MHz	20°	Long	FWD	Subs	NA	NA	NA	NA	NA
UI	10 MHz	20°	Long	FWD	Surf	NA	NA	NA	NA	NA
UI	10 MHz	45°	Shear	AFT	Subs	NA	NA	NA	NA	NA
UI	10 MHz	45°	Shear	AFT	Surf	NA	NA	NA	NA	NA
UI	10 MHz	45°	Shear	CCW	Subs	Not detected	Not detected	Not detected	Not detected	Not detected

Surface	Frequency	Angle	Mode	Direction	Focus	Amp %	SNR	Peak noise%	Noise Av %	Max noise %
UI	10 MHz	45°	Shear	CCW	Surf	Not detected	Not detected	Not detected	Not detected	Not detected
UI	10 MHz	45°	Shear	CW	Subs	Not detected	Not detected	Not detected	Not detected	Not detected
UI	10 MHz	45°	Shear	CW	Surf	Not detected	Not detected	Not detected	Not detected	Not detected
UI	10 MHz	45°	Shear	FWD	Subs	NA	NA	NA	NA	NA
UI	10 MHz	45°	Shear	FWD	Surf	NA	NA	NA	NA	NA
UI	10 MHz	65°	Shear	CCW	Surf	NA	NA	NA	NA	NA
UI	10 MHz	65°	Shear	CW	Surf	NA	NA	NA	NA	NA

Table B-4.8 UT Scan results for disk 6

OEM	Frequency	Incidence angle	Refracted Angle	Mode	Direction	SNR	Peak Amplitude	Average noise	Standard Dev.	Calibration	Cal Block	Gain
OEM 1	5	0 deg long	0	Long	-	2.02	27.15	23.3	1.12	80%	#1FBH	54.8
		5	20	Long	CW	3.33	25	4.9	5.87	80%	#1FBH	54.8
					Rad/ Ax in	5.44	31.84	4.55	7.67	80%	#1FBH	54.8
		19	45	Shear	CW	1.63	5.08	1.03	1.15	80%	SDH Ø 0.02inch	41.2
					Rad/ Ax in	1.06	4.49	1.29	0.93	80%	SDH Ø 0.02inch	41.2
		26	65	Shear	CW	0	0	0	0	80%	SDH Ø 0.02inch	37.2
					Rad/ Ax in							
		-5	20	Long	CCW	4.84	37.5	5	8.62	80%	#1FBH	54.8
					Rad/ Ax out	3.15	28.91	7.15	6.45	80%	#1FBH	54.8
		-19	45	Shear	CCW	2.9	8.01	1.15	1.8	80%	SDH Ø 0.02inch	41.2
					Rad/ Ax out	1.74	3.91	1.15	0.08	80%	SDH Ø 0.02inch	41.2
		-26	65	Shear	CCW	0	0	0	0	80%	SDH Ø 0.02inch	37.2
					Rad/ Ax out							
	10	0 deg long	0	Long	-	1.45	7.23	3.44	1.01	80%	#1FBH	46.2
		5	20	Long	CW	6.37	24.81	3.72	5.53	80%	#1FBH	46.2
					Rad/ Ax in	5.59	23.63	3.89	5.31	80%	#1FBH	46.2
		19	45	Shear	CW	2.15	4.3	1.74	0.47	80%	SDH Ø 0.02inch	44.8
					Rad/ Ax in	0	0	0	0	80%	SDH Ø 0.02inch	44.8
		26	65	Shear	CW	0	0	0	0	80%	SDH Ø 0.02inch	42.0
					Rad/ Ax in							
		-5	20	Long	CCW	13.72	41.8	3.67	9.04	80%	#1FBH	46.2
					Rad/ Ax out	4.51	22.27	4.2	4.45	80%	#1FBH	46.2
		-19	45	Shear	CCW	5.43	8.01	1.78	1.53	80%	SDH Ø 0.02inch	44.8
					Rad/ Ax out	0	0	0	0	80%	SDH Ø 0.02inch	44.8
		-26	65	Shear	CCW	1.21	6.84	3.49	0.76	80%	SDH Ø 0.02inch	42.0

					Rad/ Ax out							
OEM 2												
		Incidence angle	**Refracted Angle**	**Mode**	**Direction**	**SNR**	**Peak Amplitude**	**Average noise**	**Standard Dev.**	**Calibration**	**Cal Block**	**Gain**
	5	0 deg long	0	Long	-	1	0	0	0			
		5	20	Long	CW							
					Rad/ Ax in							
		19	45	Shear	CW	4	38	0	0			
					Rad/ Ax in							
		26	65	Shear	CW							
					Rad/ Ax in							
		-5	20	Long	CCW							
					Rad/ Ax out							
		-19	45	Shear	CCW	7.1	38	0	0			
					Rad/ Ax out							
		-26	65	Shear	CCW							
					Rad/ Ax out							
	10	0 deg long	0	Long	-	4	47	0	0	#1 FBH at 80% FSH (gate 0.1-2.0 in)	PWA1 100 (FG PM Ni)	46 dB (base gain)
		5	20	Long	CW							
					Rad/ Ax in							
		19	45	Shear	CW							
					Rad/ Ax in							
		26	65	Shear	CW	0	37	0	0			
					Rad/ Ax in							
		-5	20	Long	CCW							
					Rad/ Ax out							
		-19	45	Shear	CCW	2	0	0	0			
					Rad/ Ax out							

		-26	65	Shear	CCW	0	37	0	0			
					Rad/ Ax out							
OEM 3*												
		Incidence angle	**Refracted Angle**	**Mode**	**Direction**	**SNR**	**Peak Amplitude**	**Average noise**	**Standard Dev.**	**Calibration**	**Cal Block**	**Gain**
	5	0 deg long	0	Long	-							
		5	20	Long	CW							
					Rad/ Ax in							
		19	45	Shear	CW							
					Rad/ Ax in							
		26	65	Shear	CW							
					Rad/ Ax in							
		-5	20	Long	CCW							
					Rad/ Ax out							
		-19	45	Shear	CCW							
					Rad/ Ax out							
		-26	65	Shear	CCW							
					Rad/ Ax out							
	10	0 deg long	0	Long	-	1.8	36	0	0			
		5	20	Long	CW							
					Rad/ Ax in							
		19	45	Shear	CW							
					Rad/ Ax in							
		26	65	Shear	CW							
					Rad/ Ax in							
		-5	20	Long	CCW							
					Rad/ Ax out							
		-19	45	Shear	CCW							
					Rad/ Ax out							
		-26	65	Shear	CCW							

					Rad/ Ax out							
OEM 4												
		Incidence angle	**Refracted Angle**	**Mode**	**Direction**	**SNR**	**Peak Amplitude**	**Average noise**	**Standard Dev.**	**Calibration**	**Cal Block**	**Gain**
	5	0 deg long	0	Long	-	6.5	16	6.31	/	#2 FBH at 80% FSH	Inco718	/
		5	20	Long	CW	NA						
					Rad/ Ax in	NA						
		19	45	Shear	CW	2.18	7	0.87	/	SDH at 80% + 6 dB	Inco718	32.9 dB
					Rad/ Ax in	not seen				SDH at 80%	Inco718	
		26	65	Shear	CW	NA						
					Rad/ Ax in	NA						
		-5	20	Long	CCW	NA						
					Rad/ Ax out	NA						
		-19	45	Shear	CCW	4.25	11	0.84	/	SDH at 80% + 6 dB	Inco718	32.9 dB
					Rad/ Ax out	not seen				SDH at 80%	Inco718	
		-26	65	Shear	CCW	NA						
					Rad/ Ax out	NA						
	10	0 deg long	0	Long	-	2.83	14	6.06	/	#2 FBH at 80% FSH	Inco718	34.4 dB
		5	20	Long	CW	4.84	10	1.27	/	#2 FBH at 80% FSH	Inco718	46.7 dB
					Rad/ Ax in	1.55	11	1.11	/	#2 FBH at 80% FSH	Inco718	40.6 dB
		19	45	Shear	CW	NA						
					Rad/ Ax in	NA						
		26	65	Shear	CW	NA						
					Rad/ Ax in	NA						
		-5	20	Long	CCW	3.21	14	1.58	/	#2 FBH at 80% FSH	Inco718	46.7 dB
					Rad/ Ax out	3.26	10	0.94	/	#2 FBH at 80% FSH	Inco718	/

		-19	45	Shear	CCW	NA						
					Rad/ Ax out	NA						
		-26	65	Shear	CCW	NA						
					Rad/ Ax out	NA						

n/a means that the scans were not executed

A minus (-) means that the indication was not visible, or the value is missing

* OEM 3: No calibration was done for these scans

Table B-4.9 UT Scan results for disk 7

Frequency	Incident Angle	Refracted Angle	Mode	Direction	Peak Amplitude	SNR	Average noise	Standard Dev.
5 MHz	0	0	Long		not seen			
5 MHz	2.5	10	Long	Unk	not seen			
5 MHz	5	20	Long	CCW	not seen			
5 MHz	5	20	Long	CW	not seen			
5 MHz	5	20	Long	RI	not seen			
5 MHz	5	20	Long	RO	not seen			
5 MHz	10	45	Long	CCW	44.71	4.61	7.61	1.67
5 MHz	10	45	Long	CW	21.96	4.34	3.34	0.4
5 MHz	10	45	Long	RI	18.82	2.37	6.16	1.47
5 MHz	10	45	Long	RO	25	1.81		
5 MHz	12.5	26	Shear	RI	47	6.24	6.7	1.58
5 MHz	15	30	Shear	RI	86	7.66	8.67	2.2
5 MHz	17.5	38	Shear	RI	100	6.68	12.89	2.25
5 MHz	20	45	Shear	CCW	100	6.69	13.74	2.66
5 MHz	20	45	Shear	CW	100	9.82	12.17	2
5 MHz	20	45	Shear	RI	94	12.51	6.21	1.18
5 MHz	20	45	Shear	RO	100	6.89		
5 MHz	26	65	Shear	CCW	61	7.6	8.05	1.11
5 MHz	26	65	Shear	CW	100	6.68	10.64	2.11
10 MHz	0	0	Long		36.86	4.02	14.52	3.11
10 MHz	2.5	10	Long	Unk	36.86	4.05	9.9	5.14
10 MHz	5	20	Long	CCW	32.16	5.38	6.86	4.3
10 MHz	5	20	Long	CW	31.37	4.88	8.96	4.13
10 MHz	5	20	Long	RO	29.8	3.9	8.82	3.9
10 MHz	5	20	Long	UNK	26.67	6.52	5.74	4.66
10 MHz	7.5	15	Long	Unk	29.8	5.07	8.01	3.92
10 MHz	10	45	Long	CCW	20.39	7.03	5.1	3.64
10 MHz	10	45	Long	CW	25.88	7.74	6.16	4.35
10 MHz	10	45	Long	UNK	27.45	4.27	6.54	3.3
10 MHz	12.5	26	Shear	RI	22.75	8.37	6.49	4.77
10 MHz	15	30	Shear	RI	68.24	10.42	13.07	11.15
10 MHz	15	38	Shear	RI	100	14.34	17.43	18.2
10 MHz	20	45	Shear	CCW	85.49	9.01	13.09	14.19
10 MHz	20	45	Shear	CW	100	11.84	15.15	18.06
10 MHz	20	45	Shear	RI	90.2	12.91	17.41	16.04

Frequency	Incident Angle	Refracted Angle	Mode	Direction	Peak Amplitude	SNR	Average noise	Standard Dev.
10 MHz	20	45	Shear	RO	100	16.84	21.15	22.63
10 MHz	26	65	Shear	RI	not seen		n/a	n/a

Table B-4.10 UT Scan results for disk 8

Surface	Frequency	Angle	Mode	Direction	Focus	Amplitude	SNR	Noise avg.	Max Noise	Noise Std.
B	5 MHz	20	Long	CCW	Subs	5	1.4	1.5	4	0.5
B	5 MHz	20	Long	CCW	Surf	9	3.8	2.2	4	0.4
B	5 MHz	20	Long	CW	Subs	5	2.7	1.8	3	0.4
B	5 MHz	20	Long	CW	Surf	7	2.6	2.1	4	0.3
B	5 MHz	20	Long	RI	Surf	5	2.3	1.4	3	0.5
B	5 MHz	20	Long	RO	Surf	9	5	1.5	3	0.5
B	5 MHz	45	Shear	CCW	Subs	10	9.9	1.1	2	0.3
B	5 MHz	45	Shear	CW	Subs	12	12.1	1.1	2	0.3
B	5 MHz	45	Shear	RI	Subs	7	4.1	1.7	3	0.5
B	5 MHz	45	Shear	RI	Surf	10	14.3	1.4	2	0.5
B	10 MHz	0	Long		Subs	19	3.9	5.6	9	0.8
B	10 MHz	0	Long		Surf	15	2.8	5.6	9	1
B	10 MHz	20	Long	CCW	Subs	11	5	3.5	5	0.6
B	10 MHz	20	Long	CCW	Surf	18	3.3	3.6	8	0.7
B	10 MHz	20	Long	CW	Subs	10	2.7	3.6	6	0.6
B	10 MHz	20	Long	CW	Surf	14	2.5	4	8	0.7
B	10 MHz	20	Long	RI	Surf	10	3.5	3	5	0.6
B	10 MHz	20	Long	RO	Surf	23	4.8	5.3	9	0.9
B	10 MHz	45	Shear	CCW	Subs	26	19.3	2.8	4	0.5
B	10 MHz	45	Shear	CCW	Surf	12	4.8	1.9	4	0.4
B	10 MHz	45	Shear	CW	Subs	23	9.6	2.9	5	0.5
B	10 MHz	45	Shear	CW	Surf	15	4.6	2.2	5	0.5
B	10 MHz	45	Shear	RI	Surf	8	9.6	1.3	2	0.5
C1	5 MHz	0	Long		Subs	11	3.3	2.4	5	0.5
C1	5 MHz	20	Long	CCW	Subs	5	1.8	2.8	4	0.5
C1	5 MHz	20	Long	CW	Subs	5	3	2	3	0.2
C1	5 MHz	45	Shear	CCW	Subs	9	8	1	2	0.1
C1	5 MHz	45	Shear	CW	Subs	8	7	1	2	0.1
C1	10 MHz	0	Long		Subs	26	6	5.6	9	1.3
C1	10 MHz	20	Long	CCW	Subs	13	1.5	4.2	10	1.5
C1	10 MHz	20	Long	CCW	Surf	7	2.5	2	4	0.2
C1	10 MHz	20	Long	CW	Subs	13	2.8	3.7	7	0.9
C1	10 MHz	20	Long	CW	Surf	6	4	2	3	0.2
C1	10 MHz	45	Shear	CCW	Subs	23	2.3	3.8	12	1.8
C1	10 MHz	45	Shear	CCW	Surf	12	5.7	3.5	5	0.6

Surface	Frequency	Angle	Mode	Direction	Focus	Amplitude	SNR	Noise avg.	Max Noise	Noise Std.
C1	10 MHz	45	Shear	CW	Subs	26	3.4	4.7	11	1.8
C1	10 MHz	45	Shear	CW	Surf	7	1.4	3.5	6	0.6
C2	5 MHz	0	Long		Subs	8	3.7	2.5	4	0.5
C2	5 MHz	20	Long	CCW	Subs	5	1.6	2.2	4	0.4
C2	5 MHz	20	Long	CCW	Surf	6	6	1.2	2	0.4
C2	5 MHz	20	Long	CW	Subs	8	2.9	1.9	4	0.4
C2	5 MHz	20	Long	CW	Surf	9	9.8	1.2	2	0.4
C2	5 MHz	45	Shear	CCW	Subs	17	17.7	1.1	2	0.2
C2	5 MHz	45	Shear	CW	Subs	13	13.2	1.1	2	0.2
C2	10 MHz	0	Long		Subs	29	4.3	5.6	11	1.2
C2	10 MHz	0	Long		Surf	17	4.7	4.3	7	0.7
C2	10 MHz	20	Long	CCW	Subs	15	4.3	3.3	6	0.6
C2	10 MHz	20	Long	CCW	Surf	17	3.1	5.2	9	0.8
C2	10 MHz	20	Long	CW	Subs	24	12.2	3.3	5	0.5
C2	10 MHz	20	Long	CW	Surf	23	4.9	5.4	9	0.8
C2	10 MHz	20	Long	RO	Surf	15	3.6	5.3	8	0.8
C2	10 MHz	45	Shear	CCW	Subs	48	21.5	2.9	5	0.5
C2	10 MHz	45	Shear	CCW	Surf	15	5.1	3.8	6	0.6
C2	10 MHz	45	Shear	CW	Subs	46	11.3	3.2	7	0.7
C2	10 MHz	45	Shear	CW	Surf	12	2.6	3.9	7	0.6
D	5 MHz	45	Shear	AFT	Surf	18	13.5	1.8	3	0.4
D	10 MHz	0	Long		Surf	12	1.7	4.7	9	1
D	10 MHz	20	Long	AFT	Surf	20	2.3	9.5	14	1
D	10 MHz	20	Long	CCW	Surf	15	3.4	6.5	9	0.8
D	10 MHz	20	Long	CW	Surf	15	3.6	5.3	8	0.7
D	10 MHz	20	Long	FWD	Surf	12	2.2	4.6	8	0.7
D	10 MHz	45	Shear	AFT	Surf	15	9.5	2.7	4	0.5
D	10 MHz	45	Shear	CCW	Surf	8	3	2	4	0.3
D	10 MHz	45	Shear	CW	Surf	8	2.9	1.9	4	0.4
D	10 MHz	45	Shear	FWD	Surf	5	3	2	3	0.2

Table B-4.11 UT Scan results for disk 9

Surface D	Frequency	Angle	Mode	Direction	Focus	Amplitude	SNR	Mean Noise
D	5 MHz	45	Shear	Aft	Surf	20	4.42	3.20
D	5 MHz	45	Shear	CCW	Surf	6	3.4	2.50
D	5 MHz	45	Shear	CW	Surf	13	3.86	2.20
D	5 MHz	45	Shear	FWD	Surf	24	6.52	5.10
D	10 MHz	0	Long	NA	Surf	NA	NA	
D	10 MHz	20	Long	CCW	Surf	5	1.3	2.90
D	10 MHz	20	Long	CW	Surf	9	1.88	2.60
E	5 MHz	45	Shear	CCW	Surf	11	3.31	2.40
E	5 MHz	45	Shear	CW	Surf	7	1.8	2.50
E	5 MHz	65	Shear	CCW	Surf	11	2.82	1.70
E	5 MHz	65	Shear	CW	Surf	12	3.41	2.10
E	10 MHz	0	Long	NA	Surf	10	1.61	4.70
E	10 MHz	20	Long	CW	Surf	8	1.61	2.70
E	10 MHz	45	Shear	CCW	Surf	15	2.11	5.50
E	10 MHz	45	Shear	CW	Surf	10	2.36	5.60
E	10 MHz	65	Shear	CCW	Surf	24	3.33	4.00
E	10 MHz	65	Shear	CW	Surf	19	2.79	3.40